

Aus dem Max-Planck-Institut für biophysikalische Chemie in Göttingen

Abteilung Zelluläre Biochemie

Direktor: Prof. Dr. Reinhard Lührmann

**Determination of the Structure of the
Spliceosomal U6 snRNP from Yeast,
*Saccharomyces cerevisiae***

Dissertation

zur Erlangung des Doktorgrades

der Mathematisch-Naturwissenschaftlichen Fakultäten
der Georg-August-Universität zu Göttingen

vorgelegt von

Ramazan Karaduman

aus

Istanbul, TÜRKEI

Göttingen, 2006

D7

Referent: Prof. Dr. Ralf Ficner

Korreferent: Prof. Dr. Hans-Joachim Fritz

Tag der mündlichen Prüfung:

ANNEME

ve

BABAMA

TABLE of CONTENTS

ABSTRACT	1
INTRODUCTION	3
2.1 Chemistry of Splicing Reaction.....	3
2.1.1 A Two-Step Mechanism	3
2.1.2 Splice Site Sequence Requirements	5
2.2 Spliceosome Assembly in Yeast.....	6
2.2.1 Spliceosome Assembly and Splicing Cycle	6
2.2.2 Properties and Structures of Spliceosomal U snRNAs	9
2.2.3 Protein Composition of Spliceosomal U snRNPs	11
2.3 U6 snRNA Participates in Several Important RNA:RNA Rearrangements	14
2.4 The Features of mono-U6 snRNP Particle	16
2.4.1 Core LSm proteins of the U6 snRNP	16
2.4.2 Prp24p: A Spliceosomal Recycling Factor	20
2.4.3 Structure of U6 snRNA in mono-U6 snRNP	22
2.5 Objectives of the Work.....	25
MATERIALS and METHODS	27
5.1 Materials	27
5.1.1 Chemicals	27
5.1.2 Antisera and monoclonal Antibodies.....	29
5.1.3 Enzymes and Enzyme Inhibitors	29
5.1.4 Nucleotides.....	30
5.1.5 DNA Oligonucleotides	30
5.1.6 Bacteria and Yeast Strains.....	32
5.1.7 Plasmids	34
5.1.8 General Buffers and Solutions	35
5.1.9 Kits.....	35

5.1.10	Working Materials.....	35
5.1.11	Instruments	35
5.2	Methods.....	36
5.2.1	Proteinbiochemistry Standard Methods.....	36
5.2.1.1	Concentration Determination of Proteins.....	36
5.2.1.2	Phenol-Chloroform-Isoamylalcohol Extraction.....	36
5.2.1.3	Proteinase K Digestion	37
5.2.1.4	Denaturing Polyacrylamide Gel Electrophoresis (SDS-PAGE)	37
5.2.1.5	Western Blot Analysis.....	38
5.2.1.6	Coomassie Staining of Protein Gels	39
5.2.1.7	Silver Staining of Protein Gels.....	39
5.2.2	Molecular Biology Standard Methods.....	40
5.2.2.1	Concentration Determination of Nucleic Acids.....	40
3.2.2.2	Agarose Gel Electrophoresis of Nucleic Acids.....	40
3.2.2.3	Denaturing Polyacrylamide Gel Electrophoresis of RNA.....	41
3.2.2.4	Non-Denaturing Polyacrylamide Gel Electrophoresis of U6-Prp24 Binary Complex.....	42
3.2.2.5	Ethidium Bromide Staining of RNA Gels.....	42
3.2.2.6	Silver staining of RNA gels	43
3.2.2.7	Transformation and Isolation of Plasmids into/from <i>E. coli</i>	43
3.2.2.8	Polymerase Chain Reaction (PCR)	43
	<i>PCR for the Amplification of TAP-Marker Cassette</i>	44
	<i>PCR for the Amplification of the Fluorescent Protein-Marker Cassette</i>	44
	<i>PCR for the Amplification of PRP24 Gene from Chromosomal DNA</i>	45
	<i>PCR for Sequencing Analysis</i>	46
	<i>PCR for Characterization of Transformants</i>	46
3.2.2.9	Transformation of haploid yeast cells	47
	<i>Constructing Yeast Strain Expressing TAP-tagged Prp24p</i>	47
	<i>Constructing the Yeast Strain Expressing Fluorescent Protein (yECitrine or yECitrine-3HA)-tagged LSm Proteins</i>	48
	<i>Transformant Characterization by PCR</i>	48
	<i>Transformant Characterization by Western blot</i>	49
3.2.2.10	Constructing Bacteria Strain Overexpressing His ₆ -tagged Prp24p.....	49

3.2.2.11	Restriction Digestion of Plasmids or PCR products.....	50
3.2.2.12	Synthesis of Radioactively Labeled DNA-probes for Northern Analysis	50
3.2.2.13	Northern Blot Analysis.....	50
3.2.2.14	<i>In Vitro</i> Transcription	51
3.2.2.15	Radioactive Labeling of 5'-end of DNA-Oligonucleotides.....	52
3.2.3	Cell Culture and Growth.....	53
3.2.3.1	Growth and Culture of Bacteria	53
3.2.3.2	Yeast Cell Culture	53
3.2.3.3	Harvesting and Extract Preparation from Yeast Cells	54
3.2.4	Immunoprecipitations	56
3.2.5	Special Methods	56
3.2.5.1	Purification of Recombinant Prp24 Protein Tagged with (His) ₆ from <i>E. coli</i> cells	56
	<i>Pre-check of Overexpression:</i>	57
	<i>Ni²⁺-NTA-Affinity Chromatography:</i>	57
3.2.5.2	Tandem Affinity Purification of U6 snRNP Particles using Prp24-TAP Tagged strain	58
3.2.5.3	Glycerol Gradient Sedimentation of Purified snRNP particles.....	60
3.2.5.4	Identification of U6 snRNP proteins by Mass Spectrometry.....	61
3.2.5.5	Electron Microscopy Analysis U6 snRNP Particles	61
3.2.5.6	Isolation of Total-RNA from Yeast Cells	61
3.2.5.7	Band Shift Assays with U6-Prp24 Binary Complex.....	62
3.2.5.8	Methods for Chemical Modification of RNA	63
	<i>Modification with DMS</i>	63
	<i>Modification with CMCT</i>	64
	<i>Modification with Kethoxal</i>	65
3.2.5.9	Hydroxyl Radical Footprinting	65
3.2.5.10	<i>UV-Cross Linking Experiments</i>	67
3.2.5.11	Primer Extension Analysis of Modified U6 snRNA	68

RESULTS 70

5.1 RNA Structure and RNA-Protein Interactions in Purified Yeast U6 snRNPs 70

5.1.1	Isolation of Native U6 snRNPs from the Yeast <i>S. cerevisiae</i> , using the Tandem Affinity Purification (TAP) Method and C-terminally tagged Prp24p	70
5.1.2	Determination of the Secondary Structure of Naked U6 snRNA and U6 in Purified U6 snRNP Particles	75
5.1.3	Mapping the Binding Region of the U6 Proteins on the U6 snRNA by Hydroxyl Radical Footprinting	79
5.1.4	Cross Linking of Proteins to U6 snRNA: Identification of Prp24 and LSm Proteins' Binding Site(s)	81
5.2	RNA-Protein Interactions within the Prp24p-U6 snRNA Binary Complex	86
5.2.1	Purification of Recombinant Prp24 Protein	87
5.2.2	Determination of Binding Affinity of Prp24p-for U6 snRNA	89
5.2.3	Recombinant Prp24p Recognizes Similar Nucleotides of U6 snRNA as Native Prp24p does	90
5.2.4	Footprinting of Recombinant Prp24p Bound to the U6 snRNA .	92
5.3	Electron Microscopy Analysis of yeast U6 snRNP	94
5.3.1	U6 snRNP Has Two Morphologically-Defined Subunits	95
5.3.2	Topographic Labelling of LSm Proteins with yECitrine-Tag	96
5.3.3	Further Image Analysis of U6 snRNP Reveals Potential Flexibility within its Domains	103
5.3.4	Chemically Cross Linked Particles Exhibit a Compact Structure	105
DISCUSSION	108
5.1	RNA Structure and RNA-Protein Interactions in Purified U6 snRNPs	108
5.1.1	The Secondary Structure of U6 snRNA in Purified U6 snRNPs ...	108
5.1.2	The Binding Site of Prp24 and LSm2-8 Proteins on the U6 snRNA in the U6 snRNP particles	110
5.1.3	Prp24p and the LSm Complex Facilitate U4/U6 Association by Opening the U6 Structure	112
5.1.4	The Structure of the Yeast U6 snRNA in Native snRNPs can be adopted by Human U6 and U6 _{atac} snRNAs	114

5.2	Electron Microscopy of Yeast U6 snRNPs Reveal Structural Arrangement between Prp24p and the LSm Ring	116
5.2.1	U6 snRNPs Exhibit Two Structural Configurations	116
5.2.2	Topographic Labelling of the LSm Proteins Reveals the Arrangement of Prp24p, LSm Proteins and U6 snRNA	118
5.2.3	Possible Functional Implications of Two Forms of U6 snRNP	122
	REFERENCES	123
	APPENDIX	I

ABSTRACT

The U6 small nuclear RNA (snRNA) undergoes major conformational changes during the assembly of the spliceosome and catalysis of splicing. It associates with the specific protein Prp24p, and a set of seven LSm2–8 proteins, to form the U6 small nuclear ribonucleoprotein (snRNP). These proteins have been proposed to act as RNA chaperones that stimulate pairing of U6 with U4 snRNA to form the intermolecular stem I and stem II of the U4/U6 duplex, whose formation is essential for spliceosomal function. However, the mechanism whereby Prp24p and the LSm complex facilitates U4/U6 base-pairing, as well as the exact binding site(s) of Prp24p in the native U6 snRNP, are not well understood.

In order to understand the binding site(s) of Prp24 and LSm 2-8 proteins on the U6 snRNA, as well as to shed light on the mechanism whereby Prp24p and the LSm complex facilitate U4/U6 base pairing, purified native U6 snRNPs were thoroughly characterized by chemical structure probing, UV-cross linking and hydroxyl radical footprinting. These three methods demonstrate that the naked U6 snRNA structure is very compact, whereas in the presence of Prp24p and the LSm proteins, the RNA structure in the U6 particle is much more open. This is particularly apparent for the 3'-stem loop and a large internal asymmetrical loop of the U6 snRNA, in which several nucleotides are accessible to chemical modification in the U6 snRNP but are inaccessible to such modification in the naked U6 snRNA. Prp24p binds strongly to the left-hand part of the asymmetrical loop (nucleotides 40–60) and only weakly to the 3'-stem loop in the U6 snRNP. On the contrary, initially a binding of the LSm proteins in the U6 snRNP could not be detected. Interestingly, the 3'-stem loop of the U6 snRNA is strongly contacted by Prp24p when LSm proteins are missing, while, in the presence of both Prp24p and LSm2p-8p the 3'-stem loop assumes a more open conformation. Therefore, we suggest that Prp24p presents the Watson-Crick base pairing positions of the asymmetrical loop. In addition, in cooperation with LSm proteins, Prp24p might be involved in opening up the U6 RNA regions, whereby promoting the formation of stems I and II of the U4/U6 duplex. Interestingly, we find that the open structure of the yeast U6 snRNA in native snRNPs can also be adopted by human U6 and U6atac snRNAs.

A chaperone-like activity of LSm proteins was suggested during the U4/U6 annealing. However, how the LSm proteins interact with Prp24p in U6 snRNPs and how the LSm2p-8p complex is involved in U4 and U6 snRNA base pairing are still unclear. To learn more about how Prp24p and LSm proteins are spatially organised, we used electron microscopy. Depending on whether U6 snRNP particles were chemically fixed prior to electron microscopy sample preparation or not, yeast U6 snRNPs show two different structural configurations: (1) open or (2) a compact close form. Electron microscopy analysis of U6 snRNPs with an open form shows a slightly elongated shape with two distinct substructures. One substructure has a round shape with an accumulation of stain in its centre, which is typical for the LSm heptamer. The second substructure consists of a bundle of smaller domains and contains the other large protein mass of the U6 snRNP, the Prp24p protein. The close form of U6 snRNPs exhibits a more compact structure. Moreover, the two substructures in the close form are hardly discernable probably because the Prp24p protein overlaps the typical ring structure of the LSm proteins. Indeed, such a conformation would allow more interactions between Prp24p and LSm proteins as shown previously by yeast two hybrid analysis. Although the open form derived from unfixed U6 snRNPs shows structural heterogeneity, single particle image analysis revealed much more defined image classes with the fixed particle. This closed form might reflect indeed a biologically relevant state of U6 snRNP in solution. The positions of various LSm proteins were investigated by tagging with genetically introduced yECitrine globular protein. These results showed that the LSm4, -5, -6, -7, and -8 proteins are located at well-defined positions in the LSm ring relative to the Prp24p domain, while LSm2p and -3p are found near the Prp24p domain. Indeed, our cross linking data showed that the Prp24p and the LSm2 protein in the LSm complex contact relatively close nucleotides at the base of the U6 snRNA stem region. This further confirms that LSm2p, eventually with LSm3p, are in close proximity to the Prp24p domain. Our results also confirm the previously proposed order of LSm proteins as 4-8-2-3-5-6-7 in the LSm ring. Our data obtained by electron microscopy analysis of unfixed or fixed U6 snRNP particles suggest that different configurations of open and close forms might have important functional implications. During the transition from close to open form or vice versa, U6 snRNA might undergo further structural rearrangements, which would promote the annealing of the stems I and II of U4/U6 duplex.

INTRODUCTION

The characteristic of eukaryotic protein-coding genes is that RNA molecules are faithfully transcribed as primary transcripts (pre-mRNA) by RNA polymerase II, but then are covalently modified at both their 5'- and 3'-ends in several ways internally to form mature messenger RNA (mRNA). The maturation of pre-mRNA starts by first capping 5'-end of the pre-mRNA. An exogenous guanosine triphosphate is added via 5'-5'-pyrophosphate-bond and subsequently methylated to form m⁷G-cap of the pre-mRNA. Capping occurs almost immediately, after 30 nucleotides of RNA have been synthesized. The 5'-m⁷G-cap will later play a role in the initiation of protein synthesis and seems to protect the growing RNA transcript from degradation.

Secondly, 3'-end of pre-mRNA is altered by a second modification in which the growing transcript is cleaved at a specific site and a **poly-A tail** (100 to 200 residues of adenylic acid) is added by a *poly-A polymerase*.

The most striking feature of eukaryotic genes is that the coding sequences (exons) are interspersed with unexpressed regions (introns) and before transported into cytoplasm, the introns are removed from pre-mRNA and exons must be ligated correctly. This process is called “pre-mRNA splicing” and catalyzed by a multi-mega Dalton ribonucleoprotein complex, “spliceosome”. During the splicing reaction, the spliceosome requires several trans-acting U snRNPs (uridine-rich small nuclear ribonucleoprotein particles) and non-snRNP splicing factors. In addition, the specific interactions between *cis*-acting factors of pre-mRNA and *trans*-acting factors of spliceosome play a critical role for the catalysis reaction of nuclear splicing.

2.1 Chemistry of Splicing Reaction

2.1.1 A Two-Step Mechanism

The removals of intron sequences and the joining the exons of pre-mRNA take place via two stereo specific steps of trans-esterification reactions (Figure 2.1). In the first reaction step of splicing, the 2'-hydroxyl group of the branch site adenosine attacks the phosphodiester bond at the 5'-splice site (5'-SS). This attack

results in cleavage of the 3', 5'-phosphodiester bond at the 5'-splice site and concomitant formation of an unusual 2', 5'-phosphodiester bond between the first nucleotide of the intron and the branch site adenosine.

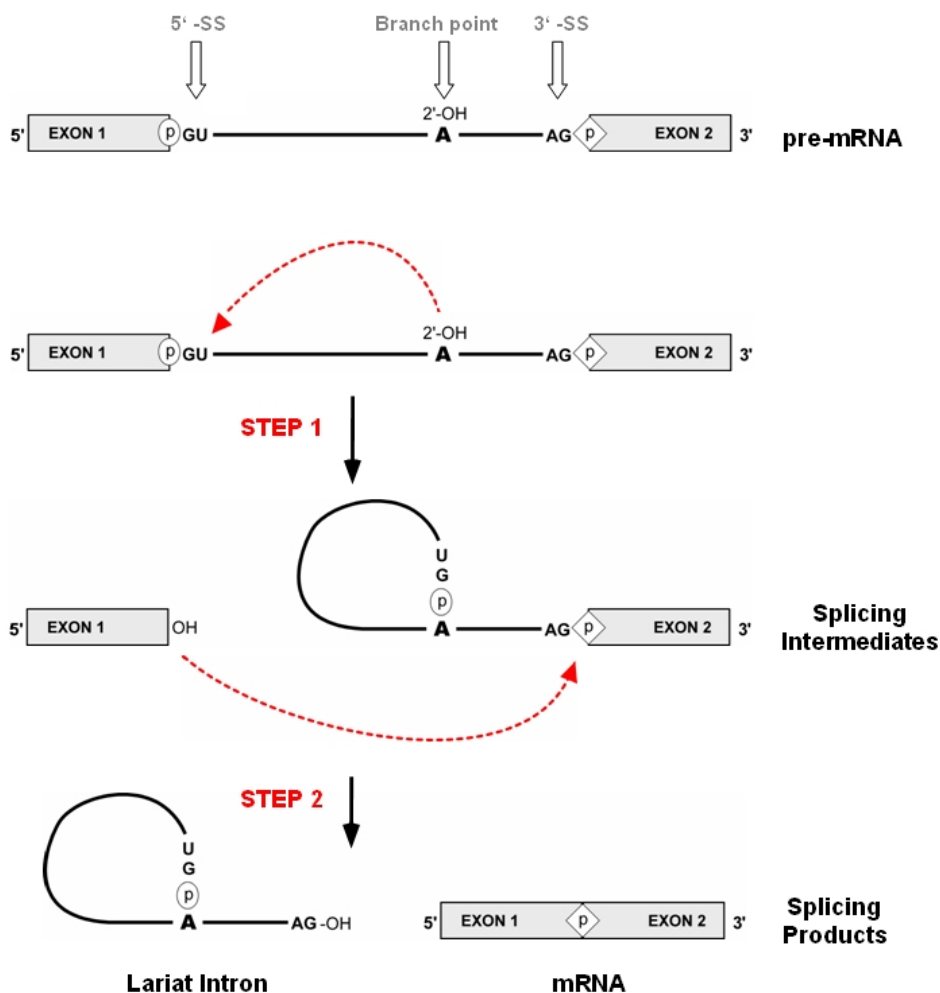


Figure 2.1 Schematic showing of splicing chemistry. In first step, 2'-OH group of branchpoint adenosine makes a nucleophilic attack at the 5'-splice site (5'-SS), resulting in splicing intermediates exon 1 (or 5'-exon) and lariat intron-exon 2 (3'-exon). In second step, the consequential 3'-OH group of exon 1 attacks at the 3'-splice site (3'-SS), causing the formation of splicing products lariat intron and mRNA.

After this reaction, the splicing intermediates, 5'-exon and intron-3'-exon lariat are formed. In the second trans-esterification step, the resulting free 3'-hydroxyl group of the 5'-exon carries out a nucleophilic attack at the 3'-splice site (3'-SS), resulting in ligation of the exons via 3', 5'-phosphodiester bonds and excision of the intron in the form of lariat. Subsequently, the lariat intron is

debranched and degraded whereas the mature mRNA is transported into cytoplasm (Moore *et al.*, 1993; Moore and Sharp, 1993; Nilsen, 1998; Burge *et al.*, 1999).

2.1.2 Splice Site Sequence Requirements

The choice of the splice sites must be determined precisely because an error of even one nucleotide would shift the reading frame in the resulting mRNA molecule and make nonsense of its message. The spliceosome and splicing reaction follow highly pre-defined sequences at splice sites. For recognition of splice sites, so-called *cis*-acting sequence elements of pre-mRNA and *trans*-acting factors of spliceosome play an essential role. Specific factors of spliceosome recognize the *cis*-elements of pre-mRNA and allow the correct trans-esterification of exons. There are four different *cis*-acting sequence elements present in a pre-mRNA (Figure 2.2).

(1) “5′-splice site” in yeast (*Saccharomyces cerevisiae*) is composed of R/GUAUGU (“/” indicates the splice site, “R” is a purine, nucleotides in bold stand for 90 % or higher conservation during evolution, and underlined nucleotides show the beginning of introns). In higher eukaryotes, consensus sequence of 5′-splice site is made of AG/GURAGU and is more variable among the organisms.

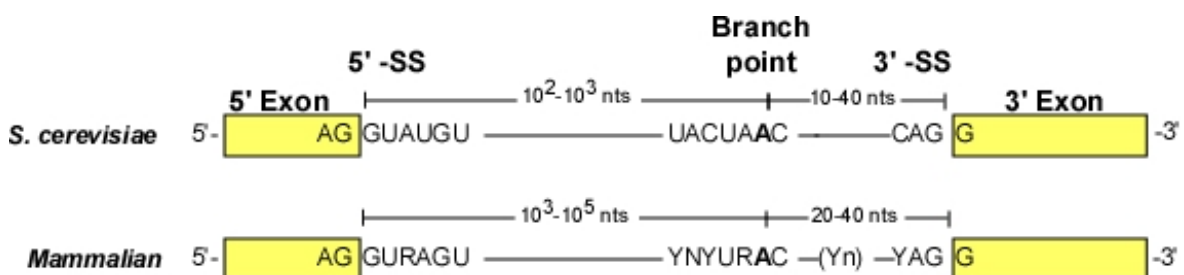


Figure 2.2 Consensus sequences of *cis*-acting intronic sequence elements. Comparison of conserved consensus sequences of intron from *S. cerevisiae* and Mammalian. 5′-SS is 5′-splicing site; 3′-SS is 3′-splicing site. The branch point adenosine is shown in bold. Polypyrimidine tract is represented with “Yn” and purines are shown with “R” and “N” stands for any nucleotide.

(2) “Branch point adenosine” is usually located 18 to 40 nucleotides upstream of the 3′-splice site and embedded in a highly conserved sequence of UACUAACA (underlined nucleotides shows the sited of branch site adenosine). In

higher eukaryotes, the branch site is inserted within YNYURACN sequence (“Y” indicates pyrimidine and “N” is any nucleotide).

(3) “Polypyrimidine tract” is found between branch point adenosine and 3′-splice site and made of 10-15 polypyrimidine nucleotides. It is not a strong *cis*-acting element of yeast pre-mRNA, however, this sequence is more common in mammals than in yeast.

(4) “3′-splice site is found at the end of the introns and consists of **YAG/G** sequence. The end of intron in higher eukaryotes is defined with invariable AG dinucleotide.

The differences in sequence requirements for splicing in yeast and metazoan may be a consequence of the way genes are organized and expressed in two types of organisms. Although a few genes in yeast contain one or two small introns, most are intron-free. In contrast, the majority of higher eukaryotic genes contain multiple introns, which range in size from 30 to several thousand nucleotides. A large number of higher eukaryotic genes also encode transcripts that are differentially spliced. The mechanisms required to accurately remove multiple introns from a single RNA precursor and to regulate cell-specific alternative splicing, may have necessitated greater flexibility in the sequence requirement for RNA splicing in higher eukaryotes.

2.2 Spliceosome Assembly in Yeast

2.2.1 Spliceosome Assembly and Splicing Cycle

The spliceosome cycle was originally described on the basis of the kinetics of appearance of different complexes in splicing reactions *in vitro* and the splicing intermediates and snRNAs that they contained (Konarska and Sharp, 1986; Cheng and Abelson, 1987). The spliceosome assembles in a highly ordered and stepwise manner and during splicing reaction and, pre-mRNA and spliceosome have to achieve several steps (Figure 2.3). First of all, consensus intronic sequences within pre-mRNA must be recognized. Subsequently, pre-mRNA must assume conformation in which ligation of the exons is favourable. As last step, splicing reaction takes place, resulting in excision of introns and production of mRNA.

A large number of *trans*-acting factors during splicing steps interact with the pre-mRNA to form the spliceosome. These factors assemble on pre-mRNA

together with preformed U snRNP particles, which contain, in addition to protein factors, an individual RNA component, called as snRNA (small nuclear RNA). Depending on the snRNA constituent of snRNP, the spliceosomal snRNPs are called as U1-, U2, U5, or U4/U6 snRNP.

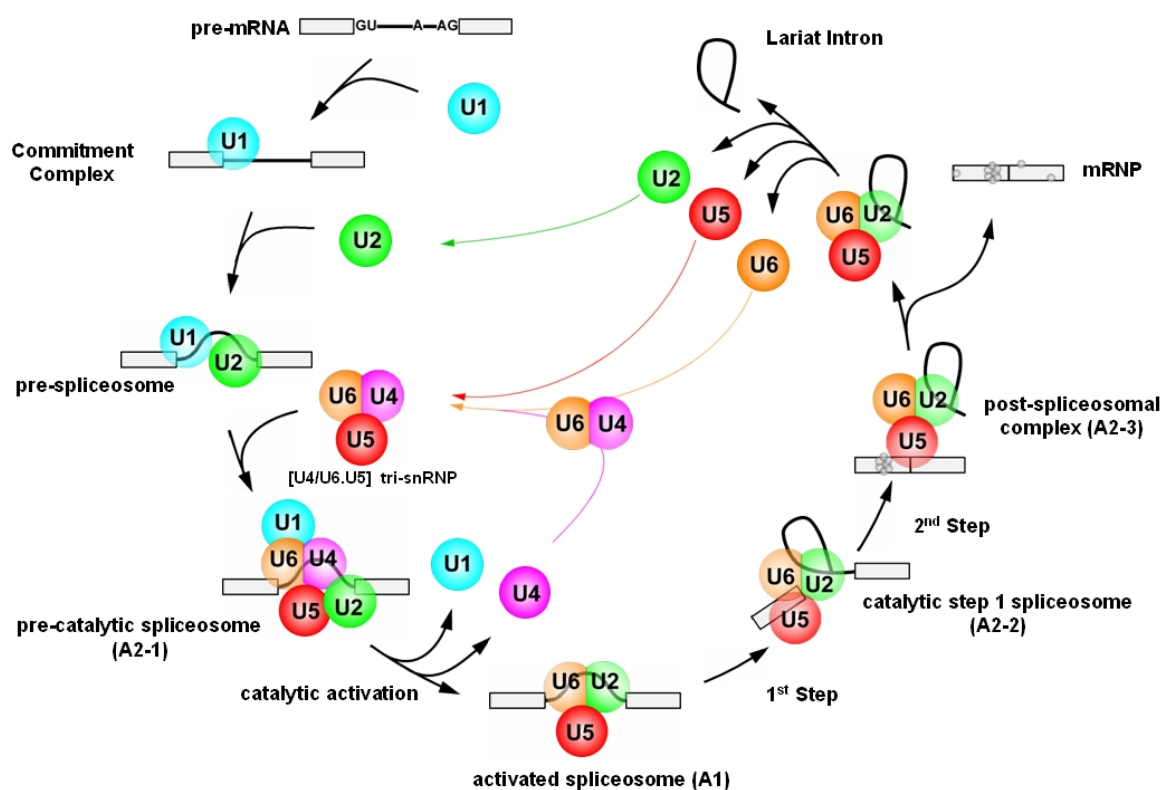


Figure 2.3 [U4/U6.U5] tri-snRNP addition model for spliceosome assembly and splicing cycle. The assembly of spliceosome is a dynamic process, which starts with interaction of U1 snRNP with the 5'-splice site forming commitment complex. Subsequently, U2 snRNP associates with the branchpoint of pre-mRNA to produce pre-spliceosome. After [U4/U6.U5] tri-snRNP joins the pre-spliceosome and, U1- and U4 snRNP particles leave the pre-catalytic spliceosome (A2-1), a catalytically active spliceosome (A1) is generated. After two transesterification steps of splicing reaction, spliceosome disassembles and its components are recycled to join the next round of splicing reaction with a new pre-mRNA (modified according to Staley and Guthrie, 1998).

The earliest even in splicing assembly is the targeting of pre-mRNA that is initiated by the interaction of U1 snRNP with the 5'-splice site, leading to the formation of commitment complex. This interaction involves base pairing between U1 snRNA and the 5'-splice site, and does not require energy. Commitment complex formation is facilitated by U1 snRNP proteins and as well as by interaction

of non-snRNP proteins with pre-mRNA (S raphin and Rosbash, 1989; Heinrichs *et al.*, 1990; Puig *et al.*, 1999; Zhang and Rosbash, 1999; Fortes *et al.*, 1999). In the following step, the U2 snRNP interacts stably with the branch site to generate the pre-spliceosome (Cheng and Abelson, 1987; Konarska and Sharp, 1987). Like the 5'-splice site, the sequence encompassing the branch point adenylate residue is highly conserved in yeast. The branch point sequence is recognized by two non-snRNP splicing factors: bbranch point binding protein (BBP or Bpb1p) and Mud2 protein (Berglund *et al.*, 1997; Berglund *et al.*, 1998). Mud2p is the yeast homolog of the large subunit of human U2AF, which binds to the polypyrimidine tract of pre-mRNA and facilitates the interaction of U2 snRNP with branch point sequence (Valc rcel *et al.*, 1996). After it is bound by BBP, the branch point is recognized by base pairing with U2 snRNA. It is suggested that although the interaction between U2 snRNA and pre-mRNA is independent of energy, stable association of U2 snRNP with the branch point requires ATP (Das *et al.*, 2000).

Next, the [U4/U6.U5] tri-snRNP joins the pre-spliceosome, generating the pre-catalytic spliceosome (A2-1). The [U4/U6.U5] tri-snRNP is formed from U5 snRNP and U4/U6 di-snRNP by a process which is independent from pre-mRNA and requires ATP for assembly (Blach and Pinto, 1989). Recent RNA crosslink studies revealed an early interaction of [U4/U6.U5] tri-snRNP with the 5'-splice site while the U1 snRNP is bound there but prior to the binding of the U2 snRNP to the branch point (Maroney *et al.*, 2000). This U2-independent interaction of [U4/U6.U5] tri-snRNP at the 5'-intron occurs via U5 snRNP-specific Prp8 protein, and unlike commitment complex formation, requires ATP.

In a subsequent step, major structural rearrangements occur that lead to the formation of catalytically activated spliceosome (A1). During this step, the base pairing between U4- and U6-snRNA is unwound (Madhani and Guthrie, 1992) and, as a result, U4 snRNA dissociates. For the catalytic activation of spliceosome, beside dissociation of U4 snRNA, U1 snRNA must be displaced from the 5'-splice site, which should next form base pairing interactions with U6 snRNA.

After formation of activated spliceosome, the two trans-esterification steps of splicing reaction can take place in the following A2-2 and A2-3 complexes. After completion of splicing reaction, the spliceosome dissociates, releasing the mRNA and excised intron, as well as the U snRNPs. The intron-lariat is degraded into its nucleotides and U snRNP components of spliceosome are recycled to take part in new rounds of splicing. After the snRNPs are released from spliceosome,

they are dissociated to single particles and the pre-spliceosomal multi-snRNP complexes are reassembled. U4- and U6 snRNA reassociate to form U4/U6 di-snRNP. Next, U5 snRNP can join U4/U6 di-snRNP to form new [U4/U6.U5] tri-snRNP particles.

2.2.2 Properties and Structures of Spliceosomal U snRNAs

The RNA constituents within spliceosomes are named as uridine-rich small nuclear RNAs or shortly U snRNAs since they are rich in uracil bases. There are five different spliceosomal U snRNAs present in cell nucleus: U1-, U2-, U4-, U5-, and U6 snRNA (Table 2.1 and Figure 2.4). In yeast, two isoforms of U5 snRNA exist: U5L (U5 long) and U5S (U5 short). The shorter U5S snRNA is the cleavage product of the longer U5L snRNA (Chanfreau *et al.*, 1997).

U snRNAs in yeast		U snRNAs in human	
U snRNA	Length (nts)	U snRNA	Length (nts)
U1	568	U1	164
U2	1175	U2	187
U4	160	U4	145
U5L	214	U5	116*
U5S	179	(-)	(-)
U6	112	U6	106

Table 2.1 Length of U snRNAs in yeast and human. Asterisk indicates that there are more than 10 isoforms of U5 snRNA, which are not shown explicitly in the table.

With the exception of U6 snRNA, all the other spliceosomal snRNAs are transcribed by RNA polymerase II and they acquire at their 5'-end a cap structure, which is composed of a 2,2,7-trimethylguanosine (m_3G) (Reddy and Busch, 1988). The specific m_3G -cap structure of snRNAs is recognized by a monoclonal anti- m_3G -antibody (Bochnig *et al.*, 1987), allowing purification of U snRNP particles by immuno affinity chromatography (Kastner and Lührmann, 1999). On the other hand, U6 snRNA is transcribed by RNA polymerase III and has been shown to carry a γ -mono-methyl phosphate cap at its 5'-end (Singh and Reddy, 1989).

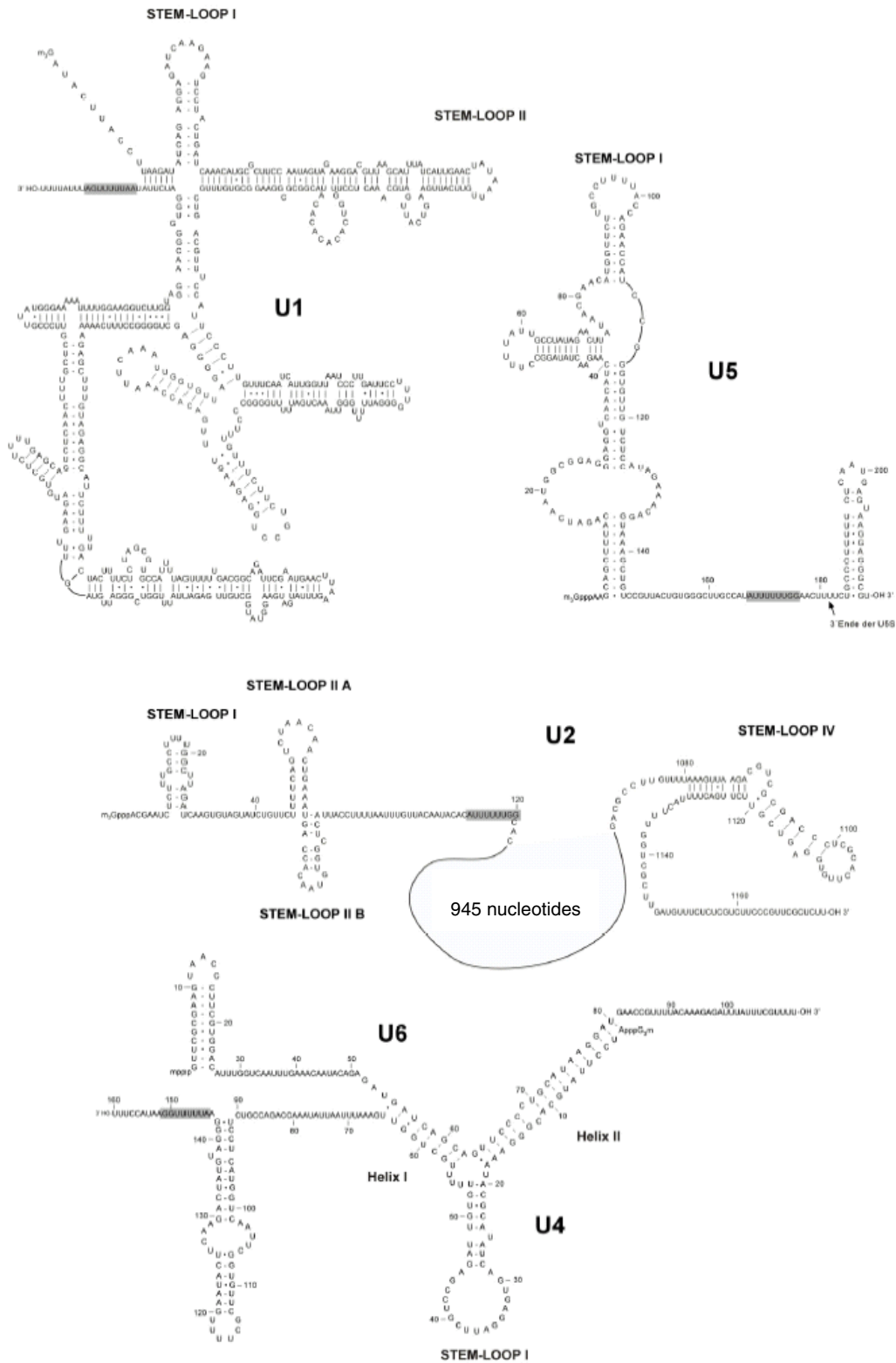


Figure 2.4 Primary sequences and proposed secondary structures of yeast U snRNAs. U snRNAs assume conserved secondary structures with single stranded regions and stem loops. The binding region of Sm proteins is shown with a grey bar.

Sequencing of various U snRNAs isolated from a wide variety of cells and organisms has revealed extensive conservation of the snRNA sequences. The essential parts of U snRNAs, in particular, are also conserved in their secondary structures (Brow and Guthrie, 1988; Guthrie and Patterson, 1988). The primary sequence of certain snRNA regions are even 100 % conserved. With few exceptions, these highly conserved regions are mostly single-stranded in the secondary structure models, and involve in base pair interactions or function as protein-binding sites. Among snRNAs, yeast U4 and U6 are virtually identical in size to their mammalian counterparts. Nonetheless, the U4 snRNAs share only limited regions of primary sequence homology.

In contrast, the U6 snRNAs can be aligned almost perfectly throughout their length; there is more than 60 % similarity over the full length of yeast and mammalian U6. The similarity of U4 and U6 snRNAs among organisms is even more pronounced when the base pairing interaction between U4 and U6 snRNAs is compared. The so called Y-shaped secondary structure of U4/U6 di-snRNA is highly conserved between yeast and man. U5 snRNAs vary in size over a two-fold range, from 214 nucleotides in yeast to 116 nucleotides in human. Similar to U4/U6 snRNA, the secondary structure of U5 snRNA shows strong conservation. The size variation of U1 and U2 snRNAs is by far the greatest for the spliceosomal snRNAs between yeast and higher eukaryotes. Both snRNAs from yeast are much longer and they contain extensive highly structured insertions as compared to their human equivalents. The functional studies showed that these yeast-specific regions of U1 and U2 snRNAs are not essential *in vivo* and are not required in the course of splicing reaction (Igel and Ares, 1988; Siliciano *et al.*, 1991).

2.2.3 Protein Composition of Spliceosomal U snRNPs

Spliceosome is composed of U snRNP particles and non-snRNP splicing factors. Biochemical comparisons of the various snRNP species have revealed two classes of snRNP proteins: those which are common to all species and those which are associated with a given snRNP particle or complex.

U1-U5 spliceosomal snRNAs each bind seven common “Sm” proteins, designated B/B', D₁, D₂, D₃, E, F, and G. These seven common proteins form a heptameric ring (Kambach *et al.*, 1999). Unlike other spliceosomal snRNAs, U6 snRNA binds a homologous group of seven “LSm” (like Sm) proteins, designated 2-8. The LSm proteins form a doughnut-shaped structure in the absence of U6 snRNA

in mammals (Achsel *et al.*, 1999).

In addition, each snRNA binds a group of snRNP-specific proteins. In yeast, many of these proteins are named as “Prp” proteins, implying their function in pre-mRNA processing (Table 2.2). Like their RNA counterparts, both common and particle specific snRNP proteins appear to be evolutionarily conserved, suggesting that they play an important role in snRNP function. It is very likely that these proteins account for the appearance of several discrete forms of the spliceosomal snRNPs.

Recent studies in yeast have shown the presence of a pre-assembled protein NTC complex (Nineteen Complex) associated with Prp19. NTC complex is suggested to join spliceosome after U1- and U4 snRNAs are dissociated and is required for stabilizing both U5- and U6 snRNA interactions with pre-mRNA (Chan *et al.*, 2003). In yeast, NTC is composed of at least 8 proteins: Prp19p, Ntc20p, Ntc25p, Isy1p, Syf1p, Syf2p, Syf3p, and Cef1p, as well as several other proteins: Cwc2p, Ecm2p, Prp45p, Cwc1p, and Sad1p (Chen *et al.*, 2002).

In addition to the snRNP proteins listed in Table 2.2, there are other splicing proteins required for RNA structural transitions in pre-mRNA splicing. Most notable of these proteins belong to a family of DExD/H-box RNA helicases (Tanner and Linder, 2001; reviewed in Brow, 2002). Although two transesterifications reactions of splicing result in no net change in the number of phosphoester bonds, at several points in the splicing cycle ATP must be hydrolyzed and at each of these steps a DExD/H-box RNA-dependent helicase is required.

Other non-snRNP splicing factors comprise the two pre-mRNA binding proteins Bbp1 and Mud2p, the two cap binding proteins Cbc1p and Cb2p, and five other proteins: Aar2p, Exo84p, Prp17p, Slu7p, and Spp2p.

Proteins	Homo sapiens					Saccharomyces cerevisiae					Proteins
	U1	U2	U5	U4/U6	U4/U6.U5	U1	U2	U5	U4/U6	U4/U6.U5	
B/B'	●	●	●	●●	●●	●	●	●	●●	●●	B
D1	●	●	●	●●	●●	●	●	●	●●	●●	D1
D2	●	●	●	●●	●●	●	●	●	●●	●●	D2
D3	●	●	●	●●	●●	●	●	●	●●	●●	D3
E	●	●	●	●●	●●	●	●	●	●●	●●	E
F	●	●	●	●●	●●	●	●	●	●●	●●	F
G	●	●	●	●●	●●	●	●	●	●●	●●	G
70K	●					●					Snp1
A	●					●					Mud1p
C	●					●					yU1-C
						●					Nam8
						●					Prp39
						●					Prp40
						●					Prp42
						●					Snu56
						●					Snu71
						●					Luc7
A'		●					●				Lea1
B''		●					●				Yib9
SF3a120		●					●				Prp21
SF3a66		●					●				Prp11
SF3a60		●					●				Prp9
SF3b155		●					●				Hsh155
SF3b145		●					●				Cus1
SF3b130		●					●				Rse1
SF3b49		●					●				Hsh49
p14		●					●				Snu17
SF3b14b		●					●				Rds3p
SF3b10b		●									
SPF30		●									
SPF31		●									
hPrp43		●					●				Cus2
220K			●		●			●		●	Prp8
200K			●		●			●		●	Brr2
116K			●		●			●		●	Snu114
102K			●		●				●	●	Prp6
100K			●		●			●			Prp28
52K			●					●			Snu40
40K			●		●						
15K			●		●			●		●	Dip1
90K				●	●				●	●	Prp3
61K				●	●				●	●	Prp31
60K				●	●				●	●	Prp4
20K				●	●						
15.5K				●	●				●	●	Snu13
110K					●					●	Snu66
65K					●					●	Prp38
										●	Snu23
										●	Spp381
27K					●						

Table 2.2 Protein components of the yeast (*S. cerevisiae*) and the human (*H. sapiens*) spliceosomal U snRNPs. Each section represents the U snRNP containing the snRNA(s) listed at the top. Proteins listed below show the U snRNP particle specific proteins from yeast and human homologues according to Brow, 2002 and Will *et al.*, 2002.

2.3 U6 snRNA Participates in Several Important RNA:RNA Rearrangements

As described above, assembly of the spliceosome is a highly dynamic process. During the steps of the spliceosome and catalysis of splicing, the U snRNPs undergo several precisely coordinated changes in composition and structure. This is particularly true for the U6 snRNP. In yeast, U6 snRNA is present in 5- to 10-fold excess over U4 snRNA and when not associated with U4 snRNA, is found in a mono-U6 snRNP particle (Hamm and Mattaj, 1989; Bordonné *et al.*, 1990). Before joining spliceosome, the U6 snRNA in mono-U6 snRNP particle must base pair with the U4 snRNA to form the U4/U6 di-snRNP (Figure 2.5). During this step, U6 snRNP undergoes a dramatic rearrangement in its secondary RNA structure. First, nucleotides of U6 snRNA that form intramolecular 3'-stem-loop (in yeast, U6 nucleotides 64-80) must be separated and positioned for base pairing with the U4 snRNA (in yeast, U4 nucleotides 1-18) to yield stem II of the U4/U6 interaction domain.

Similarly, the U6 snRNA nucleotides upstream of the 3'-stem-loop (in yeast, U6 nucleotides 55-62) base pair with the U4 snRNA (in yeast, U4 nucleotides 57-63), forming stem I of the U4/U6 duplex in the di-snRNP (Fortner *et al.*, 1994; Wolff and Bindereif, 1993). In the subsequent step, the U4/U6 di-snRNP associates with the U5 snRNP, to form [U4/U6.U5] tri-snRNP, which enters the pre-spliceosome. The addition of the [U4/U6.U5] tri-snRNP to the spliceosome triggers further RNA:RNA rearrangements, which lead to the conversion of the fully assembled pre-catalytic spliceosome into its catalytically active form (Brow, 2002; Nilsen, 2003; Staley and Guthrie, 1998).

In the active spliceosome, both stems of the U4/U6 interaction are disrupted and the U4 snRNA is released. The stem II region of U6 snRNA, once released from U4 snRNA, folds on itself to form an intramolecular stem-loop. The stem I region of U6 snRNA, once freed, base pairs with the U2 snRNA. Another major rearrangement, in which U6 snRNA is involved, is the complete displacement of U1 snRNA. After U1 snRNA is released, U6 snRNA establishes a new base pairing with the 5'-splice site. After splicing, the spliceosome dissociated and the released individual U4, U6 and U5 snRNPs are incorporated into new U4/U6 di-snRNPs and [U4/U6.U5] tri-snRNPs in preparation for the next round of splicing.

2.4 The Features of mono-U6 snRNP Particle

The mono-U6 snRNP particle from yeast consists of the U6 snRNA and eight proteins: the specific protein Prp24p, and, unlike other spliceosomal U snRNPs, a set of seven Sm-like core proteins (LSm2p, LSm3p, LSm4p, LSm5p, LSm6p, LSm7p and LSm8p) (Stevens *et al.*, 2001; see Table 2.2).

2.4.1 Core LSm proteins of the U6 snRNP

LSm proteins are known to have structural similarities to the previously characterized Sm family of proteins. A set of seven Sm proteins (Sm B/B', D₁, D₂, D₃, E, F, and G) form a heteroheptameric complex, found in a single-stranded regions of spliceosomal U1, U2, U4 and U5 snRNAs. X-ray crystallographic studies of two heterodimeric of Sm polypeptides (B/D₃ or D₁/D₂) revealed that the Sm proteins contain an Sm fold, which consists of two short stretches of conserved amino acids, named as Sm motifs 1 and 2 that are separated by a variable region (Hermann *et al.*, 1995).

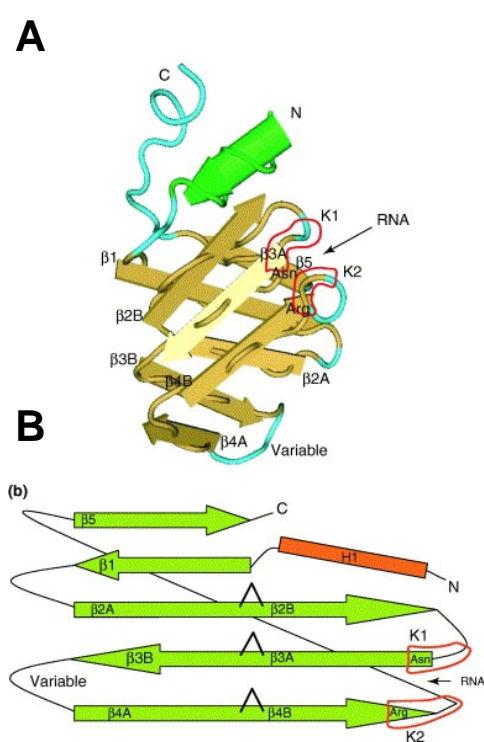


Figure 2.6 Structure of the Sm fold and model of the Sm ring. (A) and (B) shows the crystal structure of the Sm fold. The K1 and K2 are the RNA binding pockets which are labelled and outlined in red. The position of highly conserved Asp37 and Arg67 within RNA binding pockets is also shown. The model of the Sm ring (C) is shown. The positions $\beta 4$ and $\beta 5$ strands that interact between neighbouring subunits are also noted (Adapted from Khusial *et al.*, 2005).

The Sm fold is an oligonucleotide-binding barrel with a helix stacked on top (Kambach *et al.*, 1999; Figure 2.6 A and B). The oligonucleotide-binding barrel

consists of an N-terminal α -helix followed by a five-stranded anti parallel β -sheet. The first and fifth of β -strands are short and the second, third, and fourth of which are longer and bent. A loop between β 4- and β 5-strand closes the barrel. The loops between strands β 2 and β 3 and between β 4 and β 5 look toward the ring and form a nucleotide binding pocket. The α -helix and β 1-, β 2-, and β 3-strands form the Sm 1 motif. β 4 and β 5 strands appear in a second shorter sequence, called Sm 2 motif.

Based on the structures of the Sm polypeptides and biochemical data about how the polypeptides interact, a model for the Sm core complex in which seven Sm proteins formed a seven-membered ring was suggested by Kambach *et al.* [1999]. In this model (Figure 2.6 C), Sm subunits in the ring contact each other via an anti parallel interaction between the backbone of the second half of β 4- and β 5-strands and Sm ring contains a small central aperture. Indeed, electron microscopy analysis of purified human spliceosomal snRNPs confirmed a ring-shaped Sm structure with 8 nm diameter (Kastner *et al.*, 1990; Stark *et al.*, 2001).

The Sm ring assembly requires the presence of single stranded Sm site (AAUUUxUGG) within the U1, U2, U4, and U5 snRNAs (Urlaub *et al.*, 2001). Genetic, biochemical, and structural studies imply the order of the subunits in the heteroheptameric Sm ring as D₃, B, D₁, D₂, F, E, and G (Urlaub *et al.*, 2001; Stark *et al.*, 2001; Figure 2.6 C). Cross linking studies with the Sm rings to their bound RNA revealed that the Sm site binds to the Sm ring with the adenosine nucleotide bound to the SmE subunit and wraps around the central ring aperture with the guanosine nucleotide bound to the SmF subunit.

Homology searches revealed the existence of a large family of Sm-like (LSm) proteins, called LSm1p to LSm16p, which all share the Sm fold (Figure 2.7). Of the LSm proteins, LSm1p to LSm7p were shown to function during mRNA degradation in the cytoplasm. LSm2p to LSm8p were demonstrated to interact with U6 snRNA (Pannone *et al.*, 1998; Mayes *et al.*, 1999; Salgado-Garrido *et al.*, 1999; He and Parker, 2000). LSm10 and LSm11 proteins specifically bind to the U7 snRNA (Schumperli and Pillai, 2004). LSm12-16 proteins contain long C-terminal tails and associated methyltransferases (Albrecht and Lengauer, 2004).

(Figure 2.8 A; Achsel *et al.*, 1999). Sequence comparisons between open reading frames of Sm and LSm proteins proposed an order of LSm proteins in the LSm ring: LSm4823657, assuming the same arrangement as in the Sm complex (SmD₃BD₁D₂FEG) (Figure 2.8 B; Fromont-Racine *et al.*, 1997; Salgado-Garrido *et al.*, 1999). This arrangement is to some extent supported by genetic studies in yeast (Panone *et al.*, 2001) and by FRET analyses in human cells (Ingelfinger *et al.*, 2002).

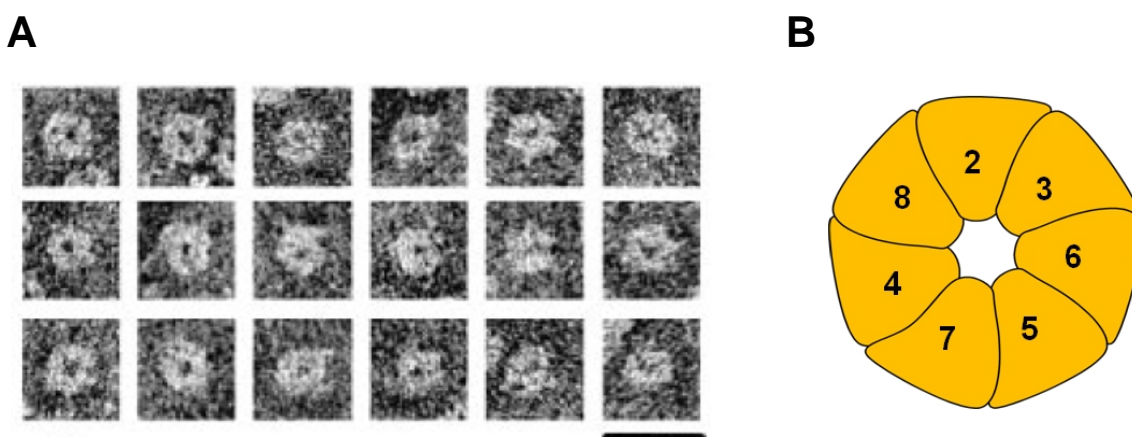


Figure 2.8 Structure of LSm ring. (A) Electron microscopy analysis of human LSm ring. The bar represents 20 nm (Adapted from Achsel *et al.*, 1999). (B) Proposed order of LSm proteins in the LSm ring.

In both yeast and human, LSm2p-8p complex binds to a uridine-rich sequence at the 3'-end of U6 snRNA (Achsel *et al.*, 1999; Mayes *et al.*, 1999; Vidal *et al.*, 1999). In human U6 snRNA, 12 nucleotides of 3'-terminus were found to be necessary and sufficient for binding to the LSm proteins, and tract of five uridines at the 3'-end was shown to be an important determinant for this binding (Achsel *et al.*, 1999). In contrast, in yeast U6 snRNA, the last 18 nucleotides at the 3'-terminus are necessary but not sufficient for U6 binding of the LSm core (Vidal *et al.*, 1999).

LSm2p-8p complex was suggested to have a chaperone-type function in facilitating multiple rearrangements of splicing complexes during pre-mRNA splicing (Achsel *et al.*, 1999; Verdona *et al.*, 2004). After splicing and spliceosome dissociation, LSm2p-8p seems to facilitate the annealing of U4- and U6 snRNPs, in order to regenerate U4/U6 di-snRNPs and [U4/U6.U5] tri-snRNPs for the next round. In yeast, some of the LSM genes are essential for viability, but *lsm1Δ*, *lsm6Δ* and

lsm7Δ cells are viable although growth is temperature-sensitive (Mayes *et al.*, 1999). Yeast extract prepared from *lsm6Δ* and *lsm7Δ* cells were found unable to continue splicing when challenged with additional pre-mRNA (Verdone *et al.*, 2004). These results further support the idea that LSm2p-8p proteins function as a chaperone complex in modifying RNA:RNA and RNA-protein interactions, in cooperation with Prp24p.

2.4.2 Prp24p: A Spliceosomal Recycling Factor

Prp24p is an essential yeast U6 snRNP protein and was first identified by genetic suppression studies in yeast as a protein involved in the U4/U6 annealing (Shannon and Guthrie, 1991). Later studies showed that recombinant Prp24p stimulates the formation of U4/U6 di-snRNA from *in vitro* U4 and U6 snRNA transcripts, but the annealing rate is not as efficient as the base pairing of U4 and U6 snRNPs in cell extracts by recombinant Prp24p (Ghetti *et al.*, 1995; Raghunathan and Guthrie, 1998). It has been suggested that Prp24p cooperates with the LSm protein complex in U4/U6 base pairing (Achsel *et al.*, 1999; Vidal *et al.*, 1999; Verdone *et al.*, 2004).

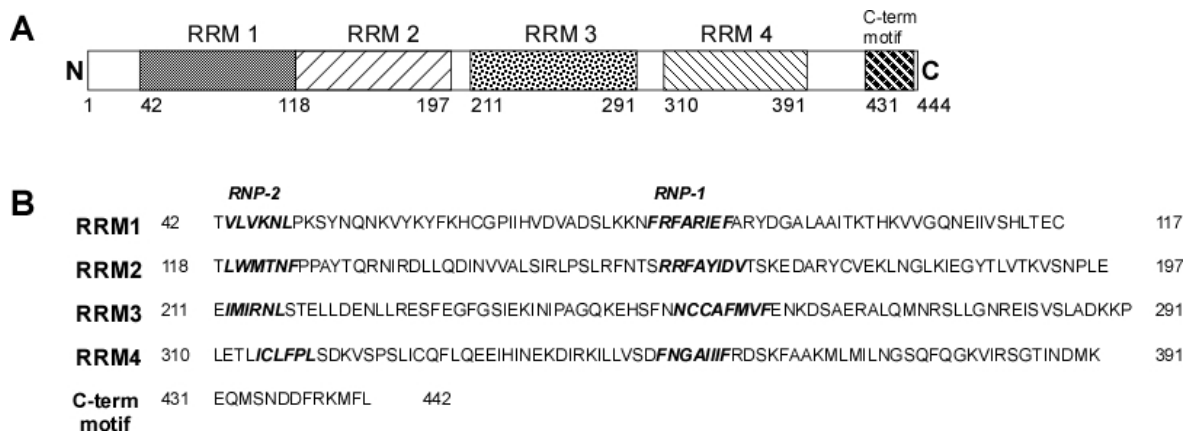


Figure 2.9 Motifs of yeast Prp24p. (A) Schematic diagram of the primary structure Prp24p. The RNA recognition motifs (RRMs) and C-terminal LSm recognition motif are shown as shaded boxes. RRM 1 and RRM 2 overlap by one amino acid, residue 118. (B) Amino acid sequence of Prp24p RRM1-4 and C-terminal LSm recognition motif. The sites of RNP-1 and RNP-2 are indicated in italics.

Yeast Prp24p contains four RNA recognition motifs (RRMs 1-4) and a highly conserved 12 amino acids at its C-terminus (Rader and Guthrie, 2002; Figure 2.9).

The functions of all four RRMs in yeast Prp24p are not known. Extragenic suppressors of the mutations in U6 snRNA showed that RRMs 2 and 3 of Prp24p may interact with U6 snRNA in mono-U6 snRNP (Vidaver *et al.*, 1999). Mutations in RRM 1 has no effect on the viability of yeast cells whereas mutagenesis of RRM 4 resulted in temperature sensitivity, suggesting that beside RRMs 2 and 3, RRM 4 is also important for Prp24p function (Vidal *et al.*, 1999; Rader and Guthrie, 2002). However, when RRM 1 is deleted, recombinant Prp24p cannot discriminate between wild-type and mutant U6 snRNA sequences *in vitro*, suggesting that RRM 1 might be required for specific binding of Prp24p to U6 snRNA (Kwan and Brow, 2005). Interestingly, the mutations in RRMs 1 and 4 of Prp24p shifted the U4/U6 di-snRNA equilibrium *in vitro* towards U6 snRNA, suggesting a model that RRMs 2 and 3 stabilizes U6 snRNA whereas RRMs 1 and 4 may bind U4 snRNA *in vitro* and bring it into close proximity with U6 snRNA (Rader and Guthrie, 2002).

The C-terminal motif is required for Prp24p-LSm interaction. Two-hybrid studies with the full-length recombinant Prp24p showed that Prp24p interacts with subunits of the LSm ring (Fromont-Racine *et al.*, 2000). However, in mutant Prp24 protein without C-terminal motif, two-hybrid interactions between Prp24p and LSm proteins are abolished, most strikingly the interaction with LSm5p, LSm7p and LSm8p. Furthermore, the deletion of C-terminal motif leads to a significant decrease in U4/U6 levels *in vivo*, suggesting that the interaction of Prp24p with the LSm proteins, mediated by the C-terminal motif promotes U4/U6 base pairing (Rader and Guthrie, 2002).

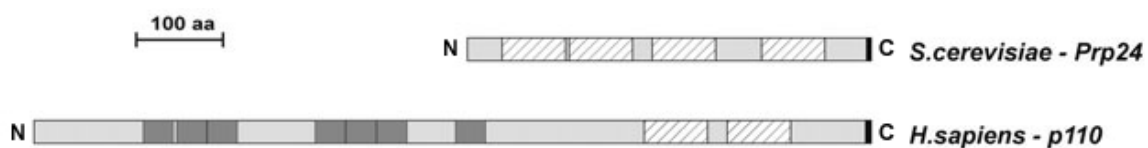


Figure 2.10 Conserved domain structures of the yeast (*S.cerevisiae*) Prp24p and human p110. The proteins are aligned with respect to their C-terminal ends. Stripped boxes are the RRMs and dark grey boxes show TPR motifs. C-terminal LSm interaction motif is indicated with a small black box (Adapted from Bell *et al.*, 2002).

Recently, a 110-kDa protein (p110 or SART3) was identified in the mammalian system as a protein distantly related to yeast Prp24p. In its C-terminal

half, the human p110 contains two RRM domains and a C-terminal LSM interaction motif (Figure 2.10; Bell *et al.*, 2002). Comparing the RRM domains between both proteins showed that, the two RRM domains of human p110 correspond to RRM domains 2 and 3 in the yeast Prp24p. The large N-terminal region of p110 carries seven tetratricopeptide repeat (TPR) domains, which have no counterpart in yeast Prp24p. The human p110 associates with U6 and U4/U6 snRNPs, but is absent from both [U4/U6.U5] tri-snRNPs and spliceosome. It is shown to be functionally related to yeast Prp24p and can greatly enhance the reassociation of the U4 and U6 snRNAs, as well as U4_{atac} and U6_{atac} snRNAs (Bell *et al.*, 2002; Damianov *et al.*, 2004).

Chemical modification studies with U6 snRNPs, enriched from yeast extracts by glycerol gradient centrifugation, showed that Prp24p binds directly to nucleotides 40-43 of the U6 snRNA (Shannon and Guthrie, 1991; Jandrositz and Guthrie, 1995). Recent *in vitro* binding experiments suggested that the primary binding site on the U6 snRNA of a C-terminally truncated form of Prp24p may lie within residues 45-58 (Kwan and Brow, 2005). Human p110 binds mainly to residues 38-57 of human U6 snRNA and residues 10-30 of the U6_{atac} snRNA (Bell *et al.*, 2002; Damianov *et al.*, 2004). These are the regions of U6 and U6_{atac} snRNAs conserved from yeast to human.

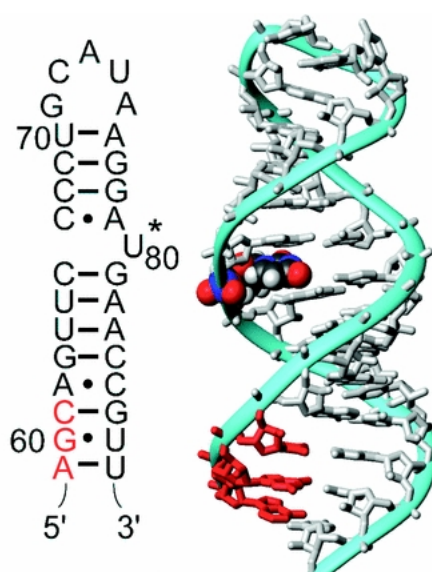
Although both Prp24p and p110 share conserved binding sites on their corresponding U6 snRNAs, it is still an open question whether they function in the same way. The human U6 snRNA fails to function in yeast extracts (Fabrizio *et al.*, 1989) and furthermore, human p110 is not able to complement mutations or deletion of Prp24p in yeast (Rader and Guthrie, 2002). The interesting absence of the TPR domains in yeast Prp24p may be responsible for the likely functional difference(s) between two proteins.

2.4.3 Structure of U6 snRNA in mono-U6 snRNP

Several secondary structures of the yeast U6 snRNA, based on genetic experiments and structure probing of partially purified U6 snRNPs have been suggested (Fortner *et al.*, 1994; Vidaver *et al.*, 1999; Jandrositz and Guthrie, 1995; Ryan *et al.*, 2002). The early structure proposed for U6 snRNA in yeast mono-U6 snRNP contains RNA with at least three intramolecular helices: the 5'-, central-, and 3'-stem loops (Figure 2.11 A). A recent model suggested that two distant regions of the U6 snRNA (positions 38-43 and 86-95) have the potential to base pair and form an intramolecular RNA duplex, called the telestem (Ryan *et al.*, 2002;

or may function as protein-recognition sites (Legault *et al.*, 1998). Additionally, a readily protonated C67-⁺A79 wobble pair adjacent to the metal binding site at U80 is present. Metal ion binding in that region is modulated by the protonation of N1 of adenine in the C-A wobble pair (Huppler *et al.*, 2002). The unprotonated state of A79 favours metal ion binding, and metal ion binding, in turn, lowers the pK_a , which results in a significant conformational change in the U6 3'-stem. At higher pH values, U80 stacks above the unprotonated A79 base. At lower pH values, U80 is flipped out of the helix and the protonated A79 base stacks upon U80 (Reiter *et al.*, 2004).

Figure 2.12 Solution structure of the yeast U6 3'-stem loop (ISL). The structure has an overall 1.4 Å resolution. The Watson-Crick paired regions adopt standard A-form helical geometry. The internal loop contains a C67-⁺A79 wobble base pair and harbours a metal binding site at U80. The GCAUA pentaloop adopts a GNR(N)A-type fold. Metal binding site is indicated with an asterisk. The AGC triad is given in red. The U80 nucleotide is shown as a space-filling model (Adapted from Butcher and Brow, 2005).



The structure of naked human U6 snRNA was obtained by theoretical calculations of maximal base pairing and by chemical and enzymatic probing (Mougin *et al.*, 2002; Harada *et al.*, 1980). The structure of the human U6 snRNA is very compact and consists of 3'-stem loop of similar length (Figure 2.13 A). The existence of an internal loop was predicted (Rinke *et al.*, 1985) and appears to be analogue to the loop adopted by yeast U6 snRNA.

Likewise, sequence of U6_{atac} snRNA, which is associated with the AT-AC minor spliceosome, exhibit some similarity to the U6 snRNAs from other organisms and can be folded into a similar secondary structure (Figure 2.13 B). In particular, over 30 nucleotides in its central region, U6_{atac} is identical above 80 % to all other U6 snRNAs.

light on the mechanism whereby Prp24p and the LSm complex facilitate U4/U6 base pairing, the U6 snRNA and proteins interactions in the U6 snRNP were thoroughly characterized by chemical structure probing, UV-cross linking, and hydroxyl radical footprinting. Using RNA structure probing techniques, we demonstrate that within the U6 snRNP a large internal region of the U6 snRNA is unpaired and contacted by Prp24p. On the other hand, the 3'-stem loop is not bound strongly by U6 proteins in native particles. Thus, our data suggest that the combined association of Prp24p and LSm proteins confers upon U6 nucleotides a conformation favourable for U4/U6 base pairing.

A chaperone-like activity of LSm proteins was suggested during the U4/U6 annealing. However, how the LSm proteins interact with Prp24p in U6 snRNPs and how the LSm2p-8p complex is involved in U4 and U6 snRNA base pairing are still unclear. To learn more about how Prp24p and LSm proteins are spatially organised, both unfixed and chemically fixed U6 snRNP particles were investigated by electron microscopy. The unfixed U6 snRNP particles reveal an open form with two substructures: a round ring-like LSm domain and a more angular Prp24p domain. Unlike unfixed U6 snRNPs, chemically fixed U6 particles exhibit a close form, where two substructures observed by unfixed U6 particles, can be hardly distinguished. Interestingly, statistical image analysis of both forms of the U6 snRNP showed that the close form in the fixed U6 snRNP contain a more uniformly defined structure, which in turn suggests that the close form might indicate a biologically relevant configuration of U6 snRNPs. To investigate the positions of LSm protein entities, we developed a novel method where each individual LSm protein was genetically tagged at its C-terminus with a 30 kDa globular γ ECitrine protein. Labelling of LSm proteins with γ ECitrine protein showed that the arrangement of the LSm proteins relative to the Prp24p domains is not random. Moreover, it can be predicted that the Prp24p domain is linked to the LSm ring at well-defined positions where LSm2p and LSm3p are located. Our data also confirm the proposed arrangement of the LSm proteins (4-8-2-3-5-6-7) in the LSm ring.

MATERIALS and METHODS

5.1 Materials

5.1.1 Chemicals

Acetic acid	Merck, Darmstadt
Acetone	Merck, Darmstadt
Acetonitrile	Merck, Darmstadt
Acrylamide solutions (ready to use)	Roth, Karlsruhe
Rotiphorese gel 30 (30 % Acrylamide, 0.8 % Bis-acrylamide, 37.5:1)	
Rotiphorese gel 40 (40 % Acrylamide/Bis-Acrylamide, 29.1:0.9)	
Agarose electrophoresis grade	Invitrogen, Netherlands
Ammonium bicarbonate	Merck, Darmstadt
Ammonium peroxydisulfate (APS)	Merck, Darmstadt
Bacto-Agar	Difco, USA
Bacto-peptone	B&D, USA
Boric acid	Merck, Darmstadt
Bovine serum albumine (BSA)	Boehringer, Mannheim
Bradford-Assay Solution	Bio-Rad, Munich
Bromophenol blue	Merck, Darmstadt
Cacodylic acid	Fluka, Switzerland
Calcium chloride	Merck, Darmstadt
Calmodulin beads	Stratagene, USA
Coomassie Brilliant Blue R 250	Serva, Heidelberg
1-cyclohexyl-3-(2-morpholinoethyl)	
carbodiimide metho-p-toluene sulfonate (CMCT)	Sigma, Taufkirchen
α -cyano-4-hydroxy-cinnamic acid	Sigma, Taufkirchen
DNA-size marker	Roth, Karlsruhe
Dimethylsulfoxide (DMSO)	Roth, Karlsruhe
Dimethylsulfate (DMS)	Fluka, Switzerland
1,4-dithiothreitol (DTT)	Merck, Darmstadt
D-(+)-monoglucose	Merck, Darmstadt
DOBA powder	Q-Biogene, USA
Dodecyl sulfate sodium salt (SDS)	Merck, Darmstadt

EDTA (ethylene diamine-N,N,N',N'- tetraacetic acid)	Roth, Karlsruhe
EGTA (ethylene glycol bis(2-amoniethyl)-tetraacetic acid)	Roth, Karlsruhe
Ethanol	Merck, Darmstadt
Ethidium bromide (10mg/ml)	Roth, Karlsruhe
β -ethoxy- α -ketobutyral aldehyde (kethoxal, KE)	Research Organic Inst.
Ficoll 400,000	Sigma, Taufkirchen
Formaldehyde	Merck, Darmstadt
Formamide	Merck, Darmstadt
Glutaraldehyde 25 % aqueous solution	EM Sciences
Glycerol	Merck, Darmstadt
Glycin	Merck, Darmstadt
Glycoblue	Ambion, Frankfurt
HEPES (N-[2-hydroxyethylpiperazine-N'-2-ethane sulfonic acid], free acid)	Roth, Karlsruhe
Hydrochloric acid	Merck, Darmstadt
IgG Sepharose 6 Fast flow	Pharmacia, Freiburg
Imidazole	Merck, Darmstadt
Iodoacetamide	Merck, Darmstadt
L-amino acids	USB, Cleveland, Ohio
LB-Agar	BIO 101, USA
LB-Medium	BIO 101, USA
Lithium acetate	Sigma, Taufkirchen
Methanol	Merck, Darmstadt
Milk powder	Prema, Radolfzell
2-Mercaptoethanol	Roth, Karlsruhe
Ni-NTA-Agarose	Qiagen, Hilden
Nitrocellulose	Merck, Darmstadt
Nonidet P-40 (NP-40)	Fluka, Switzerland
Phenol	Roth, Karlsruhe
Phenol/chloroform/isoamyl alcohol (25:24:1)	Roth, Karlsruhe
Potassium hyroxide	J T Baker
Potassium chloride	Merck, Darmstadt
Polyethylene glycol (PEG) 3350	Sigma, Taufkirchen
Protein (pre)-stained molecular weight marker	Bio-Rad, USA
Phenyl- methyl- sulfonylfluorid (PMSF)	Roche, Mannheim
Protein-A-Sepharose CL-4B (PAS)	Pharmacia, Freiburg
Salmon sperm DNA (10mg/ml)	Stratagene, USA
Siliconized glass beads	Supeka
Silver nitrate	Merck, Darmstadt

Sodium acetate	Merck, Darmstadt
Sodium carbonate	Merck, Darmstadt
Sodium chloride	Merck, Darmstadt
Sodium citrate	Merck, Darmstadt
Sodium hydrogen carbonate	Merck, Darmstadt
<i>di</i> -Sodium hydrogen phosphate	Merck, Darmstadt
Sodium phosphate	Merck, Darmstadt
Sodium thiosulfate pentahydrate	Merck, Darmstadt
TEMED (N,N,N',N'-tetramethylethylene diamine)	Sigma, Taufkirchen
tri-Fluoro acetic acid	Fluka, Switzerland
Tris-(hydroxymethyl)aminomethan	Roth, Karlsruhe
Triton X-100	Sigma, Taufkirchen
tRNA (from <i>Escherichia coli</i>)	Boehringer, Mannheim
Tween 20	Sigma, Taufkirchen
Urea	Merck, Darmstadt
Yeast extract	BD, USA
Xylene cyanol FF	Sigma, Taufkirchen

5.1.2 Antisera and monoclonal Antibodies

anti-Rabbit Peroxidase	Dianova, Hamburg
HA-Tag Polyclonal Antibody	BD, USA
Living Colors YFP Monoclonal Antibody	BD, USA
anti-Prp24p rabbit-antiserum	Dr. C. Guthrie, USA
Peroxidase-antiperoxidase complex (PAP)	Sigma, Taufkirchen

5.1.3 Enzymes and Enzyme Inhibitors

AMV Reverse Transcriptase	USB, Cleveland, Ohio
Pfu DNA Polymerase (2.5 U/ μ l)	Stratagene, USA
Aprotinin	Serva, Heidelberg
Benzamidine	Serva, Heidelberg
Chymostatin	Serva, Heidelberg
Complete™ Protease Inhibitor Tablets, EDTA-free	Roche, Mannheim
Leupeptin	Serva, Heidelberg
Pepstatin A	Serva, Heidelberg
Taq DNA Polymerase	Dep. of Lührmann
Klenow enzyme	Stratagene, USA
Proteinase K	Sigma, Taufkirchen
Restriction Enzymes	NEB, Schwalbach

RNasin (RNase inhibitor; 40 U/ μ l)	Promega, USA
RNase A (1 μ g/ μ l)	Ambion, USA
RNase T1 (1 U/ μ l)	Ambion, USA
RQ DNase I (1 U/ μ l)	Promega, USA
TEV Protease, Recombinant (10 U/ μ l)	Invitrogen, Netherlands
Trypsin	Invitrogen, Netherlands
T4 polynucleotide kinase	NEB, Schwalbach
T7 RNA polymerase	Dep. of Lührmann

5.1.4 Nucleotides

Nucleoside-5'-triphosphate (100 mM) (ATP, CTP, GTP, UTP)	Pharmacia, Freiburg
Deoxynucleoside-5'-triphosphate (100 mM) (dATP, dCTP, dGTP, dTTP)	Pharmacia, Freiburg
di-Deoxynucleoside-5'-triphosphate (100 mM) (ddATP, ddCTP, ddGTP, ddTTP)	Pharmacia, Freiburg
Radionucleotide:	
[α - ³² P] UTP	Pharmacia, Freiburg
[α - ³² P] dATP	Pharmacia, Freiburg
[γ - ³² P] ATP	Pharmacia, Freiburg

5.1.5 DNA Oligonucleotides

Oligo <i>PRP24</i>	Description	Sequence
1	For_ Oligo_TAP	5'-CAAGAGCAGATGTCCAACGACGATTTTCGCAA ATGTTTCTAGGTGAGTCCATGGAAAAGAGAAG-3'
2	Rev_ Oligo_TAP	5'-CTAAAATGACATCCTATTAGAAGTTCGTCCTT CTCCGGTTCGGTTAGTACGACTCACTATAGGG-3'
3	For_check_oligo_ <i>PRP24</i>	5'-CACTCAGTATACGGCTTCCC-3'
4	Rev_check_oligo_ <i>PRP24</i>	5'-CTTGGGTTTATATCACTGC-3'

Oligo <i>LSM2</i>	Description	Sequence
5	For_ Oligo_ <i>LSM2</i> _YFP	5'- GCTACAAGACGCTACCAGAAGGGAGGTAATGAC TGAAAGAAAAGGTGACGGTGCTGGTTA-3'
6	Rev_ Oligo_ <i>LSM2</i> _YFP	5'-AAAATAATGAGAAAAAATGCCATGAGGATAGA CTGCATAATTCGATGAATTCGAGCTCG-3'
7	For_check_oligo_ <i>LSM2</i>	5'-TAGTTGACCAAGAAGTGGTC-3'
8	Rev_check_oligo_ <i>LSM2</i>	5'-CCATGAGGATAGACTGACTA-3'

Oligo LSM3	Description	Sequence
9	For_ Oligo_LSM3_YFP	5'-CTCTAATCAGCACGCCCTCTGAAGATGACGAT GGCGCAGTGGAGATAGGTGACGGTGCTGGTTA-
10	Rev_ Oligo_LSM3_YFP	5'-AATAAAAAAATACGTACTGTTCCCTTTGTTTT TCCTCCTTTGCTCGATGAATTCGAGCTC-3'
11	For_check_oligo_LSM3	5'-CATCACGCACACTCAAGAAA-3'
12	Rev_check_oligo_LSM3	5'-ATCAGATTGGCTCCTCCTT-3'

Oligo LSM4	Description	Sequence
13	For_ Oligo_LSM4_YFP	5'-CCGTCCAACATCATTTAACAGCTCTTCTCCAC AAAAGGTCGAATTTGGTGACGGTGCTGGTTA-3'
14	Rev_ Oligo_LSM4_YFP	5'-GTACCAATATATTTATATATGTACATAATTATT ATACAAAATTTGTTTCGATGAATTCGAGCTC-3'
15	For_check_oligo_LSM4	5'-AATGCTGAGAGCAGTAAAGC-3'
16	Rev_check_oligo_LSM4	5'-CACCAGAAAGTCAACCTGTA-3'

Oligo LSM5	Description	Sequence
17	For_ Oligo_LSM5_YFP	5'-TTGCCATCCTGTGCCAGGCGGCAAAAAGACC CCTACGGAGGCGTGGGTGACGGTGCTGGTTA-3'
18	Rev_ Oligo_LSM5_YFP	5'-TATTTTTTTAGATGCACTATACAAATTCGCGT TAATTTTGCCTTTTCGATGAATTCGAGCTCG-3'
19	For_check_oligo_LSM5	5'-TGAGTCTACCGGAGATTTG-3'
20	Rev_check_oligo_LSM5	5'-AATGAATTGTACGGTGCGA-3'

Oligo LSM6	Description	Sequence
21	For_ Oligo_LSM6_YFP	5'-TCTTTTGGAGGGGCACGCAGGTCATGTATATCA GTGAACAAAAAATAGGTGACGGTGCTGGTTA-3'
22	Rev_ Oligo_LSM6_YFP	5'-AACCAACTTGCTCATTCTACATATAATCCAT TAGAGGAGATAAGTTCGATGAATTCGAGCTGCTCG- 3'
23	For_check_oligo_LSM6	5'-ATGCCAAATAAGCAACGTCG-3'
24	Rev_check_oligo_LSM6	5'-GTGCTAAACTCGCAAAGTCA-3'

Oligo LSM7	Description	Sequence
25	For_ Oligo_LSM7 YFP_HA	5'-TCTCTTAAAGTCCGCCGAAGGTTCTGATGTAC TATATATGCAAAAAGGTGACGGTGCTGGTTA-3'
26	Rev_ Oligo_LSM7 YFP_HA	5'-TTTTCAACTGTAAGGAAGGGAGTTATATGAGA TTATATTAAACTCGATGAATTCGAGCTCG-3'
27	For_check_oligo_LSM7	5'-CGCATGTACGTGTATACTAC-3'
28	Rev_check_oligo_LSM7	5'-TTCAACTGTAAGGAAGGGAG-3'

Oligo LSM8	Description	Sequence
29	For_ Oligo_LSM8_YFP	5'-CGAAAATGAGCATGTAATATGGGAAAAAGTGTAC GAATCAAAGACAAAAGGTGACGGTGCTGGTTA-3'
30	Rev_ Oligo_LSM8_YFP	5'-ATTATTATTATTATTATTATTATTACTATT ATTGCAACTATATCGATGAATTCGAGCTCG-3'
31	For_check_oligo_LSM8	5'-ATGTCAGCCACCTTGAAGA-3'
32	Rev_check_oligo_LSM8	5'-CGTGACGGGTAATGCTTAA-3'

Oligo PRP24 overexpression	Description	Sequence
37	For_ Oligo_PRP24_exp	5'-CCTGGGATCCATGGAGTA TGGACATCACGCTAGACC-3'
38	Rev_ Oligo_PRP24_exp	5'-GCGGCCGGGTACCCTACT CACCTAGAAACATCTGCG-3'

Oligo Primer extension	Description	Sequence
39	yU6 94_112	5'-AAAACGAAATAAATCTCT-3'
40	yU6 68_84	5'-GTTTCATCCTATGCAGG-3'

5.1.6 Bacteria and Yeast Strains

Name	Genotype	Description
HB101	<i>supE44, hsdS20 (r_B⁻ m_B⁻)recA13, ara-14, proA2, lacY1, galk2, rpsL20, xyl-5, mtl-1, leuB6, thi-1</i>	a general host for plasmids that do not contain α -complementation
Rosetta	F ⁻ <i>ompThsdS_B (r_B⁻ m_B⁻) gal dcm lacY1, pRARE2² (C_M^R) pAR5615 (A_P^R)</i>	a general host for recombinant protein expression, which supplies tRNAs for AGG, AGA, AUA, CUA, CCC, GGA codons on a compatible chloramphenicol-resistant plasmid
TR2 α	MAT α , <i>trp1-Δ1, his3-Δ, ura3-52, lys2-801, ade2-101</i>	haploid MAT α , dissected from TR1 a/a (Sikorski und Hieter, 1989)
YRK3	MAT α , <i>trp1-Δ1, his3-Δ, ura3-52, lys2-801, ade2-101, PRP24::TAP Tag-TRP1, C-term</i>	haploid yeast strain like TR2 α , in which TAP tag was inserted at the C-terminus of PRP24 using plasmid pBS1479 (this study)

YEK1	MATa, <i>trp1-Δ1</i> , <i>his3- Δ</i> , <i>ura3-52</i> , <i>lys2-801</i> , <i>ade2-101</i> , <i>PRP24::TAP Tag-TRP1</i> , C-term, <i>LSM7::yECitrine-3HA Tag-Sp HIS5</i> C-term	haploid yeast strain like YRK3, in which yECitrine-3HA tag was inserted at the C-terminus of <i>LSM7</i> using plasmid pKT239 (Elif Karagöz)
YRK10	MATa, <i>trp1-Δ1</i> , <i>his3- Δ</i> , <i>ura3-52</i> , <i>lys2-801</i> , <i>ade2-101</i> , <i>PRP24::TAP Tag-TRP1</i> , C-term, <i>LSM7::yECitrine-3HA Tag-Sp HIS5</i> C-term, <i>LSM2::yECitrineTag-Ca URA3</i> C-term	haploid yeast strain like YRK3 and YEK1, in which yECitrine tag was inserted at the C-terminus of <i>LSM2</i> and yECitrine-3HA tag was inserted at the C-terminus of <i>LSM7</i> using plasmid pKT175 and pKT239 (this study)
YRK11	MATa, <i>trp1-Δ1</i> , <i>his3- Δ</i> , <i>ura3-52</i> , <i>lys2-801</i> , <i>ade2-101</i> , <i>PRP24::TAP Tag-TRP1</i> , C-term, <i>LSM4::yECitrineTag-Ca URA3</i> C-term	haploid yeast strain like YRK3, in which yECitrine tag was inserted at the C-terminus of <i>LSM4</i> using plasmid pKT175 (this study)
YRK12	MATa, <i>trp1-Δ1</i> , <i>his3- Δ</i> , <i>ura3-52</i> , <i>lys2-801</i> , <i>ade2-101</i> , <i>PRP24::TAP Tag-TRP1</i> , C-term, <i>LSM8::yECitrineTag-Ca URA3</i> C-term	haploid yeast strain like YRK3, in which yECitrine tag was inserted at the C-terminus of <i>LSM8</i> using plasmid pKT175 (this study)
YRK14	MATa, <i>trp1-Δ1</i> , <i>his3- Δ</i> , <i>ura3-52</i> , <i>lys2-801</i> , <i>ade2-101</i> , <i>PRP24::TAP Tag-TRP1</i> , C-term, <i>LSM5::yECitrineTag-Ca URA3</i> C-term	haploid yeast strain like YRK3, in which yECitrine tag was inserted at the C-terminus of <i>LSM5</i> using plasmid pKT175 (this study)
YRK15	MATa, <i>trp1-Δ1</i> , <i>his3- Δ</i> , <i>ura3-52</i> , <i>lys2-801</i> , <i>ade2-101</i> , <i>PRP24::TAP Tag-TRP1</i> , C-term, <i>LSM6::yECitrineTag-Ca URA3</i> C-term	haploid yeast strain like YRK3, in which yECitrine tag was inserted at the C-terminus of <i>LSM6</i> using plasmid pKT175 (this study)
YRK16	MATa, <i>trp1-Δ1</i> , <i>his3- Δ</i> , <i>ura3-52</i> , <i>lys2-801</i> , <i>ade2-101</i> , <i>PRP24::TAP Tag-TRP1</i> , C-term, <i>LSM2::yECitrineTag-Ca URA3</i> C-term	haploid yeast strain like YRK3, in which yECitrine tag was inserted at the C-terminus of <i>LSM2</i> using plasmid pKT175 (this study)
YRK17	MATa, <i>trp1-Δ1</i> , <i>his3- Δ</i> , <i>ura3-52</i> , <i>lys2-801</i> , <i>ade2-101</i> , <i>PRP24::TAP Tag-TRP1</i> , C-term, <i>LSM3::yECitrineTag-Ca URA3</i> C-term	haploid yeast strain like YRK3, in which yECitrine tag was inserted at the C-terminus of <i>LSM3</i> using plasmid pKT175 (this study)

5.1.7 Plasmids

Plasmid	Description
pBS1479	Shuttle vector containing TAP tag; ARS, CEN; Amp ^R , <i>K.I. TRP1</i> (Bertrand Séraphin)
pRS314	Shuttle vector containing ARS, CEN; Amp ^R , <i>TRP1</i> (Sikorski and Hieter, 1989)
pRS315	Shuttle vector containing ARS, CEN; Amp ^R , <i>HIS5</i> (Sikorski and Hieter, 1989)
pRS316	Shuttle vector containing ARS, CEN; Amp ^R , <i>URA3</i> (Sikorski and Hieter, 1989)
pKT239	Shuttle vector, pFA6a, containing yECitrine-3HA tag; ARS, CEN; Amp ^R , <i>S.p. HIS5</i> (Sheff and Thorn, 2004)
pKT175	Shuttle vector, pFA6a, containing yECitrine tag, ARS, CEN; Amp ^R , <i>C.a. URA3</i> (Sheff and Thorn, 2004)
pUC18-T7 U1 cod. reg.	coding region of U1 snRNA cut with HindIII/EcoRI, for Random-Primer- Labelling; Dep. of Lührmann, Dr. P. Fabrizio
pUC18-T7 U2 cod. reg.	coding region of U2 snRNA cut with PstII/XhoI, for Random-Primer- Labelling; Dep. of Lührmann, Dr. P. Fabrizio
pUC18-T7 U4 cod. reg.	coding region of U4 snRNA cut with EcoRI/BamHI, for Random-Primer- Labelling; Dep. of Lührmann, Dr. P. Fabrizio
pUC18-T7 U5 cod. reg.	coding region of U5 snRNA cut with PvuII, for Random-Primer- Labelling; Dep. of Lührmann, Dr. P. Fabrizio
pETM-11	pBR322 based vector, containing N _{term} -His ₆ -tag, TEV protease site; <i>f1 ori</i> ; Kan ^R (G. Stier, EMBL, Heidelberg)
pETM-42	pBR322 based vector, containing N _{term} -His ₆ -MBP-tag, TEV protease site; <i>f1 ori</i> ; Kan ^R (G. Stier, EMBL, Heidelberg)
pETM-60	pBR322 based vector, containing N _{term} -NusA-His ₆ -tag, TEV protease site; <i>f1 ori</i> ; Kan ^R (G. Stier, EMBL, Heidelberg)
pRK-1	pETM-11 vector, containing N _{term} -His ₆ -tag-TEV protease site- <i>PRP24</i> (this study)
pRK-3	pETM-42 vector, containing N _{term} -His ₆ -MBP-tag-TEV protease site- <i>PRP24</i> (this study)
pRK-5	pETM-60 vector, containing N _{term} -NusA-His ₆ -tag-TEV protease site- <i>PRP24</i> (this study)

5.1.8 General Buffers and Solutions

<u>10 x TBE</u>	<u>RNA-loading buffer</u>	<u>Protein-loading dye</u>
0.89 M Tris	1 x TBE	60 mM Tris/ HCl pH 6.8
0.89 M Boric acid	50 % Formaldehyde	1 mM EDTA
25 mM EDTA pH 8.0	0.1 % (w/v) Bromophenolblue	16 % Glycerol
	0.1 % (w/v) Xylane cyanol	2 % (w/v) SDS
		0.1 % (w/v)
		bromophenolblue
		50 mM DTT

5.1.9 Kits

ABI PRISM™ Dye Desoxy Cycle Sequencing Kit	Applied Biosystems
ECL Western Blot Detection Kit	Pharmacia, Freiburg
GFX-PCR DNA and Gel Band Purification Kit	Pharmacia, Freiburg
Expand Long Template PCR Mix	Roche, Mannheim
Prime It II Random Primer Labeling Kit	Stratagene, USA
QIAquick Gel Extraction Kit	Qiagen, Hilden
QIAfilter Mini and Maxi Preparation Kit	Qiagen, Hilden

5.1.10 Working Materials

Dialysis Membranes MCW 6000-8000 Da	Spektrapor, USA
NylonMembrane Hybond N+ or XL	Pharmacia, Freiburg
Parafilm	Roth, Karlsruhe
Pipettes	Eppendorf, Hamburg
ProbeQuant™ G-50 Micro Columns	Pharmacia, Freiburg
Protran Nitrocellulose Membrane	Schleicher, Dassel
X-ray film Kodak Biomax	Kodak, USA
Siliconized object slide	ICN Biomedicals, Ohio
0.8 x 4-cm Poly-Prep columns	Bio-Rad, USA
Cassettes for film exposure	Kodak, USA
Whatman 3MM Paper	Whatman Paper, U.K.
10-well multitest slides	ICN Biomedicals, Ohio

5.1.11 Instruments

ABI PRISM 310 Genetic Analyser	Applied Biosystems
Autoclaves	H+PLabortechnik, Munich

DNA Thermocycler (PCR)	Hybaid Omni Gene,U.K.
Gel Documentation	Bio-Rad, Munich
Gel Electrophoresis Devices	MPI-BPC
Gel Dryer Model 583	Bio-Rad, Munich
Gradient Master Model 106	BioCamp Instruments
Head-over-Tail Rotor	Cole-Parmer, USA
pH-Meter	Mettler, Switzerland
Phosphorimager Typhoon 8600	Molecular Dynamics
Developing machine X-Omat	Kodak, USA
Sorvall Rotors (SLC 6000, SS34, T865, T647.5, TH-660)	Kendro, USA
French press	MPI bpc
Power supplies	Pharmacia, Freiburg
Spectrophotometer Ultrospec 3000 pro	Pharmacia, Freiburg
Speed Vac concentrator 5301	Eppendorf, Hamburg
UV-Lamps, 254nm	Bachhofer
UV-Stratalinker 2400	Stratagene, USA
Desktop centrifuges with and without cooling	Heraeus, Hanau
Ultracentrifuges	Sorvall; Kendro, USA

5.2 Methods

5.2.1 Proteinbiochemistry Standard Methods

5.2.1.1 Concentration Determination of Proteins

The concentration of the proteins was determined by the method of Bradford (Bradford *et al.*, 1976). The protein probes were diluted up to 800 μ l in water and 200 μ l of Bradford-solution was added. After incubation for 10 min at room temperature, the absorption of the samples at 595 nm was measured by a spectrophotometer. To determine the concentrations of the samples, BSA solutions with known concentrations were used.

5.2.1.2 Phenol-Chloroform-Isoamylalcohol Extraction

The Phenol-Chloroform-Isoamylalcohol extraction (PCI-extraction) was used for separating proteins from nucleic acids. The solution was extracted with the same volume of PCI-solution and very well mixed. To separate the aqueous and

organic phases, the suspension was centrifuged for 5 min at room temperature and 13 000 rpm. The upper aqueous phase containing nucleic acids were precipitated by the addition of 1/10 Vol. 3 M NaOAc pH 5.2 and 2.5 Vol. with ethanol (abs). In the case of too low amounts of RNA, 15-30 μg of glycoblu was added. The lower organic phase containing proteins were precipitated with 5 Vol. of cold-acetone. Both nucleic acids and proteins were incubated overnight at -20°C or at least one hour at -80°C . Subsequently, they were precipitated for 20 min at 4°C and 13 000 rpm. The pellet was washed with 70 % (v/v) Ethanol and precipitated again as above mentioned. The pellet was finally dried under vacuum and resuspended in an appropriate buffer.

PCI-extraction solution

50 % (v/v) Phenol

48 % (v/v) Chloroform

2 % (v/v) Isoamylalcohol

equilibrated with TE-buffer

TE-buffer pH 7.5

10 mM Tris/HCl pH 7.5

1 mM EDTA

5.2.1.3 Proteinase K Digestion

All proteinase K digestions were done at 1% (w/v) SDS, 7.5 mM EDTA, and $1\mu\text{g}/\mu\text{l}$ proteinase K concentrations. Reaction was incubated for 30 min at 37°C . RNA was extracted by PCI-extraction and precipitated.

5.2.1.4 Denaturing Polyacrylamide Gel Electrophoresis (SDS-PAGE)

To separate total proteins from each other, denaturing SDS-polyacrylamide gel electrophoresis was performed according to Laemmli (1970). Depending on the resolution, the size of the gels was varied. 12 % or the case may be 10 % polyacrylamid gels (37.5:1) with high TEMED concentration (0.33 % v/v) were prepared. Protein samples were dissolved in an appropriate volume of protein loading buffer and denatured at 96°C for 5 min before loading on gel. Gels were run vertically in SDS-PAGE running buffer until bromophenol blue dye reached the bottom of the gel. The protein bands were visualized by either Coomassie or by silver staining.

Stacking-Gel Buffer (4 x)

500 mM Tris/HCl pH 6.8
0.4 % (w/v) SDS

Separating-Gel Buffer (4 x)

1.5 M Tris/HCl pH 8.8
0.4 % (w/v) SDS

SDS-PAGE running buffer

25 mM Tris-HCl, pH 6.8
192 mM Glycine
1 % (w/v) SDS

5 % Stacking-Gel Solution (per 10 ml)

1.7 ml Roti Gel 30 (30:0.8; Acr:Bis-Acry)
2.5 ml 4 x Stacking-Gel Buffer
50 μ l 10 % (w/v) APS & 25 μ l TEMED

10 % Separating-Gel Solution (per 30 ml)

10 ml Roti Gel 30 (30:0.8; Acr:Bis-Acry)
7.5 ml 4 x Separatory-Gel Buffer
100 μ l 10 % (w/v) APS
100 μ l TEMED

12 % Separating-Gel Solution (30 ml)

12 ml Roti Gel 30
7.5 ml 4 x Separatory-Gel Buffer
100 μ l 10 % (w/v) APS
100 μ l TEMED

5.2.1.5 Western Blot Analysis

Western blot analysis was performed according to very well-known protocols (Burnette, 1981). After performing high-TEMED SDS-polyacrylamide gel electrophoresis, proteins were transferred on a nitrocellulose membrane by wet-blotting. The transfer was carried out at least for 2 h at 70 V and for proteins bigger than 250 kDa, the time was prolonged up to 3 h. Before incubating with antibodies, the nitrocellulose membrane after the transfer was blocked in 5 % (w/v) milk powder-TBS-Tween for 1 h at room temperature or over night at 4 °C. Then, the membrane was washed twice with TBS-Tween shortly, once for 15 min, and twice for 5 min. After incubating with primary antibody, the membrane was washed again with TBS-Tween as above mentioned. Next, the membrane was incubated with 1:50 000 diluted secondary anti-Rabbit antibodies which are coupled to peroxidase. After repeated washing steps, the development was performed by enhanced chemiluminescence (ECL) following manufacturer's instructions.

Western blotting-buffer

1.5 L SLAB 4
0.6 L Methanol
0.9 L ddH₂O

SLAB 4 (per 5 L)

30 g Tris/HCl
142.6 g Glycin
5 gr SDS

TBS-Tween

20 mM Tris/HCl pH 7.5

150 mM NaCl

0.1 % Tween-20

5.2.1.6 Coomassie Staining of Protein Gels

Coomassie Brilliant Blue R-250 is an aminotriarylmethane dye that forms strong but not covalent complexes with proteins, most probably by a combination of *van der Waals* forces and electrostatic interactions with NH_3^+ groups. Coomassie staining of protein gels was performed according to protocol from Sambrook *et al.*, 1989. After running SDS-polyacrylamide gel, it was stained with coomassie staining solution for 30 min at room temperature and subsequently destained with destaining solution at room temperature until protein bands were clearly visible. The gel was scanned and then transferred on a Whatmann paper and dried at 80°C for 1 hour.

Coomassie Staining Solution

40 % (v/v) Methanol

10 % (v/v) Acetic Acid

1 % (w/v) Coomassie Brilliant Blue R-250

Destaining Solution

40 % (v/v) Methanol

10 % (v/v) Acetic Acid

5.2.1.7 Silver Staining of Protein Gels

Staining SDS-Polyacrylamide with silver solutions relies on differential reduction of silver ions that are bound to the side chains of amino acids. Silver staining is ~100-1000-fold more sensitive than staining with Coomassie Brilliant Blue and capable of detecting as little as 0.1-1.0 ng of polypeptide in a single band. Silver staining of protein gels was performed according to protocol from Blum *et al.*, 1987. During the procedure, all the solutions were 10 times of the gel volume and all steps were performed on a shaker. The protein gel was first fixed in 50 % methanol/ 12 % acetic acid solution at least for 30 min or over night. After fixation, the gel was washed twice with 50 % ethanol following and once with 30 % ethanol for 20 min each. This step is necessary in order to avoid decomposition of thiosulfate and subsequent Ag_2S formation. The gel was then treated with 0.8mM $\text{Na}_2\text{S}_2\text{O}_3$ for exactly 60 seconds, and immediately washed three times with ddH₂O to remove the thiosulfate from the surface. After that, it was incubated with 0.012 M AgNO_3 / 0.026 % formaldehyde solution for 20 min. The stained gel, then, washed

three times with ddH₂O. The gel was treated shortly with 0.56 M Na₂CO₃, 0.0185% formaldehyde, 16 μM Na₂S₂O₃ solution to remove excess silver from the surface of the gel. The solution was changed; the gel was developed in the same solution until protein bands could be seen. The developing was stopped with 50 % methanol/ 12 % acetic acid solution and then replaced by 5% acetic acid. The gel was scanned and then transferred on a Whatmann paper and dried at 80°C for 1 hour.

5.2.2 Molecular Biology Standard Methods

5.2.2.1 Concentration Determination of Nucleic Acids

The absorption of DNA or RNA aqueous solutions was measured by spectrophotometer at 260 nm and 280 nm by using a blank solution, which usually contains the buffer where nucleic acids were resuspended. The concentration was then calculated using pre-determined absorption values according to Sambrook *et al.*, 1989. The ratio of OD₂₆₀ / OD₂₈₀ determined the purity of the nucleic acid solution, which was 2.0 for pure RNA or oligonucleotides, and 1.8 for pure DNA. The lower ratios showed protein contamination, which has to be removed by PCI-extraction.

1 OD₂₆₀ = 50 μg/ml double-stranded DNA

1 OD₂₆₀ = 33 μg/ml single-stranded DNA

1 OD₂₆₀ = 40 μg/ml single-stranded RNA

3.2.2.2 Agarose Gel Electrophoresis of Nucleic Acids

The agarose gel electrophoresis of nucleic acids was performed according to standard protocol from Sambrook *et al.*, 1989. Depending on the size of the nucleic acid fragments, the concentration of the agarose was varied between 1.0 % and 2.0 %. For detection, agarose gel contained 0.5 μg/ml (w/v) ethidium bromide and nucleic acids were separated horizontally at 100-150 V in 1 x TBE buffer. The bands were visualized with UV-light at 254 nm.

<u>Agarose gel solution</u>	<u>Agarose gel loading buffer (5 x)</u>
1 x TBE	30 % (w/v) Glycerol
1.0-2.0 % (w/v) Agarose	5 mM EDTA
0.5 µg/ml (w/v) ethidium bromide	0.25 % (w/v) Bromophenolblue
	0.25 % (w/v) Xylene Cyanol FF

Migration Rates of the Marker Dyes through Agarose Gels		
Agarose concentration, % (w/v)	Xylene Cyanol FF	Bromophenolblue
0.7-1-7	4000 bp	300 bp
2.5-3.0	800 bp	100 bp

3.2.2.3 Denaturing Polyacrylamide Gel Electrophoresis of RNA

The RNA fragments up to 2000 nts were separated from each other on denaturing polyacrylamide-urea gels containing urea. Depending on the size of the RNA fragments, the concentration of polyacrylamide was varied between 5 % and 20 % (Sambrook *et al.*, 1989). Before loading on the gel, RNA samples were resuspended in 5 µl of RNA loading buffer and denatured for 1.5 min to 3 min at 96 °C. The electrophoresis was performed in 1 x TBE buffer until xylene cyanol reached the bottom of the gel. The RNA fragments on the gel were visualized either by ethidium staining or by silver staining. In the case of radioactively labeled samples, RNA molecules were detected by autoradiography.

RNA Gel solutions (per 20 ml)

8 M (w/v) Urea
5 %-20 % Rotiphorese 40
2 ml 10 x TBE
100 µl 10 % (w/v) APS & 10 µl TEMED

Migration Rates of the Marker Dyes through Denaturing Polyacrylamide Gels		
Polacryalmide gel, %	Xylene Cyanol FF	Bromophenolblue
5.0	130 bases	35 bases
6.0	106 bases	29 bases
8.0	76 bases	26 bases
10.0	55 bases	12 bases
20.0	28 bases	8 bases

3.2.2.4 Non-Denaturing Polyacrylamide Gel Electrophoresis of U6-Prp24 Binary Complex

To investigate the interaction between U6 snRNA and Prp24 protein, non-denaturing polyacrylamide gel electrophoresis was performed where RNA-protein complex was under native conditions. For this purpose, 1 mM thick, 6 % and 10 % polyacrylamide (80:1 acrylamide:bis-acrylamide) gels were prepared. Before loading on gel, samples were mixed with glycerol at a final concentration of 4 %. Electrophoresis was carried out at 4 °C. U6 snRNA-Prp24p complexes were separated for 1-1½ h at 9 W in 0.5 x TBE buffer. Subsequently, gel was transferred on a Whatmann paper and dried at 80°C for 30 min.

<u>RNA 6 % Solution (30 ml)</u>	<u>RNA 10 % Solution (30 ml)</u>
6 ml 30 % Acrylamide	10 ml 30 % Acrylamide
1.125 ml 2 % Bis-acrylamide	1.875 ml 2 % Acryl-amide
1.5 ml 10 x TBE	1.5 ml 10 x TBE
150 µl 25 % (w/v) APS & 15 µl TEMED	150 µl 25 % (w/v) APS & 15 µl TEMED

Migration Rates of the Marker Dyes through Non-Denaturing Polyacrylamide Gels		
Polacryalmide gel,%	Xylene Cyanol FF	Bromophenolblue
6.0	260 bp	65 bp
8.0	160 bp	45 bp
10.0	90 bp	30 bp

3.2.2.5 Ethidium Bromide Staining of RNA Gels

Ethidium bromide staining of polyacrylamide gels was performed when the amount of RNA molecules was high enough to be detected. Ethidium bromide staining is easy to perform but has certain detection limits. When low amounts of RNA were present, the bands were detected by silver staining. Polyacrylamide gel was soaked into a solution containing 400 µg ethidium bromide and incubated for 30 min at room temperature. The gel was washed twice shortly with ddH₂O in order to get rid of the excess ethidium bromide. The bands were visualized with UV-light at 254 nm.

3.2.2.6 Silver staining of RNA gels

Silver staining of RNA gels was performed according to protocol from Merrill *et al.*, 1983. During the procedure, at least a 10-fold volume of the gel volume was required for all solutions and all steps were performed on a shaker. First, the gel was fixed in 40 % methanol/ 10 % acetic acid solution at least for 30 min or over night. After fixation, the gel was washed twice with 10 % ethanol/ 5 % acetic acid solution for 15 min in order to dissolve and remove interfering substances. After that, it was washed shortly with ddH₂O and subsequently stained in 12 mM AgNO₃ solution for 20 min. Stained gel was washed shortly twice with ddH₂O. Then, it was treated shortly with 0.28 M Na₂CO₃/ 0.0185 % formaldehyde solution to remove excess silver from the surface of the gel. The solution was changed; the gel was developed in the same solution until RNA bands were visual. The developing was stopped with 5 % acetic acid solution. The gel was scanned and then transferred on a Whatmann paper and dried at 80 °C for 1 hour.

3.2.2.7 Transformation and Isolation of Plasmids into/from *E. coli*

The chemically competent cells were prepared according to CaCl₂ method from Cohen *et al.*, 1972. A overnight-50 ml *E. coli* culture with an OD₆₀₀ of 0.3 was washed with 25 ml of 50 mM ice cold CaCl₂. Cells were afterwards were resuspended in 3 ml of 50 mM ice cold CaCl₂ and glycerol was added to a final concentration of 10 %. Competent cells were kept at -80°C. The transformation of the plasmids was performed according to standard protocol from Sambrook *et al.*, 1989. 10-50 ng of DNA was mixed with 50 µl of competent cells and incubated on ice for 30 min. Heat-shock was performed for 1 min at 42 °C and cells were immediately chilled on ice for 1 min. Subsequently, 800 µl of LB-medium was added and incubated for 1 h at 37 °C. Cells were centrifuged briefly and cell pellet was resuspended in 50 µl of 10 mM Tris/HCl pH 7.5. Cells were plated on the selection media (LB-Kan^R or LB-Amp^R) and incubated for 1-2 days at 37 °C. The isolation of the plasmid DNA from bacteria was carried out using QIAfilter mini- and maxi-prep kits according to manufacturer's instruction.

3.2.2.8 Polymerase Chain Reaction (PCR)

In PCR reactions, either plasmid DNA or yeast chromosomal DNA were used as templates. The reactions were performed in a DNA thermocycler using either Taq- or Pfu-polymerase or the kit: Expand long template PCR mix. PCR conditions

were different depending on template and kind of DNA-polymerase. The PCR products were purified from the reaction using *QIAquick PCR Purification Kit* according to manufacturer's instructions.

PCR for the Amplification of TAP-Marker Cassette

TAP-marker cassette was amplified from plasmid pBS1479 using oligonucleotide primers which are 48 nucleotides-long homologous to region of a certain gene. A typical PCR reaction contained:

Plasmid DNA (pBS1479)	0.1-0.4 μg
10 x Taq buffer	10 μl
dNTP mix (each 1.25 mM dATP, dGTP, dCTP, and dTTP)	12 μl
Primer forward (10 pmol/ μl)	6 μl
Primer reverse (10 pmol/ μl)	6 μl
Taq-polymerase (5u / μl)	1 μl
with ddH ₂ O up to 100 μl	

<u>PCR program</u>		<u>Cycle</u>
5 min	94 °C	1 x
30 s	94 °C	
30 s	48 °C	50 x
1 min/kb	72 °C	
5 min	72 °C	1 x

PCR for the Amplification of the Fluorescent Protein-Marker Cassette

To introduce fluorescent protein tags to the LSm proteins at their C-terminal, yECitrine and yECitrine-3HA tags were amplified by PCR from plasmids pKT 175 or pKT239 using oligonucleotide primers which are 48 nucleotides-long homologous to region of a certain gene. A typical PCR reaction contained:

Plasmid DNA (pKT175, Aat II digested; pKT239)	0.05-0.1 μg
10 x Buffer 1	10 μl
Primer forward (10 pmol/ μl)	3 μl
Primer reverse (10 pmol/ μl)	3 μl
dNTP mix (each 1.25 mM dATP, dGTP, dCTP, and dTTP)	28 μl
Expand long template PCR mix (5 U/ μl)	1.5 μl
with ddH ₂ O up to 100 μl	

PCR program		Cycle
2 min	94 °C	1 x
20 s	94 °C	
30 s	65 °C	25 x
1 min/kb	68 °C	
7 min	68 °C	1 x

PCR for the Amplification of PRP24 Gene from Chromosomal DNA

To overexpress recombinant Prp24 protein in *E. coli*, *PRP24* gene was amplified by PCR from yeast chromosomal DNA using expression oligonucleotide primers for *PRP24*. A typical PCR reaction contained:

Chromosomal yeast DNA (0.5 $\mu\text{g}/\mu\text{l}$)	2 μl
10 x Pfu buffer	10 μl
Primer forward (10 pmol/ μl)	10 μl
Primer reverse (10 pmol/ μl)	10 μl
dNTP mix (each 1.25 mM dATP, dGTP, dCTP, and dTTP)	8 μl
100 % (v/v) DMSO	10 μl
Pfu-polymerase (5 U/ μl)	2 μl
with ddH ₂ O up to 100 μl	

PCR program		Cycle
2 min	94 °C	1 x
15 s	94 °C	
30 s	65 °C	30 x
½ min/kb	72 °C	
5 min	72 °C	1 x

PCR for Sequencing Analysis

In the case of PCR for subsequent sequencing analysis with ABI Prism 310 Genetic Analyzer, PCR reaction was performed according to manufacturer's instructions using fluorescently-labeled nucleotides. A typical PCR reaction contained:

PCR fragment (0.3 $\mu\text{g}/\mu\text{l}$)	1 μl
10 x Big Dye Sequencing Buffer	2 μl
Primer forward (3.2 pmol/ μl)	1 μl
Primer reverse (3.2 pmol/ μl)	1 μl
Big Dye	4 μl
with ddH ₂ O up to 20 μl	

<u>PCR program</u>		<u>Cycle</u>
1 min	96 °C	1 x
30 s	96 °C	
30 s	55 °C	25 x
4 min	60 °C	

PCR for Characterization of Transformants

To analyze whether a transformant contained the correct integration of a tag of interest, chromosomal DNA was isolated from transformant yeast cells and PCR analysis was performed using checking oligonucleotide primers. A typical PCR reaction contained:

Chromosomal yeast DNA	0.5-1.0 μl
10 x Taq buffer	2 μl
dNTP mix (each 1.25 mM dATP, dGTP, dCTP, and dTTP)	2.4 μl
Primer forward (10 pmol/ μl)	1.2 μl
Primer reverse (10 pmol/ μl)	1.2 μl
Taq-polymerase (5u / μl)	0.1 μl
with ddH ₂ O up to 20 μl	

PCR program		Cycle
1 min	94 °C	1 x
30 s	94 °C	
30 s	48 °C	50 x
1 min/kb	72 °C	
5 min	72 °C	1 x

3.2.2.9 Transformation of haploid yeast cells

Constructing Yeast Strain Expressing TAP-tagged Prp24p

To construct the yeast expressing TAP tagged Prp24p, the C-terminal TAP cassette was amplified by PCR from the plasmid pBS1479 using oligonucleotides 1 and 2. Transformation was carried according to Puig *et al.*, 2001 using yeast strain TR2 and LiOAc method. 50 ml of yeast culture was grown over night until its OD₆₀₀ reached 0.6-1.0 per ml. Cells were washed with 10 mM Tris/ HCl pH 7.5. Subsequently, yeast cells were resuspended in 25 ml of LiT solution with 10 mM DTT and incubated for 40 min at room temperature with gentle shaking. After centrifuging, yeast cells were resuspended in 750 μ l of LiT solution (with 10 mM DTT). For the following transformation reactions, 100 μ l of the yeast cells was mixed with 50 μ l LiT, 5 μ l of Salmon sperm DNA (10 μ g/ μ l, denat.), and different amounts of PCR product (1 μ g-50 μ g). A positive control with 500 ng pRS314 (*TRP1*) plasmid and a negative control without DNA were included. After incubation of the mixtures for 10 min at room temperature, 300 μ l of PEG solution was added and incubated further for 10 min at room temperature. Heat-shock was performed for 15 min at 42 °C. After heat-shock, yeast cells were centrifuged briefly. Cell pellet was resuspended in 1 ml of YPD-medium and incubated for 1 h at 30 °C. This step is required for the recovery of the yeast cells. After recovery, cells were precipitated again and resuspended carefully in 100 μ l of 10 mM Tris/HCl pH 7.5. 50-100 μ l of cells were plated on the selection media (SD-TRP) and incubated for 2-3 days at 30 °C.

<u>LiT solution</u>	<u>PEG solution</u>
10 mM Tris/HCl pH 7.5	2 g PEG 3350
100 mM LiOAc	2 ml LiT solution
sterile filtered	dissolved at 50 °C and sterile filtered

Constructing the Yeast Strain Expressing Fluorescent Protein (yECitrine or yECitrine-3HA)-tagged LSm Proteins

To construct the yeast expressing yECitrine-LSm tag, the C-terminal fluorescent protein marker cassette was amplified by PCR from the plasmids pKT175 or pKT239 (only for LSm7p) using appropriate oligonucleotides 5-32. Transformation was carried according to Knop *et al.*, 1999 using yeast strain TR2 and LiOAc method. 50 ml of yeast culture was grown over night until its OD₆₀₀ reached 0.6-1.0 per ml. Cells were washed with ddH₂O and once more with 2 ml of SORB. Subsequently, yeast cells were resuspended in 360 μ l of SORB and 40 μ l of Salmon sperm DNA (10 μ g/ μ l, denat.) For the following transformation reactions, 50 μ l of the yeast cells was mixed with 1 μ g/ μ l of PCR product. A positive control with 250 ng pRS315 (*HIS5*) or pRS316 (*URA3*) plasmids and a negative control without DNA were included. After mixing well, 6V of PEG/LiOAc/TE solution was added and incubated further for 30 min at room temperature. Subsequently, DMSO was added at a final concentration of 10 % and heat-shock was performed for 15 min at 42 °C. After heat-shock, yeast cells were centrifuged briefly. Cell pellet was resuspended in 100 μ l of 10 mM Tris/HCl pH 7.5. 50-100 μ l of cells were plated on the selection media (SD-*HIS* or SD-*URA*) and incubated for 2-3 days at 30 °C.

<u>SORB</u>	<u>PEG/LiOAc/TE</u>
10 mM Tris/HCl pH 7.5	10 mM Tris/HCl pH 7.5
100 mM LiOAc	100 mM LiOAc
1 mM EDTA	1 mM EDTA
1 M Sorbitol	40 % (w/v) PEG 3350
Sterile filtered	dissolved at 50 °C and sterile filtered

Transformant Characterization by PCR

The correct integration of either TAP cassette or fluorescent marker cassette into yeast genomic DNA was verified by PCR. Single colonies were picked up from SD-*TRP* plates and cultured in 1 ml YPD-medium about 17-18 h at 30 °C. Cells were centrifuged and resuspended in 100 μ l TE/SDS and vortexed for 15 min at room

temperature. Subsequently, 500 μ l of 1 x TE buffer and extracted with 600 μ l PCI. The upper phase containing chromosomal DNA was precipitated with 0.7 V of isopropanol by centrifuging for 30 min at 4°C and 13 000 rpm. DNA pellet was resuspended in 20 μ l of ddH₂O. PCR reaction for checking the integration was performed using checking oligonucleotides for *PRP24* or *LSM* genes.

1 x TE

10 mM Tris/HCl pH 7.5

1 mM EDTA

TE/SDS

10 mM Tris/HCl pH 7.5

1 mM EDTA

0.3 % (w/v) SDS

Transformant Characterization by Western blot

Western blot was used in order to check whether integrated TAP cassette or fluorescent marker cassette was expressed correctly in yeast cells. Single colonies were picked up and inoculated in a 1.5 ml of YPD-medium over night. Next day, cells were centrifuged and resuspended in 100 μ l of protein loading buffer. Cells were disrupted with acid washed glass beads (about 30 μ l of beads were used) by vortexing 5 times for 30 seconds. Cells were kept in between steps on ice. After disruption, cells were boiled for 4 min at 95 °C, followed by centrifuging for 2 min at 4 °C. Subsequently, 50-100 μ l of supernatant was loaded on a 12 % high-TEMED SDS-PAGE. After running the gel, the proteins were blotted to a nitrocellulose membrane and incubated with primary antibody. For TAP-cassette, the membrane was incubated with PAP antibody in 1:2000-dilution. For fluorescent marker cassette, first membrane was incubated either with α -YFP antibody (1:2000 dilution) for yECitrine tagged LSm proteins (except of LSm7p) or with α -HA antibody (1:1000 dilution) for yECitrine-3HA tagged LSm7p.

3.2.2.10 Constructing Bacteria Strain Overexpressing His₆-tagged Prp24p

The *PRP24* gene was amplified by PCR from yeast genomic DNA using oligonucleotides 37 and 38. The resulting fragment was double-digested NcoI / Acc65 I and subcloned into NcoI / Acc65I-digested pETM-11 vector. The resulting plasmid was transformed in the *E. coli* strain HB 101. The transformants were selected on LB plates containing 30 μ g/ μ l Kanamycin. Single-colonies were picked up and the subcloned *PRP24* fragments were analyzed by sequencing. Subsequently, plasmids containing *PRP24* without mutations were isolated using QIAfilter mini- and maxi-prep kits according to manufacturer's instruction. This

plasmid were then further transformed in the *E. coli* strain Rosetta (DE3, pLYSs).

3.2.2.11 Restriction Digestion of Plasmids or PCR products

The restriction enzyme reactions were performed using appropriate enzyme and buffers according to manufacturer's instructions (New England Biolabs and Sambrook *et al.*, 1989). The digested products were analyzed on an agarose gel and subsequently purified from the gel using *QIAquick Gel Extraction Kit* (Qiagen) or *GFX-PCR DNA and Gel Band Purification Kit* (Amersham/Pharmacia). The ligation of restriction enzyme digested fragments was carried out using T4 DNA-ligase at 16 °C over night (Sambrook *et al.*, 1989).

3.2.2.12 Synthesis of Radioactively Labeled DNA-probes for Northern Analysis

To detect the complementary RNAs in a Northern Blot analysis, radioactively labeled DNA probes were synthesized from their corresponding DNA templates using *Prime It II Random Primer Labeling Kit* (Stratagene). DNA templates were digested with restriction enzymes from their corresponding plasmids and purified from agarose gel using *QIAquick Gel Extraction Kit* (Qiagen). During labeling, a mixture of 1 μ l DNA template, 23 μ l ddH₂O and 10 μ l of random nanomer primers were denatured at 95 °C for 5 min and subsequently cooled down at room temperature over 5 min in order to allow hybridization. In the following, 10 μ l of dATP primer buffer, 5 μ l of [α -³²P] dATP and five units of Klenow enzyme were added into the reaction and incubated for 10 min at 40 °C. The reaction was stopped by 2 μ l of 0.5 mM EDTA solution. Labeled DNA-probes were purified from free radioactive dATP by *ProbeQuant™ G-50 columns*. For Northern Blot Analysis, 20-30 x 10⁶ cpm of the labeled DNA-probes were used.

3.2.2.13 Northern Blot Analysis

Northern Blot Analysis was made in order to detect a specific RNA molecule using complementary radioactively labeled DNA-probes. After performing a denaturing polyacrylamide gel electrophoresis, RNA molecules were transferred on a nylon membrane by wet-blotting over night at 18V and 4 °C. Next day, the nylon membrane was blocked with pre-hybridization buffer for 2 h at 42 °C in order to prevent unspecific bindings. In order to detect RNA fragments, the nylon membrane was hybridized for 24-48 h with radioactively labeled-DNA probes. After hybridization, the nylon membrane was washed twice with wash buffer 1 for

5 min at room temperature, twice with wash buffer 2 for 5 min at room temperature, and once more with wash buffer 2 for 30 min at 50 °C. After washing steps, RNA fragments were visualized by autoradiography.

<u>Pre-/ Hybridization Buffer</u>	<u>20 x SSC</u>
25 mM Na ₃ PO ₄ pH 6.5	300 mM Na-Citrate
6 x SSC	3 M NaCl
5 x Deinhardt's solution	
0.5 % (w/v) SDS	<u>100 x Deinhardt's solution</u>
50 % (v/v) Deionized formamide	2 % (w/v) Polyvenylpyrrolodase
0.1 mg/ml Salmon sperm DNA (5 min denat.)	2 % (w/v) BSA
(10-20 x 10 ⁶ cpm / probe)	2 % (w/v) Ficoll 400
<u>Wash Buffer 1 (500 ml)</u>	<u>Wash Buffer 2 (800 ml)</u>
2 x SSC	2 x SSC
0.5 % (w/v) SDS	0.1 % (w/v) SDS
<u>Wet-blotting buffer</u>	
25 mM Na ₃ PO ₄ pH 6.5	

3.2.2.14 *In Vitro* Transcription

In vitro transcription of RNA transcripts were carried out using different DNA templates. Depending on the type of expression promoters of DNA templates, different DNA polymerases such as SP6, T7, or T3 were used. In the experiments, U6 snRNA was synthesized with cold or radioactively labeled ribonucleotides. Gene on plasmid DNA coding for U6 snRNA is under the control of T7-polymerase and the plasmid DNA was cut with Bam HI restriction endonuclease at 3' end of U6 gene in order to perform a run-off transcription. The synthesis of radioactively labeled U6 snRNA was performed using [α -³²P] UTP in a small volume of reaction whereas the transcription of cold U6 snRNA was carried out in a larger preparative scale. The transcription reactions were incubated for 2 h at 37 °C. In order to purify the transcript from the template and free ribonucleotides, whole reaction mixture was loaded on a denaturing polyacrylamide RNA gel. In the case of radioactively labeled RNA, the transcript was detected by autoradiography whereas cold transcript was visualized by UV-shadowing at 312 nm. The RNA bands were cut out from the gel, chopped into smaller pieces and 500 μ l of elution buffer was added. The elution was done over night at 4 °C by *head-over-tail* incubation.

Subsequently, the transcript was purified from elution buffer and gel pieces by PCI-extraction and precipitated with ethanol. The concentration of the cold RNA was measured photometrically. From the radioactively labeled U6 snRNA, 1 μ l was counted in a scintillation counter according to Cerenkov protocol and specific activity of the U6 transcript was calculated.

Radioactively Labeled RNA

1 μ l linearized plasmid (1 μ g/ μ l)
 1 μ l 10 x transcription buffer (NEB)
 1 μ l 10 x NTPs (5 mM ATP, CTP, GTP; 1 mM UTP)
 1 μ l DTT (100 mM)
 0.5 μ l RNasin (40 U/ μ l)
 2 μ l [α -³²P] UTP (3000 Ci/mmol)
 1 μ l T7 polymerase (20 U/ μ l)
 2.5 μ l ddH₂O

Cold RNA

10 μ l linearized plasmid (1 μ g/ μ l)
 10 μ l 10 x transcription buffer
 10 μ l NTPs (25 mM each)
 10 μ l DTT (100 mM)
 5 μ l RNasin (40 U/ μ l)
 9.6 μ l MgCl₂ (100 mM)
 10 μ l T7 polymerase (20 U/ μ l)
 35.4 μ l ddH₂O

Elution Buffer

500 mM NaOAc pH 5.2
 1 mM EDTA
 2.5 % (v/v) 1:1 Phenol/Chloroform

Equation to calculate the quantity of radioactive RNA

synthesized in an *in vitro* transcription reaction

$$\text{RNA (pmoles)} = \frac{\text{Total cpm}}{2.2 \times 10^6 \text{ cpm}} \times \frac{2 + (\text{age of } ^{32}\text{P})}{2 \times \text{SA } ^{32}\text{P} (\mu\text{Ci}/\text{pmole})} \times \frac{[\text{UTP} (\mu\text{M})]}{[^{32}\text{P} \text{ UTP} (\mu\text{M})] \times \# \text{ of Us}}$$

3.2.2.15 Radioactive Labeling of 5'-end of DNA-Oligonucleotides

In order to use as primers in primer extension analysis, DNA oligonucleotides (yU6 68_84 or yU& 94_112) were radioactively labeled at their 5'-end using [γ -³²P] ATP and T4-polyucleotide kinase. Before labeling, DNA-oligonucleotide was gel-purified and its concentration was adjusted to 5 pmol/ μ l. The reaction was carried out for 40 min at 37 °C. After incubation, the reaction volume was brought to 50 μ l with CE buffer so that the radioactively labeled oligonucleotide could be purified from not incorporated free [γ -³²P] ATP using *ProbeQuant*TM G-50 columns. The eluate of the G-50 column was PCI extracted and ethanol precipitated. The precipitate was resuspended in 30 μ l of CE buffer.

Labeling Reaction

2 μ l oligonucleotide (5 pmol/ μ l)
1 μ l 10 x T4-polynucleotide kinase buffer (NEB)
6 μ l [γ - 32 P] (6000 Ci/mmol, 10 mCi/ml)
1 μ l ddH₂O

CE-Buffer

10 mM Caco. acid/KOH pH 7.0
0.2 mM EDTA

3.2.3 Cell Culture and Growth

3.2.3.1 Growth and Culture of Bacteria

E. coli bacteria cells were grown according in LB (Luria Bertani)-medium or on LB-plates (Sambrook *et al.*, 1987). Depending on the transformed plasmid, which contains genes for antibiotic resistance, LB medium contained 100 μ g/ml Ampicillin 30 μ g/ μ l Kanamycin, or 30 μ g/ μ l Chloramphenicol. For longer storage, 500 μ l of bacteria cells was mixed with 250 μ l of 50 % sterile glycerol and kept at -80 °C.

LB-Medium

1 % (w/v) Bacto-Trypton
0.5 % (w/v) Yeast extract
1 % (w/v) NaCl
1.0 % (w/v) Bacto-Agar in the case of LB-plates

3.2.3.2 Yeast Cell Culture

S. cerevisiae yeast cells were cultivated according to standard methods in YPD medium or on YPD-plates. To prepare YPD plates, first YP-medium was autoclaved for 15 at 121 min and cooled down to 50 °C. Subsequently, sterile 50 % glucose was added to the YP medium to a final concentration of 2 %. Afterwards, this medium was poured into Petri dishes and waited until the agar polymerized. The plates were stored at room temperature. Yeast cells were picked from a glycerol stock culture and streaked on YPD-plates. Yeast cells were incubated 2-3 days at 23 °C, 25 °C or 30 °C, depending on the phenotype of the cells. For a longer storage of the cells, the plates were sealed with a parafilm and kept at 4 °C up to 3 months. For the liquid cultures of yeast cells, usually 5-10 ml of pre-culture in YPD medium was prepared and incubated over night at the optimal temperature. OD₆₀₀ of the cells in pre-culture was measured and usually 10 OD of cells was inoculated around 3 pm into 2 liters of YPD culture in a 5 L Erlenmeyer

flask. Next day, at about 9 am, cells reached OD₆₀₀ of 3-5 / ml. For a longer storage in YPD medium, 800 µl of yeast cells were mixed with 400 µl of sterile 50 % glycerol and kept at -80 °C.

In order to select the right transformants after transformation of a plasmid or a piece of DNA, synthetically depleted medium (SD-medium) was used. This mixture contained all the essential amino acids except of the amino acid used as selection marker.

YPD-medium

2 % (w/v) Bacto pepton
1 % (w/v) Yeast extract
2 % (w/v) Glucose (sterile filtered)
1 % (w/v) Bacto agar in the case of YPD-plates

SD-medium

43.7 g/L DOBA powder
0.77 g /L amino acid mixtures (Bio 101)

DOBA powder

1.7 g Yeast Nitrogen Base
20 g Dextrose
5 g Ammonium Sulfate
17 g Agar

3.2.3.3 Harvesting and Extract Preparation from Yeast Cells

Total extract preparation from yeast cells were performed for U6 snRNP purification according to Puig *et al.*, (2001) and for U1 snRNP according to Lin *et al.*, (1985) and Umen & Guthrie (1995). Yeast cells from corresponding yeast strains were grown over night at 30 °C up to OD₆₀₀ of 2.5-5.0 and then were centrifuged for 10 min at 5 600 rpm using SLC-6000 rotor. Cell pellet was washed with 500 ml of cold ddH₂O per 2 L yeast culture. After this step, extract preparation for U6 snRNP and U1 snRNP purifications differ from each other. When extract was prepared for following U6 snRNP purification, cells were resuspended in 10 ml of ddH₂O, transferred into a 50-ml Falcon tube and centrifuged for 15 min at 4000 and 4 °C. After supernatant was discarded, packed cell volume was measured and cells were shock frozen in liquid nitrogen. Then, cells were resuspended in one packed cell volume of Buffer A. Cells were thawed quickly in a 23 °C-water bath and cooled down in between on ice. Afterwards, cells were disrupted by passing once through French press at a pressure of 21 800 psi. After disruption, the concentration of KCl in cell lysate was adjusted to 200 mM by 2 M KCl. Then, cell lysate was

centrifuged for 30 min at 17 000 rpm (25 000 g) using SS-34 rotor in order to get rid of cell debris. Supernatant of former centrifugation step was transferred into a new tube and further centrifuged for 1 h at 37 000 rpm (100 000 g) using T-865 rotor or for 50 min at 42 000 rpm (100 000 g) using T-647.5 rotor. After this centrifugation step, cell lysate was separated into three different phases: uppermost white layer included lipids and liposomes; middle reddish phase contained total cell extract; and pellet enclosed ribosomes, fine cell debris, and genomic DNA. Middle phase containing total cell extract was recovered with a help of a Pasteur-pipette and dialyzed 2 x 1 ½ h against Buffer D. Finally, dialyzed extract was shock-frozen in liquid nitrogen and stored at -80 °C.

When extract was prepared for following U1 snRNP purification, after washing cells with 500 ml of cold ddH₂O, cells were resuspended in 10 ml of Buffer A. After measuring the volume of cell suspension, the concentration of KCl was adjusted to 200 mM by adding 2 M KCl. This cell-paste was dropped into liquid nitrogen to make yeast-beads with 3 – 6 mM diameter. Consequently, 50 ml of these yeast beads were disrupted by grinding with a mortar grinder for 15 min until yeast beads turned into a whitish cell-powder. During this step, to cool down, liquid nitrogen was continuously added into mortar grinder. Cell powder was stored at -80 °C until needed. For extract preparation, cell powder was first quickly thawed in a 23 °C-water bath and further 1h at 4 °C until all cell powder was liquid. This cell lysate was treated exactly as above. Middle phase after two centrifugation steps was dialyzed 2 x 1 ½ h against Buffer D and dialyzed extract was shock-frozen in liquid nitrogen and stored at -80 °C.

Buffer A

10 mM Hepes/KOH pH 7.9
10 mM KCl
1.5 mM MgCl₂
8 % (v/v) Glycerol
0.5 mM DTT
0.5 mM PMSF
2 mM Benzamidine
1 μM Leupeptin
2 μM Pepstatin A
4 μM Chymostatin
2.6 μM Aprotinin

Buffer D

20 mM Hepes/KOH pH 7.9
50 mM KCl
0.2 mM EDTA
20 % (v/v) Glycerol
0.5 mM DTT
0.5 mM PMSF
2 mM Benzamidine

3.2.4 Immunoprecipitations

During this work, immunoprecipitations were performed to analyze snRNP particles from different yeast extracts. Antigen-antibody interactions allowed us to further purify the certain complexes containing corresponding antigen. Experiments in this study with U6 snRNPs were performed using anti-Prp24p and anti-YFP antibodies or using non-immune serum (NIS).

As a first step, antibodies were coupled to Protein A-Sepharose in a tube. Amount of antibodies used per assay changed between 8 μ l (anti-Prp24p antibody) and 14 μ l (anti-YFP antibody). For coupling, 50 μ l of protein A-Sepharose beads were needed per assay. Depending on the number of samples that are assayed, proportionally more bead slurry can be coupled with correspondingly increases amounts of antibody. The coupled beads can be distributed afterward between the different tubes. First, protein A-Sepharose beads were equilibrated by washing (2-3 x) with PBS-buffer. Then, antibody was incubated with equilibrated beads for 1-2 h at 4 °C by using a head-over-tail rotor. After coupling, beads were washed three times with 500 μ l of PBS-buffer per 50 μ l beads and were overlaid with 15 μ l of PBS-buffer. Subsequently, samples were added to the prepared antibody-coupled protein A-Sepharose beads and incubated at least 1 h at 4 °C by head-over-tail rotation. After binding, beads were washed four times with PBS-buffer. After last wash, beads were resuspended in 100 μ l of PBS-buffer and samples were digested with proteinase K. RNA was extracted with PCI, precipitated with ethanol, and resuspended in an appropriate buffer.

PBS (phosphate-buffered saline)-Buffer

20 mM Na₂HPO₄ pH 8.0

130 mM NaCl

3.2.5 Special Methods

3.2.5.1 Purification of Recombinant Prp24 Protein Tagged with (His)₆ from *E. coli* cells

Recombinant yeast Prp24 protein tagged with 6 x Histidines at its N-terminus was overexpressed in *E. coli* strain Rosetta and purified under native conditions using Ni²⁺-NTA affinity resin. To overexpress Prp24p, *E. coli* strain Rosetta was transformed with expression plasmid pRK-1. A single colony was inoculated into a

LB-Kanamycin (30 $\mu\text{g}/\mu\text{l}$)-Chloramphenicol (30 $\mu\text{g}/\mu\text{l}$) liquid pre-culture and grown overnight at 37 °C. Next day, OD₆₀₀ of cells was measured and cells were further inoculated into 1 L of LB-Kanamycin-Chloramphenicol liquid pre-culture in such a way that final OD₆₀₀ was 0.3 after 2-3 h of incubation at 37 °C. When reached OD₆₀₀ of 0.3, 1 ml of cells was kept before induction. Production of Prp24p was induced with 2 mM IPTG and expression was carried on overnight at 25 °C. Next day, another 1 ml of cells was saved after induction. Cells were centrifuged for 20 min at 5 600 rpm using SLC-6000 rotor. Cell pellet was washed with 500 ml of cold ddH₂O. Cells were then resuspended in 10 ml of ddH₂O and transferred into a 50-ml Falcon tube and centrifuged for 30 min at 4000 and 4 °C. After supernatant was discarded, packed cell volume was measured and cells were shock frozen in liquid nitrogen.

Pre-check of Overexpression:

Before processing the cells further, induction and expression of recombinant Prp24p was pre-checked. For this purpose, OD₆₀₀ of 1 ml-fractions kept before and after induction were measured. Cells were centrifuged and resuspended in 200 μl of pre-check buffer per OD₆₀₀. Subsequently, 2 μl of Lysozyme (100 $\mu\text{g}/\mu\text{l}$) and RQ-DNase I (2 U/ μl) per OD₆₀₀ were added and reactions were incubated at 37 °C. After incubation, 30 μl of cell lysate was mixed with 50 μl protein-loading buffer and boiled for 5 min at 96 °C. Lysate was loaded on a 12 % SDS-polyacrylamide gel and overexpression was detected by staining with Coomassie Brilliant Blue R-250.

Ni²⁺-NTA-Affinity Chromatography:

After making sure of the overexpression level, cells were thawed and resuspended in lysis buffer up to 20 ml. To cell suspension, 100 μl of lysozyme (100 $\mu\text{g}/\mu\text{l}$) was added and incubated for 10 min on ice. After that, cells were disrupted by sonication while cooling with ice-cold ddH₂O and were centrifuged for 30 min at 11 200 rpm (15 000 g) using SS-34 rotor in order to get rid of cell debris. A clear cell lysate was obtained after this step. Nucleic acids were removed from the cleared lysate by precipitation with 3 % (w/v) streptomycin sulfate for 1 h at 4 °C, followed by centrifugation step as above. Supernatant was loaded in a 10 ml 0.8 x 4-cm BioRad Poly-Prep column containing 1 ml of Ni²⁺-NTA-Agarose beads and incubated for 1 h at 4 °C by using a head-over-tail rotor. After binding to Ni²⁺-NTA-

Agarose beads, the column was drained by gravity flow and washed with 50 ml of each wash buffer I, II and III. Elution of the proteins specifically from Ni²⁺-NTA column was performed by elution buffer consisting of different imidazole concentrations. First elution was carried out with 1 ml of elution buffer containing 100 mM imidazole. Subsequently, the elution was carried on with 5 fractions of 2.5 ml of elution buffer containing 325 mM imidazole. The concentration of recombinant Prp24 protein was measured by the method of Bradford (3.2.1.1). The detection of Prp24 was performed by loading 40 μ l of sample on a 12 % SDS-polyacrylamide gel and staining with Coomassie Brilliant Blue R-250. To detect possible contamination of Prp24p with nucleic acids, 10 μ l of sample was loaded on a 10 % denaturing-polyacrylamide gel and analyzed by ethidium bromide staining.

Pre-check Buffer

50 mM Tris/HCl pH 8.0
 300 mM NaCl
 5 mM Imidazole
 1.5 mM MgCl₂
 1 x EDTA-free protease inhibitors

Lysis Buffer

20 mM Tris/HCl pH 8.0
 150 mM NaCl
 10 mM Imidazole
 0.2 % NP-40
 1 x EDTA-protease inhibitors
 2 mM β -mercaptoethanol

Wash Buffer I

20 mM Tris/HCl pH 8.0
 150 mM NaCl
 10 mM Imidazole
 2 mM β -mercaptoethanol

Wash Buffer II

20 mM Tris/HCl pH 8.0
 1 M NaCl
 10 mM Imidazole
 2 mM β -mercaptoethanol

Wash Buffer III

20 mM Tris/HCl pH 8.0
 150 mM NaCl
 50 mM Imidazole
 2 mM β -mercaptoethanol

Elution Buffer

20 mM Tris/HCl pH 8.0
 150 mM NaCl
 100 or 325 mM Imidazole
 2 mM β -mercaptoethanol

3.2.5.2 Tandem Affinity Purification of U6 snRNP Particles using Prp24-TAP Tagged strain

“Tandem Affinity Purification (TAP)” consists of two isolation steps: employing first an IgG matrix and then calmodulin affinity beads (Puig *et al.*, 2001).

Yeast strains expressing TAP-tagged Prp24 protein was constructed as it was described. To purify native U6 or U1 snRNPs, TAP method (Puig *et al.*, 2001) and TAP-tagged Prp24 or Snu71 proteins were used, respectively. Frozen yeast extracts from these constructed yeast strains were thawed quickly in a 23 °C-water bath. Subsequently, the buffer composition of extract was adjusted to 10 mM Tris /HCl pH 8.0, 150 mM NaCl, and 0.1 % NP-40. IgG-Sepharose beads (100 µl beads per extract from 4 L of yeast culture) were washed with IPP 150 buffer and incubated with yeast extract in a 50 ml-Falcon tube for 2 h at 4 °C by using a head-over-tail rotor. After binding to IgG-Sepharose beads, batches of extract were transferred into 10 ml 0.8 x 4-cm BioRad Poly-Prep columns. IgG-Sepharose beads were then washed three times with 10 ml of IPP 150 buffer and followed by washing once with TEV cleavage buffer. After washing steps, cleavage by TEV protease was performed on the beads using 1 ml of TEV cleavage buffer and 100 U of TEV protease. IgG-Sepharose beads were incubated for 2h at 16 °C by using a head-over-tail rotor. In another poly-prep column, 100 µl of Calmodulin affinity resin (per extract from 8 L of yeast culture) were washed with 10 ml of calmodulin binding buffer. After TEV protease cleavage, particles were eluted from IgG-Sepharose beads directly into the column containing calmodulin affinity resin. The dead-volume in IgG-Sepharose beads were washed with 200 µl of TEV cleavage buffer. After that, the buffer composition of eluate in calmodulin affinity beads was adjusted by adding 3 V of calmodulin binding buffer and 0.003 V of 1 M CaCl₂. Calmodulin affinity beads were incubated at least for 1 h at 4 °C by using head-over-tail. After binding to calmodulin resin, column was drained by gravity flow and washed three times with 10 ml of calmodulin binding buffer. To elute the particles, calmodulin resin was incubated with an appropriate volume of elution buffer for 20 min and eluate was collected by gravity flow.

IPP 150

10 mM Tris /HCl pH 8.0

150 mM NaCl

0.1 % NP-40

TEV Cleavage buffer

10 mM Tris /HCl pH 8.0

150 mM NaCl

0.1 % NP-40

0.5 mM EDTA

1 mM DTT

Calmodulin Binding Buffer

10 mM Tris /HCl pH 8.0
 150 mM NaCl
 0.1 % mM NP-40
 1 mM Mg(OAc)₂
 1 mM Imidazole
 2 mM CaCl₂
 10 mM β-mercaptoethanol

Elution Buffer

10 mM Tris /HCl pH 8.0
 150 mM NaCl
 0.02 % NP-40
 1 mM Mg(OAc)₂
 1 mM Imidazole
 20 mM EGTA
 10 mM β-mercaptoethanol

3.2.5.3 Glycerol Gradient Sedimentation of Purified snRNP particles

After isolating U6 and U1 snRNPs by TAP method, to obtain more homogeneous particles for electron microscopy analysis, they were further purified by glycerol gradient centrifugation. Particles were layered on a linear 10-30 % glycerol gradient containing 200 mM KCl. When particles were fixed during the gradient centrifugation, 0.1 % (w/v) final concentration of glutaraldehyde was added to 30 % glycerol gradient solution. U6 snRNP particles were sedimented for 15 h at 45 000 rpm at 4 °C whereas U1 snRNP particles were centrifuged for 12 h at 30 000 rpm at 4 °C. In both cases, SW-60 (TH-660) rotor was used. After centrifugation, 24 fractions of 175 μl were collected from the bottom of the gradient tube by using a bottom-fraction-collector. The fractions of interest for electron microscopy analysis were determined by photometrical detection of RNA concentration at 260 nm. 50 μl from peak fractions were analyzed by electron microscopy. The rest of the fractions were extracted by PCI. Proteins were analyzed by SDS-polyacrylamide gel electrophoresis followed by silver staining. RNA part of the fractions were loaded on a denaturing polyacrylamide gel and visualized by silver staining.

10 x Gradient 200 buffer

200 mM Hepes/KOH pH 7.9
 2 M KCl
 15 mM MgCl₂
 2 mM EDTA

10 % Glycerol Gradient Solution (50 ml)

5 ml 10 x Gradient 200 Buffer
 7.135 g 87 % Glycerol
 25 μl 0.1 M PMSF & 25 μl 0.1 M DTT

30 % Glycerol Gradient Solution (50 ml)

5 ml 10 x Gradient 200 Buffer
 21.155 g 87 % Glycerol
 25 μl 0.1 M PMSF & 25 μl 0.1 M DTT
 (20 μl 25 % (w/v) Glutaraldehyde)

3.2.5.4 Identification of U6 snRNP proteins by Mass Spectrometry

Protein from the gradient fractions were separated on a SDS-polyacrylamide gel and stained with silver. The visible bands of fractions containing the greatest amount of U6 snRNP proteins were cut out and digested with trypsin by the method of Shevchenko (Shevchenko *et al.*, 1996). When a protein could not be identified unambiguously by matrix-assisted laser desorption/ionization mass spectrometry, liquid chromatography tandem mass spectrometry was performed (Shevchenko *et al.*, 1996).

3.2.5.5 Electron Microscopy Analysis U6 snRNP Particles

Negative staining of the particles was carried out by double carbon film method (Kastner *et al.*, 1990). For electron microscopy, snRNP particles were adsorbed on a small piece of carbon film. Film was transferred to a well filled with 2 % uranyl formate in water and incubated for 2 min. Carbon film was lifted from the staining solution with an electron microscopy grid covered with a perforated carbon film. A second carbon film floated in another well containing 2 % uranyl formate was placed on top of the first film. After blotting, the grid was stored either at room temperature or liquid nitrogen. Images were taken at a magnification of 100 000 using a Philips CM20 operated at 120 kV. The particles were picked from raw images either manually or semi-automatically using software collection Imagic-5 (van Heel *et al.*, 1996). In particular, particle images were iteratively classified and aligned following the "reference-free alignment" protocol (Dube *et al.*, 1993). Class averaging was performed based on multivariate statistical analysis (MSA) of the aligned particle images followed by hierarchical ascendant classification (HAC; van Heel *et al.*, 1984). The class averages contained about 25 images per class.

3.2.5.6 Isolation of Total-RNA from Yeast Cells

In order to isolate total yeast RNA, 25 ml of yeast cells (TR2a) were grown until OD₆₀₀ of 1.0. Cells were centrifuged and resuspended in 400 μ l of AE-buffer per 1 OD₆₀₀. Each 400 μ l of aliquot was mixed with 40 μ l of 10 % (w/v) SDS and mixed by vortexing for 30 sec and incubated for 15 min at room temperature. To this mixture, 440 μ l of phenol (equilibrated with AE-buffer) was added and mixed again for 30 sec. Subsequently, mixture was boiled for 4 min at 65 °C and shock-frozen in an ethanol/dry ice bath. To separate phases, mixture was centrifuged for

10 min at room temperature. Aqueous upper phase was extracted twice by PCI, ethanol precipitated, dried under vacuum and resuspended in 20 μ l ddH₂O. The concentration of isolated total-RNA was determined by a photometer at 260 nm.

AE-Buffer

50 mM NaOAc pH 5.2

10 mM EDTA

3.2.5.7 Band Shift Assays with U6-Prp24 Binary Complex

For band shift assays, recombinant Prp24 protein at different concentrations was incubated with varying concentrations of *in vitro* transcribed U6 snRNA or total-RNA from yeast cells. Reconstitution was carried out in binding buffer for 20 min at 4 °C. For UV-cross linking experiments, U6-Prp24 binary complex was reconstituted in a binding buffer omitting tRNA and BSA. Protein-RNA complexes were then analyzed by 6 % or 10 % non-denaturing polyacrylamide gel electrophoresis. When radioactively labeled *in vitro* transcribed U6 snRNA was used, gel was transferred on a 3 mM Whatmann paper, dried for 30 min at 80 °C and visualized by autoradiography. In case of experiments with total-yeast RNA, protein-RNA complexes were analyzed by Northern.

The apparent Prp24-U6 snRNA dissociation constant (K_d) was calculated according to formula $K_d = [R] \times [P] / [PR]$ where [R] is the concentration of unbound RNA, [P] signifies the concentration of free protein, and [PR] stands for the concentration of protein-RNA complex (Black *et al.*, 1998). To determine the ratio of unbound U6 snRNA to U6 snRNA in the binary complex ($[R] / [PR]$), certain concentration of U6 snRNA was titrated out with different concentrations of Prp24 protein and quantified by Phosphor Imager.

Binding Buffer

30 mM Tris /HCl pH 7.5

150 mM NaCl

8 mM MgCl₂

2 mM DTT

4 % Glycerol

0.1 μ g/ μ l tRNA

40 μ g/ μ l BSA

Binding Buffer for UV-cross linking assays

30 mM Tris /HCl pH 7.5

150 mM NaCl

8 mM MgCl₂

2 mM DTT

4 % Glycerol

3.2.5.8 Methods for Chemical Modification of RNA

In order to investigate secondary structure of U6 snRNA in isolated native U6 snRNPs as well as to obtain first clues of possible protein-RNA interactions, different RNA-modification reagents were applied (Ehresmann *et al.*, 1987; Krol and Carbon, 1989; Moine *et al.*, 1997). These reagents modify unpaired nucleotides, while base-paired nucleotides or those bound by protein remain unmodified. For this purpose, native U6 snRNPs were isolated using TAP method and incubated with one of the following reagents: DMS (*dimethylsulfate*), CMCT (*1-cyclohexyl-3-(2-morpholinoethyl)-carbodiimide metho-p-toluene sulfonate*), or Kethoxal (β -*ethoxy-a-ketobutyraldehyde*) (also see Figure 3.1).

Modification with DMS

U6 snRNPs were isolated using TAP method and the concentration of the U6 particles was measured by a photometer at 260 nm. 3.3 pmol of isolated native particles or 2 pmol of *in vitro* were diluted to 200 μ l with CaCo-Buffer and 1 μ g of *E. coli* tRNA. To initiate the reaction, 2.5 μ l of DMS solution was added and incubated for 40 min on ice. 2 pmol of *in vitro* transcribed U6 snRNA was incubated in the presence of 1 μ g *E. coli* tRNA, and 2.5 μ l of DMS as described above. As controls, *in vitro* transcribed U6 snRNA or native U6 snRNP was incubated without DMS solution. The reaction was stopped with 50 μ l of DMS-Stop-Buffer and RNA was precipitated with ethanol in the presence of 10 μ g of glycoblue and ethanol. Precipitated RNA was resuspended in 100 μ l of TES-Buffer and extracted with 100 μ l of PCI. The aqueous phase was once more ethanol precipitated and resuspended in 3.5 μ l of CE-buffer.

CaCo-Buffer

50 mM Cacodylic acid/KOH pH 7.0
50 mM KCl

TES-Buffer

10 mM Tris/HCl pH 7.5
1 mM EDTA
0.1 % (w/v) SDS

DMS-Stop-Buffer

1 M Tris/HOAc pH 7.5
2 M β -mercaptoethanol
12.5 mM EDTA

CE-Buffer

10 mM Cacodylic acid/KOH pH 7.0
0.2 mM EDTA

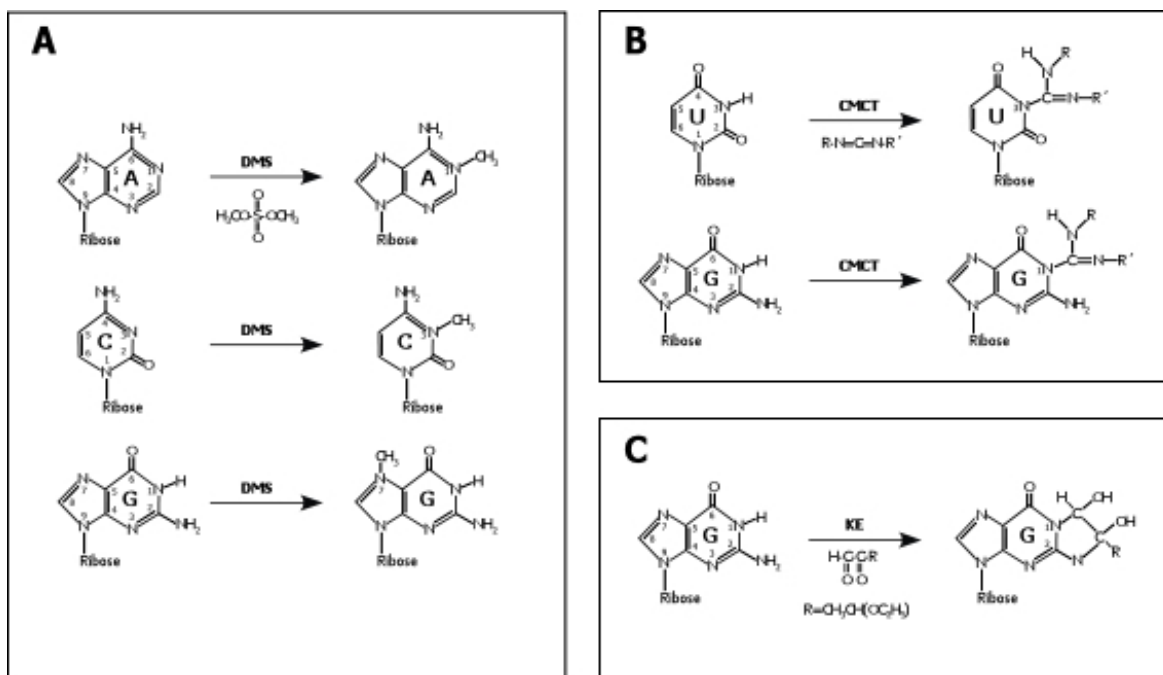


Figure 3.1 Chemical Modification of RNA with DMS, CMCT, and Kethoxal. (A) Methylation of N1-A and N3-C with DMS. **(B)** Modification of N3-U and N1-G sites with CMCT. **(C)** Modification of N1- and N2-G positions with Kethoxal. Since cyclic adduct of guanine is sensitive to basic pH, it must be stabilized in a buffer containing borate ions (Ehresmann *et al.*, 1987).

Modification with CMCT

Modification experiments with CMCT were performed in 100 μ l of borate buffer, which contained 3.3 pmol of native U6 snRNPs and 12.5 μ l of CMCT-solution. Reaction was carried out for 60 min on ice and stopped with 10 μ g of glycogen, 3 M NaOAc pH 5.2, and ethanol (abs). 2 pmol of *in vitro* transcribed U6 snRNA was incubated in the presence of CMCT and treated as described above. As controls, *in vitro* transcribed U6 snRNA or native U6 snRNP was incubated without CMCT solution. RNA was precipitated and processed as above (see 3.2.4.8.1). In the end, RNA pellet was resuspended in 3.5 μ l of CE-buffer.

Borate-Buffer

50 mM Borate/KOH pH 8.0
50 mM KCl
10 mM MgCl₂

CMCT-Solution

0.4 M CMCT prepared freshly
in borate buffer

Modification with Kethoxal

Kethoxal reactions were carried out with 3.3 pmol of U6 snRNPs in 100 μ l of Ca-Co buffer and 2 μ l of kethoxal from stock solution was added to initiate the reaction. Reaction was carried out for 80 min on ice and stopped by 20 μ g of glycoblu, 15 μ l of 3M NaOAc /Borate and 400 μ l of ethanol (abs). 2 pmol of *in vitro* transcribed U6 snRNA was incubated in the presence of 2 μ l of kethoxal and treated as described above. As controls, *in vitro* transcribed U6 snRNA or native U6 snRNP was incubated without kethoxal solution. After precipitation, RNA was resuspended in 100 μ l of TES /Borate and further processed as above (see 3.2.4.8.1). In the end, RNA pellet was resuspended in 3.5 μ l of CE /Borate buffer.

3 M NaOAc /Borate

3 M NaOAc pH 5.2

50 mM Borate /KOH pH 7.0

TES /Borate

10 mM Tris /HCl pH 7.5

1 mM EDTA

50 mM Borate /KOH pH 7.0

0.1 % (w/v) SDS

CE /Borate

10 mM Cacodylic acid /KOH pH 7.0

0.2 mM EDTA

50 mM Borate /KOH pH 7.0

3.2.5.9 Hydroxyl Radical Footprinting

Using the method of hydroxyl radical footprinting, binding area of a protein on RNA can be analyzed since hydroxyl radicals (\bullet OH) can attack riboses and cleave the sugar-phosphate backbone of RNA if not protected by protein (Celander and Cech, 1990; Dixon *et al.*, 1991; Powers and Noller, 1995). In the reaction, hydroxyl radicals were produced from ascorbic acid through so called a *Fenton reaction* as it follows: $[\text{Fe}(\text{EDTA})]^{2-} + \text{H}_2\text{O}_2 \rightarrow [\text{Fe}(\text{EDTA})]^- + \text{OH}^- + \bullet\text{OH}$. Fe^{2+} ion was complexed to the reagent of EDTA in order to constrict the action radius of the hydroxyl radicals. During this study, hydroxyl radical footprinting technique was applied to investigate protein-RNA interactions in native U6 snRNPs as well as in U6 snRNA-Prp24p binary complex.

Hydroxyl radical footprinting experiments with native U6 snRNPs were performed as follows. U6 snRNPs were isolated using TAP method and the concentration of the U6 particles was measured by a photometer at 260 nm. 3.3

pmol of isolated native particles was diluted to 200 μ l with CaCo-Buffer. To initiate hydroxyl radical reaction, 8 mM Fe (II)-EDTA, 0.005 % (v/v) H₂O₂, and 5 mM ascorbic acid were added and particles were incubated for 10 min on ice. 2.0 pmol of *in vitro* transcribed U6 snRNA was incubated in the presence of 1 μ g *E. coli* tRNA, 0.5 mM Fe(II)-EDTA, 0.005 % (v/v) H₂O₂, and 5 mM ascorbic acid as described. As controls, *in vitro* transcribed U6 snRNA or native U6 snRNP was incubated without Fenton reagents. After incubation, the reactions were stopped with 23 μ l stop-mix and 800 μ l of ethanol (abs). After precipitation, RNA was resuspended in 100 μ l of TES buffer and extracted with 100 μ l of PCI. The aqueous phase was once more ethanol precipitated and resuspended in 3.5 μ l of CE-buffer.

For the investigation of U6 snRNA-Prp24p binary complex with hydroxyl radicals, first 0.6 pmol of *in vitro* transcribed non-radioactive U6 snRNA was incubated with increasing amounts of recombinant Prp24 protein (0.02 μ M, 0.2 μ M, 0.7 μ M, and 1 μ M) in a final volume of 40 μ l binding buffer. Subsequently, the reaction mixture was diluted with CaCo-buffer to a final volume of 200 μ l. To initiate hydroxyl radical reaction, 0.5 mM Fe (II)-EDTA, 0.003 % (v/v) H₂O₂, and 2.5 mM ascorbic acid were added and particles were incubated for 10 min on ice. As controls, *in vitro* transcribed non-radioactive U6 snRNA or U6 snRNA-Prp24p complex with the highest amount of Prp24 protein concentration (1 μ M) was incubated in the absence of Fenton reagents. The reactions were stopped and further processes as in above. Finally, RNA was resuspended in 3.5 μ l CE-buffer. The cleavage products were analyzed by primer extension .

Fe (II)-EDTA Stock Solution

20 mM (NH₄)₂Fe(SO₄)₂
40 mM EDTA

H₂O₂ solution (0.4 %)

30 % H₂O₂ was diluted 1:75 with ddH₂O

Stop Mix

1 μ l Glycoblue (10 μ g/ μ l)
2 μ l 2 M Thiourea
20 μ l 3 M NaOAc pH 5.2

Fe (II)-EDTA, H₂O₂, ascorbic acid, and stop mix solutions were all prepared freshly before using in the experiment. To prepare Fe (II)-EDTA solution, 1:10 dilutions of 0.4 M (NH₄)₂Fe(SO₄)₂ and 0.8 M EDTA first mixed and subsequently further diluted 1:1 with ddH₂O.

3.2.5.10 UV-Cross Linking Experiments

Any direct contact between an amino acid chain of a protein and a base of the RNA is susceptible to UV-light (254 nm). UV-irradiation of RNA-protein complexes will result in a zero-length cross link and one covalent bond between the RNA and the protein (Urlaub *et al.*, 2005). To investigate such possible protein-RNA contacts in native U6 snRNP particle as well as in U6 snRNA-Prp24p binary complex, UV-cross linking experiments were performed. 25 μ l droplets of sample were divided on a pre-cooled 10-well multi-test slide. The glass slide with the samples was put on top of an aluminum block placed on ice. Samples were UV-irradiated for 2 min at a distance of 2 cm from UV source (UV-lamps, 254 nm, 8 W).

UV-cross linking experiments with native U6 snRNPs were as follows. U6 snRNPs were isolated using TAP method and 13.5 pmol of U6 snRNPs were UV-irradiated. Samples were then pooled together and digested with proteinase K as described above. RNA was extracted with PCI, precipitated with ethanol, and resuspended in 3.5 μ l of CE-buffer. 27 pmol of native U6 snRNA, which was isolated from native U6 snRNP by proteinase K digestion and PCI-extraction, was also UV-irradiated as described above. UV-irradiated native U6 snRNA was precipitated with ethanol and resuspended in 3.5 μ l of CE-buffer. As controls, native U6 snRNA or native U6 snRNP was not UV-irradiated, precipitated with ethanol, and resuspended in 3.5 μ l of CE-buffer.

In order to identify cross linked proteins, immunoprecipitation of UV-irradiated samples was performed under conditions where protein-protein interactions within the particles were disrupted and only a single protein-RNA was co-precipitated. For this purpose, 57 pmol of U6 snRNPs were UV-irradiated as above. In case of determining U6 snRNA-Prp24 protein cross links, protein-protein interactions were disrupted with 1 % (w/v) SDS. However, when U6 snRNA-LSm protein cross links were investigated, 1.5 % SDS (w/v) was used. Samples were incubated for 10 min at 37 °C and further for 10 min at 70 °C. After cooling down to room temperature, one volume of 10 % (v/v) Triton X-100 was added to a final concentration of 5 % (v/v) in order to chelate excess SDS. Subsequently, samples were diluted with 6 volumes of PBS and mixture was transferred to the prepared antibody-coupled protein A-sepharose beads. Immunoprecipitation was performed with anti-Prp24p antibodies when U6 snRNA-Prp24p cross links were studied. U6 snRNA-LSm protein cross links were analyzed by immunoprecipitation with anti-YFP antibodies. As control, 57 pmol of U6 snRNPs were treated and

immunoprecipitated without UV-irradiation. To check the non-specific binding to protein A-sepharose beads, both non-irradiated and irradiated samples were immunoprecipitated with non-immune serum (NIS). After immunoprecipitation, samples bound to beads were incubated with proteinase K and RNA was extracted with PCI. RNA pellet was finally dissolved in 2.0 μ l of CE-buffer. Cross linking products were analyzed by primer extension.

For the UV-cross linking experiments with U6 snRNA-Prp24p complex, 0.6 pmol of *in vitro* transcribed radioactively labeled U6 snRNA was reconstituted with 1 μ M recombinant Prp24 protein in a final volume of 15 μ l binding buffer. Complexes were UV-irradiated as described above. To check the efficiency of U6 snRNA-Prp24 cross linking, samples were digested with 3 μ g RNase A and/or RNase T1 by incubating for 30 min at 52 °C and loaded on a SDS-polyacrylamide gel. RNA bands were visualized by autoradiography. When cross linked sites in binary complex were analyzed, 0.6 pmol of *in vitro* transcribed non-radioactively labeled U6 snRNA was reconstituted with recombinant Prp24p and UV-irradiated as above. Subsequently, samples were digested with proteinase K. Extracted RNA was precipitated with ethanol and resuspended in 3.5 μ l of CE-buffer.

3.2.5.11 Primer Extension Analysis of Modified U6 snRNA

Primer extension was used to analyze U6 snRNA, which was recovered after a reaction. With primer extension, a certain region of U6 snRNA was hybridized to a radioactively labeled DNA oligonucleotide (yU6_68-84 and yU6_94-112) and complementary cDNAs were elongated by reverse transcriptase. The progression of reverse transcriptase on U6 snRNA template was blocked when a U6-nucleotide was cleaved out with hydroxyl radicals; specifically modified with a reagent; or cross linked to a peptide fragment (Ehresmann *et al.*, 1987). The produced cDNAs in varying sizes were then analyzed by denaturing polyacrylamide gel electrophoresis.

For primer extension reactions, 1 μ l of recovered RNA was incubated with 1.5 μ l of HY-mix for 1 min at 96 °C. Hybridization of oligonucleotides to U6 snRNA was allowed by cooling the samples down to room temperature. In order to be able to identify the exact positions of cDNA fragments, a sequencing reaction was carried out using 100 fmol of *in vitro* transcribed U6 snRNA as a template and 0.5 μ l of either dideoxynucleotides (ddNTPs). After hybridization step, 2.5 μ l of RT-mix was added to samples and incubated for 45 min at 43 °C. After incubation,

reactions were stopped with 6.5 μ l of RNA loading buffer and RNA-cDNA hybrids were denatured for 3 min at 96 °C. In the end, 10 μ l of reaction mixture was loaded on a 0.4 mm denaturing 10 % polyacrylamide gel and cDNA fragments were separated for 2 h at 65 W. Radioactively labeled cDNA fragments were then detected by autoradiography.

HY-Mix

0.5 μ l [γ -³²P] ATP labeled
DNA oligonucleotide
0.25 μ l 10 x HY-buffer
0.75 μ l ddH₂O

10 x HY-Buffer

0.5 M Tris /HCl pH 8.4
0.6 M NaCl
0.1 M DTT

RT-Mix

2.15 μ l ddH₂O
0.25 μ l 10 x RT-buffer
0.1 μ l dNTP Mix (each 5 mM dATP,
dGTP, dCTP, and dTTP)
0.1 μ l Reverse Transcriptase

10 x RT-Buffer

0.5 M Tris /HCl pH 8.4
0.6 M NaCl
0.1 M MgCl₂
0.1 M DTT

ddNTPs: each 0.5 mM ddATP, ddGTP
ddCTP, and ddTTP

RESULTS

5.1 RNA Structure and RNA-Protein Interactions in Purified Yeast U6 snRNPs

5.1.1 Isolation of Native U6 snRNPs from the Yeast *S. cerevisiae*, using the Tandem Affinity Purification (TAP) Method and C-terminally tagged Prp24p

To purify the yeast U6 snRNP particles for our structural investigations, a yeast strain expressing TAP-tagged Prp24 was constructed. The TAP tag consists of two IgG binding domains of *Staphylococcus aureus* protein A and a calmodulin-binding peptide (CBP) separated by a tobacco etch virus (TEV) protease cleavage site (Puig *et al.*, 2001). The TAP method involves the amplification of the TAP tag as well as nearby *TRP1* marker (from *Kluyveromyces lactis*) and the introduction of this construct into yeast cells at the C-terminus of Prp24p in-frame with its coding region (see also Figure 4.2).

The TAP-cassette coding for the C-terminal TAP-tag was amplified from plasmid pBS1479 by PCR using for_ and rev_TAP oligonucleotides. Both primers contained a region of similarity to the *PRP24* gene (48 nucleotides long) and a constant priming region on the pBS1479 plasmid. Forward primer hybridized at the 5'-end of the CBP coding sequence and reverse primer in the vector downstream of the selection marker (see also Figure 4.1 A). In addition, forward primer was designed in such a way that stop codon of *PRP24* gene was deleted and the last C-terminal residue was fused in-frame to the TAP tag (Puig *et al.*, 2001). The amplified PCR product was extracted with PCI, precipitated with ethanol, and loaded on a 1 % Agarose gel to confirm the quality of PCR reaction (Figure 4.1 B).

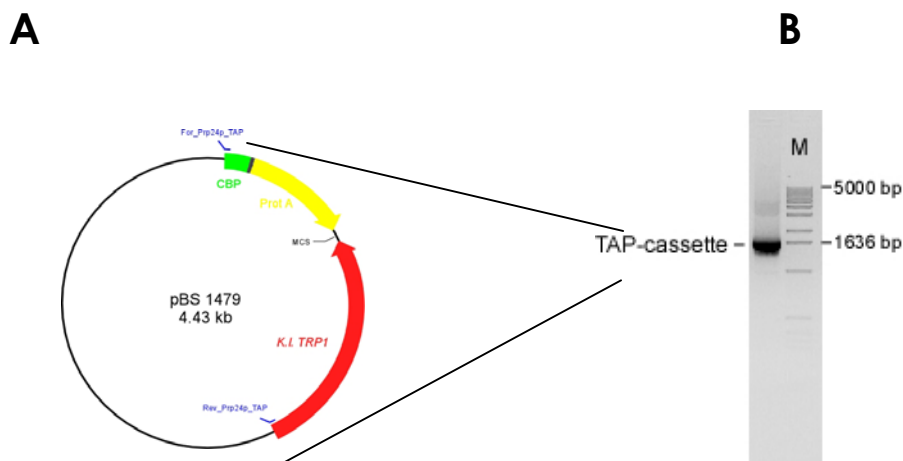


Figure 4.1 PCR amplification of the TAP-cassette. (A) Schematic representation of plasmid pBS 1479 and TAP-cassette. (B) 1 % Agarose gel electrophoresis of the amplified TAP-cassette. M is DNA ladder in base pairs.

Next, the wild type *TR2* haploid cells were transformed with *PRP24*-TAP-cassette using 1, 20, and 50 μg of amplified DNA (see also Figure 4.2). Transformants were incubated 3-4 days at 30 $^{\circ}\text{C}$ on tryptophane deficient synthetic dextrose plates (*SD-TRP*). Transformants grew normally like parent *TR2* cells without any detectable growth defect. After transformant cell colonies were visible enough, single colonies were picked and streaked out on fresh *SD-TRP* plates. After further incubation at 30 $^{\circ}\text{C}$, clones were screened by PCR analysis and Western blot.

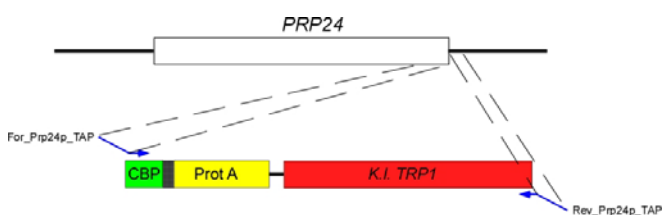


Figure 4.2 C-terminal genomic tagging of *PRP24* gene with TAP-cassette. The strategy of tagging of Prp24p with TAP tag at its C-terminus is illustrated schematically.

In order to verify the correct integration of the TAP-cassette at the 3' -end of *PRP24* gene, PCR analysis was performed. Chromosomal DNA was isolated from putative positive colonies and PCR reaction was carried out using checking oligonucleotides for *PRP24* (Figure 4.3). Forward check primer annealed in the

middle of the *PRP24* gene and reverse check primer was designed to recognize the 3'-untranslated region of the *PRP24* gene.

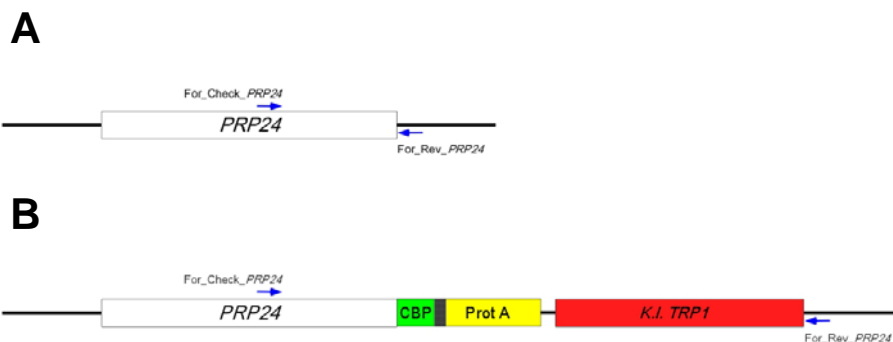


Figure 4.3 Schematic representation of the PCR analysis to verify the correct integration of the TAP-cassette. With the designed primers, positive colonies would result in longer PCR product (**B**) than wild type cells (**A**) as TAP-cassette was inserted at the downstream of *PRP24* gene.

After amplification with checking oligonucleotides, PCR products were loaded on a 1 % Agarose gel, and Figure 4.4 A shows the result of the PCR analyses. The putative positive clone (Figure 4.4 A, lane 2) gave rise to a PCR product of 2567 base-pairs long, whereas wild type cells (Figure 4.4 A, lane 1) led to a PCR fragment of only 971 base-pairs long. This indicates that the cells from this clone incorporated the TAP insert at the C-terminus of *PRP24* gene. To check for the expression of the TAP-tag at the C-terminus of Prp24 protein, Western blot was carried out (Figure 4.4 B). Western blot was developed with a peroxidase anti-peroxidase complex (PAP) that detects Prot A within the TAP-tag. The Prp24 protein has a molecular weight of 51 kDa. The molecular weight of the TAP-tagged Prp24p is expected to be 71 kDa as the TAP-tag itself has a size of 20 kDa. Western blot analysis of the positive clone (Figure 4.4 B, lane 2), which had the correct integration into the genome showed a positive signal at about 71 kDa. However, analysis of the wild type cells resulted only background levels of the signal about 71 kDa (Figure 4.4.B, lane 1). Therefore, this clone expresses the TAP-tag at the C-terminus of Prp24p and was chosen as the recombinant strain carrying Prp24p-TAP-tag for the rest of the study.

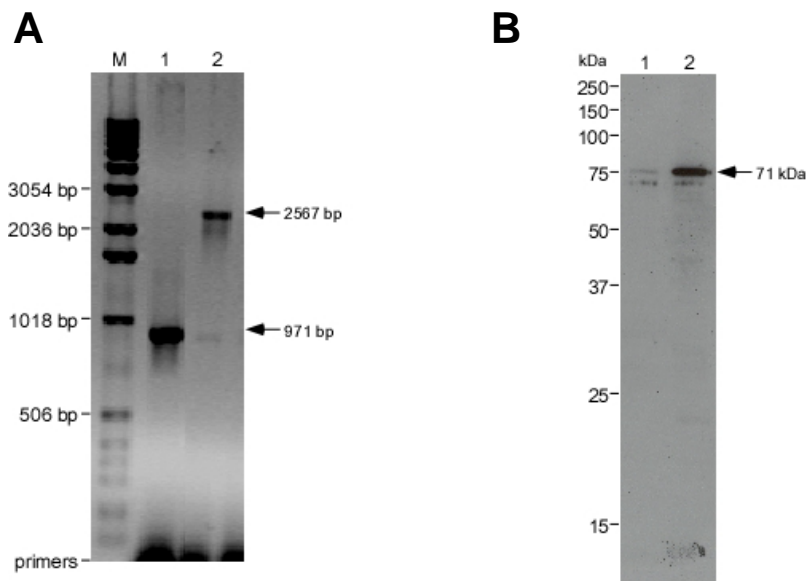


Figure 4.4 Transformant characterizations by PCR analyses and Western blot. (A) Chromosomal DNA was isolated from both wild type (lane 1) and positive colony (lane 2) and PCR products amplified with *PRP24_check* oligonucleotides were loaded on a 1 % Agarose gel. Arrows mark the size of the PCR product of the wild type (971 base-pairs) and of the positive colony (2567 base-pairs). M is DNA ladder in base pairs. **(B)** Expression of TAP-tag in wild type cells (lane 1) and in positive colony (lane 2) was analyzed by Western blot using PAP antibody. Arrow shows the size of the TAP-tagged Prp24p. The size marker in kDa is shown on the left.

After the fusion of the TAP-tag to the Prp24 protein, the yeast strain expressing the Prp24p-TAP tag was used for the tandem affinity purification of U6 snRNPs. The whole-cell extract from 8 L of yeast culture was prepared and U6 snRNP particles were purified by the TAP-method (Figure 4.5 A). The Prp24 protein and its associated components were initially passed through IgG-Sepharose beads. After washing, the bound material was eluted from the beads by TEV protease cleavage. The eluate of the first column was then incubated with calmodulin affinity resin in the presence of Ca^{2+} ion, which is required by calmodulin binding peptide for binding. Elution of the bound material from calmodulin beads were performed by chelating Ca^{2+} ions from the solution with EGTA molecules. To improve efficiency of the elution, calmodulin beads were incubated with the elution buffer for 20 min. After the first elution, the beads were incubated second time with the elution buffer as above. All of the buffers used during TAP purification contained 0.1 % (w/v) detergent (NP-40) in order to decrease unspecific binding of proteins to the beads. However, the elution buffer contained 0.02 % (w/v) NP-40 since higher concentrations of any detergent

interfered with electron microscopy sample preparation. To obtain highly purified particles for mass spectrometry as well as for electron microscopy analysis, the eluate was subjected to an additional purification step by glycerol-gradient centrifugation. The first eluate was loaded on a 10 % -30 % (v/v) glycerol gradient containing 200 mM KCl and U6 particles were sedimented for 15 h at 45 000 rpm using TH-660 rotor. After sedimentation, 24 fractions of 175 μ l were collected from bottom to top using a bottom-fraction collector. Protein and RNA contents of the each fraction were extracted by PCI. Proteins were analyzed by SDS-polyacrylamide gel electrophoresis whereas RNA content was loaded on a denaturing-polyacrylamide gel. Figure 4.5 A shows the snRNA distribution across the gradient. Fractions 15-18 contained only U6 snRNA and were essentially free of any other snRNA. In Figure 4.5 B, the protein composition of each fraction is shown.

Proteins co-sedimenting with the U6 snRNA in the peak fractions 16 and 17 were identified by mass spectrometry in collaboration with Dr. Henning Urlaub (Bioanalytical Mass Spectrometry Group, Max-Planck-Institute of Biophysical Chemistry). Visible protein bands from fractions 16 and 17 were cut out and corresponding bands were pooled. The proteins in the bands were then digested with trypsin according to Shevchenko *et al.*, 1996. For mass spectrometry, 0.5-1.0 μ l of supernatant of the digest was analyzed by MALDI-MS-TOF mass spectrometer under standard conditions using the thin-layer technique (Vorm *et al.*, 1994). When a protein could not be identified unambiguously by MALDI-MS fingerprint, or when, in addition to the main protein component, the MALDI spectra revealed the potential presence of several other less-abundant proteins, LC-MSMS was performed (Hartmuth *et al.*, 2002). Proteins from sequenced peptides were identified by database search against the NCBI database using Mascot as a search engine.

Mass spectrometry analysis showed the presence of seven distinct proteins in fractions 16 and 17: Prp24p and six of the LSm2-8 proteins, LSm4, LSm7p, LSm8p, LSm2p, LSm5p, and LSm6p. This is the essentially the same set of proteins that was found in purified U6 snRNPs (Stevens *et al.*, 2001). From the excised protein bands of fraction 16 and 17, no tryptic fragments of LSm3p could be sequenced. In fact, LSm proteins are in principle difficult to detect by mass spectrometry, due to the paucity of tryptic fragments obtained, and for this reason, probably eluded mass spectrometric detection. Indeed, the presence of LSm3p in our purified U6 snRNPs could be demonstrated independently when LSm3p (10 kDa) was

additionally tagged with a 30 kDa yECitrine tag in the Prp24p-TAP-tag strain. TAP tag purified U6 snRNPs contained stoichiometric amounts of LSm3p-yECitrine fusion protein, which was detected as a 40 kDa protein (see section 4.3.2 and Figure 4.19 C).

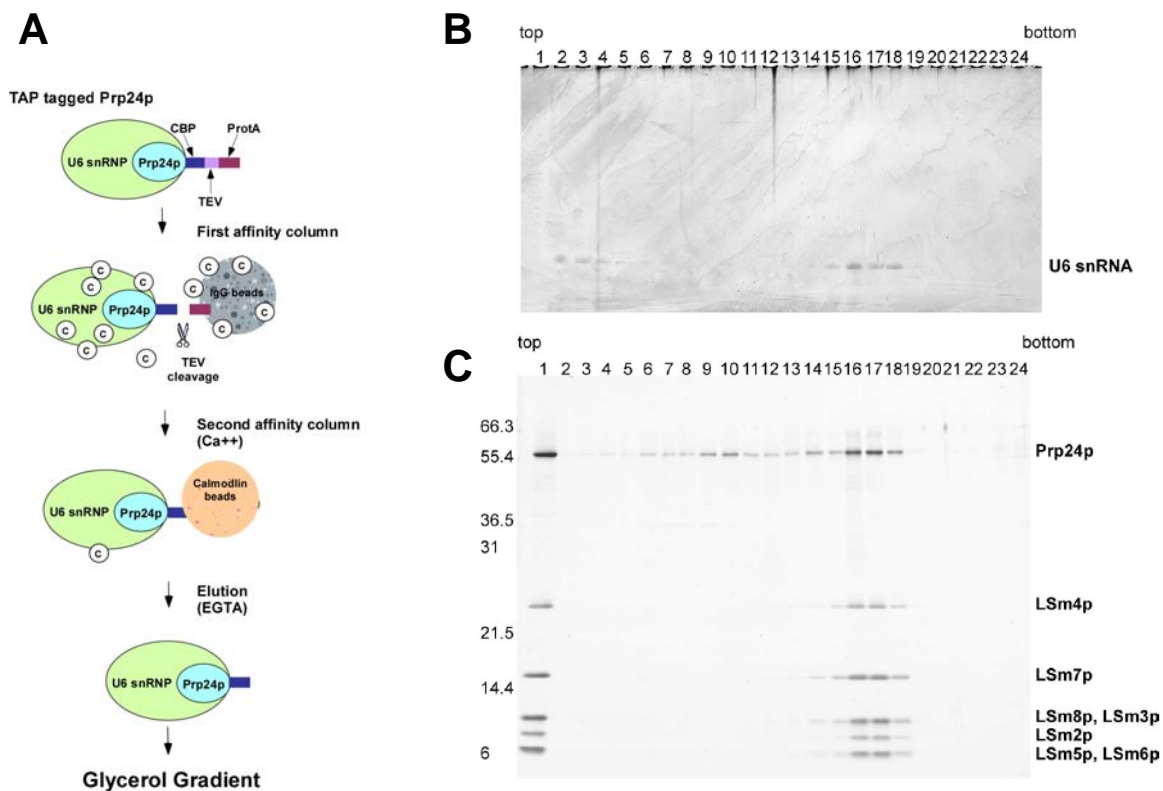


Figure 4.5 Purification of the yeast U6 snRNP with tagged Prp24p using the TAP method. The U6 snRNP was purified from whole-cell extract by two affinity purification steps (Puig *et al.*, 2001), followed by sedimentation on a 10 % -30 % (v/v) glycerol gradient (**A**). Gradient fractions, numbered above each lane, were analyzed for their (**B**) RNA and (**C**) protein content by denaturing PAGE or SDS-PAGE, respectively. Gels in (**B**) and (**C**) were stained with silver. The identity of the bands is indicated on the right.

5.1.2 Determination of the Secondary Structure of Naked U6 snRNA and U6 in Purified U6 snRNP Particles

The availability of highly pure U6 snRNPs allowed us first to investigate the structure of the U6 snRNA within these purified particles and, second, to determine how and where U6-associated proteins, in particular Prp24p, contact the U6

snRNA. We addressed these questions by initially analyzing the structure of the U6 snRNA in the purified U6 snRNP and comparing it to that of the naked U6 snRNA synthesized by *in vitro* transcription. For this purpose, we used three chemical reagents: demethylsulfate (DMS), 1-cyclohexyl-3-(2-morpholinoethyl) carbodiimide metho-*p*-toluene sulfonate (CMCT), and β -ethoxy- α -ketobutryal aldehyde (kethoxal or KE). These reagents act at the Watson-Crick base-pairing positions of a nucleotide: DMS modifies adenine and cytosine; CMCT modifies uracil and, to a lesser extent, guanine; while KE modifies guanine only (Moine *et al.*, 1997; also see Figure 3.1). Reactivity of a nucleotide towards any of these reagents is indicative of it being unpaired. Lack of reactivity indicates a paired status in the naked RNA and, either a paired status or an interaction with a protein in the RNP. Modifications were detected by primer extension with reverse transcriptase, which cannot read through the modified bases and stops after transcribing the nucleotide immediately preceding the modified base (Ehresmann *et al.*, 1987).

To determine the secondary structure of U6 snRNA in native particles, U6 snRNP was isolated by TAP method and incubated with the chemical reagents, DMS, CMCT, or kethoxal. To investigate the secondary structure of the naked U6 snRNA without proteins, *in vitro* transcribed U6 snRNA was treated with the reagents as in the case of U6 snRNP. To detect the modified bases, two radioactively labelled DNA oligonucleotides were used: γ U6_68-84 annealed U6 snRNA between 68th and 84th nucleotides and γ U6_94-112 at the very 3'-end. These oligonucleotides allowed us to analyze modifications of 75 % of all U6 snRNA nucleotides, ranging from nucleotides 2 to 89.

Representative examples of the chemical probing experiments are shown in Figure 4.6. The modification patterns of naked U6 snRNA (lane 2 in each of Figure 4.6 A-F) are compared directly to U6snRNA in native U6 snRNPs (lane 3 in each of Figure 4.6 A-F). The overall results, described in detail below, are summarised in Figure 4.6 G and H. Bases were assigned to a colour-coded group according to the intensity of modification observed. Blue implies no modification, pink implies only weak modification, and red implies strong modification by the chemical reagent. The classification of bases in this mode, resulting from our analysis, is shown superimposed on the secondary-structure models of the naked U6 snRNA (Figure 4.6 G) and that of the U6 snRNA in the snRNP particle (Figure 4.6 H).

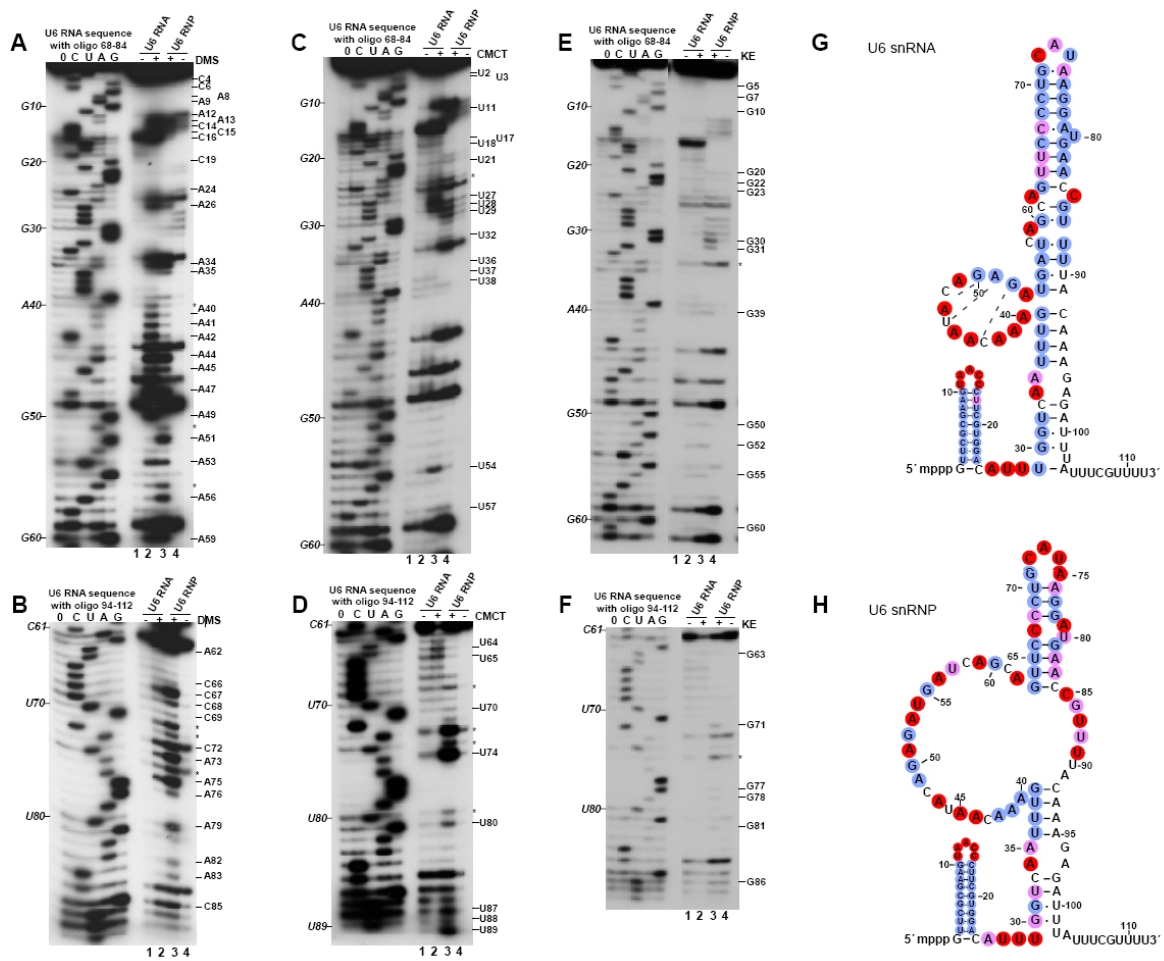


Figure 4.6 Structure-probing of purified U6 snRNPs with DMS, CMCT, and kethoxal. Primer extension reactions were carried out with two radiolabelled oligonucleotides, complementary to nucleotides 68–84 of the U6 snRNA (**A**, **C** and **E**) or 94–112 (**B**, **D** and **F**). In each gel, the positions where reverse transcription was blocked because of chemical modification of the base are shown on the right. Lanes C, U, A and G correspond to sequencing ladders made with the same oligonucleotide ("0", no ddNTP). Asterisks (*) indicate the nucleotides that showed an unusual reactivity to the chemical probes. Primer extension analyses of naked U6 snRNA (lanes 1 and 2 of each gel) and of U6 snRNA within isolated U6 snRNP (lanes 3 and 4) are shown. In each panel, in lanes 2 and 3 ("+" reagent) the reaction mixture was complete, while in lanes 1 and 4 ("–" reagent) the chemical reagent was omitted. (**G**) Comparison of the deduced secondary structures of naked U6 snRNA and (**H**) U6 snRNA in the snRNP. The accessibilities of the bases towards DMS, CMCT, and kethoxal are represented by coloured disks superimposed on the secondary structure models of the naked (**G**) U6 snRNA and (**H**) of the U6 snRNA in the snRNP particle. Bases protected from modification, blue; bases weakly modified, pink; bases strongly modified, red.

A first overall comparison of the naked U6 snRNA structure with that in the particle reveals that the RNA is very compact in the naked RNA state and more open in the protein-bound RNP state (compare Figure 4.6 G and H). This is most pronounced in two regions. The first is the U6 3'-stem-loop (nucleotides G63–C84). In the naked RNA, most of the nucleotides are not modified, except for C72, which is highly modified. However, in the RNP, the very same structural element (i.e. nucleotides 63–84) contains six highly modified bases, with four out of five of the loop bases exposed to modifications (Figure 4.6 B and D, lanes 2 and 3). The second region comprises nucleotides proposed to form the upper telestem (see Figure 4.6 G and H, and below for details). The three adenosine bases (A40–A42) assumed to form part of the ascending strand of the upper telestem are clearly accessible to modification by DMS in the naked RNA (Figure 4.6 A, lane 2). However, nucleotides U87–U89 (Figure 4.6 D, lane 2) proposed to form the descending strand of the upper telestem are not accessible to CMCT modification, suggesting that they are base-paired. Their most reasonable partners are G60, U57 and A56, which are also protected as shown in Figure 4.6 G (blue disks). In conclusion, this demonstrates clearly that the upper telestem structure is not formed in the naked RNA.

Interestingly, nucleotides A40–A42 and U87–U89 show the opposite modification pattern in the U6 snRNP when compared to the naked RNA. Whereas adenosine bases A40–A42 are no longer accessible to modification (Figure 4.6 A, lane 3), nucleotides U87–U89 are fully accessible (Figure 4.6 D, lane 3). In fact, the whole region from C85 to U89 appears to be predominantly single-stranded (Figure 4.6 H). We therefore conclude that the descending strand of the proposed upper telestem is essentially unpaired, making the existence of the upper telestem in the U6 snRNP also unlikely. Importantly, our footprinting data further indicate that protection of A40–A42 from modification in the U6 snRNP is most likely due to interaction with a protein. In contrast to the upper telestem, the lower telestem is compatible with our structure mapping data. In both the naked U6 snRNA and U6 snRNP, U36 to G39 were fully protected (Figure 4.6 C and E, lanes 2 and 3).

In addition, we reproducibly observed protection of G30–U32 in the U6 snRNA. The same nucleotides are somewhat less protected in the U6 snRNP (Figure 4.6 C and E, lanes 2 and 3). Their potential base-pairing partners are A99–U101. Although structural data for these latter nucleotides are difficult to obtain, we propose that this small helix (G30–C33, G98–U101) exists as an extension to the

lower telestem in the naked U6 snRNA. However, the same helix may not be stable in the U6 snRNP. In conclusion, our data indicate that as a result of interaction of Prp24p and the LSm2p–8p proteins with U6 snRNA, a significant number of bases are more exposed in the snRNP than in the naked snRNA.

5.1.3 Mapping the Binding Region of the U6 Proteins on the U6 snRNA by Hydroxyl Radical Footprinting

The experiments with chemical reagent have already given an initial indication as to where Prp24 and LSm proteins likely interact with the U6 snRNA. For example, A40-A42 are not protected in the naked RNA but are protected in the RNP, suggesting that they are bound by U6 proteins. In order to further characterize the protein-RNA interactions thoroughly in purified U6 snRNP, protection of the U6 snRNA backbone in the particle was assayed by hydroxyl radical footprinting. Hydroxyl radicals attack hydrogen of the ribose moiety at positions C1 and C4, leading to the excision of the base and scission of the ribose phosphate backbone (Herzberg and Dervan, 1984; Celander and Cech, 1990; Figure 4.7 A). Since susceptibility of the RNA backbone to hydroxyl radical cleavage is independent of secondary structure, protection of the ribose phosphate backbone from cleavage results only from interaction with proteins or tertiary RNA-RNA interactions that mask the ribose moieties.

For hydroxyl radical experiments, U6 snRNP was isolated by TAP method and incubated with the *Fenton reagent*, which produced hydroxyl radicals (see 3.2.5.9). Naked U6 snRNA, produced by *in vitro* transcription was also incubated with hydroxyl radicals. Additional incubations were performed to control for background RNA cleavage by omitting the *Fenton reagent* for naked U6 snRNA or for native U6 snRNP (Figure 4.7 B, lanes 1 and 4). The protection pattern of the U6 snRNA in the U6 snRNP was analyzed by primer extension using the DNA oligonucleotides as described above. Reverse transcriptase fell off when a base excised out of RNA backbone, causing a stop in cDNA synthesis.

Figure 4.7 B shows the primer extension analysis of hydroxyl radical experiment. Most of the nucleotides in the 5'-half of the U6 RNA in the U6 snRNP are protected to various degrees (see also Figure 4.7 C for summary). A footprint is observed for nucleotides involved in base-pairing, as well as for single-stranded nucleotides, extending from C4 to G60.

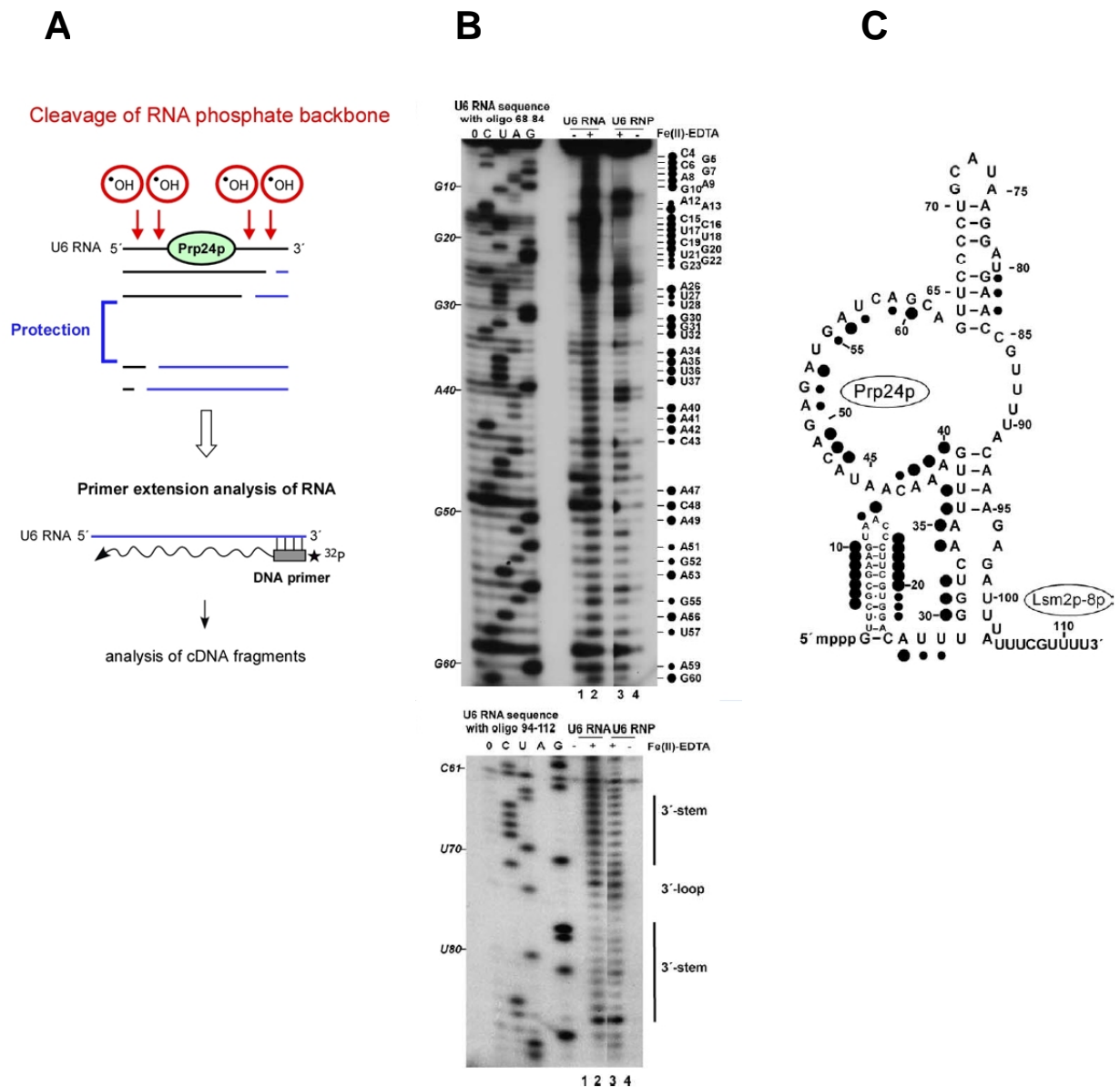


Figure 4.7 Mapping the binding regions of U6 proteins by hydroxyl radicals. (A) shows footprinting experiments schematically. Primer extension reactions were carried out with two radiolabelled oligonucleotides, annealed to the U6 snRNA at (B) nucleotides 68–84 or (C) 94–112. The nucleotide positions where reverse transcription was blocked due to the removal of the base are marked by black dots on the right. Lanes C, U, A and G correspond to sequencing ladders made with the same oligonucleotide. Note that in (C) the lane A is missing. Large dots indicate strong protection, and small dots indicate moderate or slight protection. Modification products from naked U6 snRNA (lanes 1 and 2 of each gel) and isolated U6 snRNP (lanes 3 and 4) are shown; in each case, for lanes 2 and 3 (“+” Fe(II)-EDTA) the reaction mixture was complete, while for lanes 1 and 4 (“–” Fe(II)-EDTA) hydroxyl radicals were omitted. (D) Summary of the U6 nucleotides protected from hydroxyl radicals in the U6 particle (black dots). The Figure shows the secondary structure of the yeast U6 snRNA in the U6 particle, which was established in this study.

The 5'-stem-loop appears to be complexed tightly with the protein(s): nucleotides of both strands of the stem are protected, as well as two out of the five loop nucleotides. Also, several nucleotides of the large internal loop show various degrees of ribose protection; including A40, A41, A42 and C43 (Figure 4.7 B, upper panel). In contrast to the 5'-stem-loop, we find that the 3'-stem-loop of the U6 snRNA in the U6 particle is not protected significantly from hydroxyl radical cleavage (Figure 4.7 B, lower panel, compare lane 2 with lane 3). Only a few nucleotides maybe protected slightly (i.e. positions 81, 82 and 83 of the descending 3'-stem). Therefore, this region does not appear to be contacted strongly by U6 proteins.

5.1.4 Cross Linking of Proteins to U6 snRNA: Identification of Prp24 and LSM Proteins' Binding Site(s)

To obtain independent evidence for contact points between proteins and the U6 snRNA, we performed UV-cross linking of purified U6 particles. Affinity purified U6 snRNPs were transferred on a pre-cooled 10-well multi-test slide embedded on ice and irradiated for 2 min with 254 nm UV-light. After digestion of the proteins of U6 snRNP with proteinase K, the sites of cross links were detected by primer extension. The proteolytic peptide fragment of the protein UV-cross linked to the RNA base blocks the progression of the reverse transcriptase on the RNA template, and the enzyme stops after transcribing the nucleotide immediately before the cross linked base (Urlaub *et al.*, 2002; also see Figure 4.8 A). Since cross linking induced by UV-irradiation at short wavelengths might also induce strand breaks or cause intra-RNA cross links, (both of these also lead to stops or stuttering of the reverse transcriptase), controls were performed to distinguish between reverse transcriptase stops or natural stops (Urlaub *et al.*, 2002). For this purpose, reverse transcriptase patterns from three RNAs were compared: (1) U6 snRNA from UV-irradiated U6 snRNP particles, (2) UV-irradiated naked U6 snRNA and, (3) non-irradiated naked U6 snRNA.

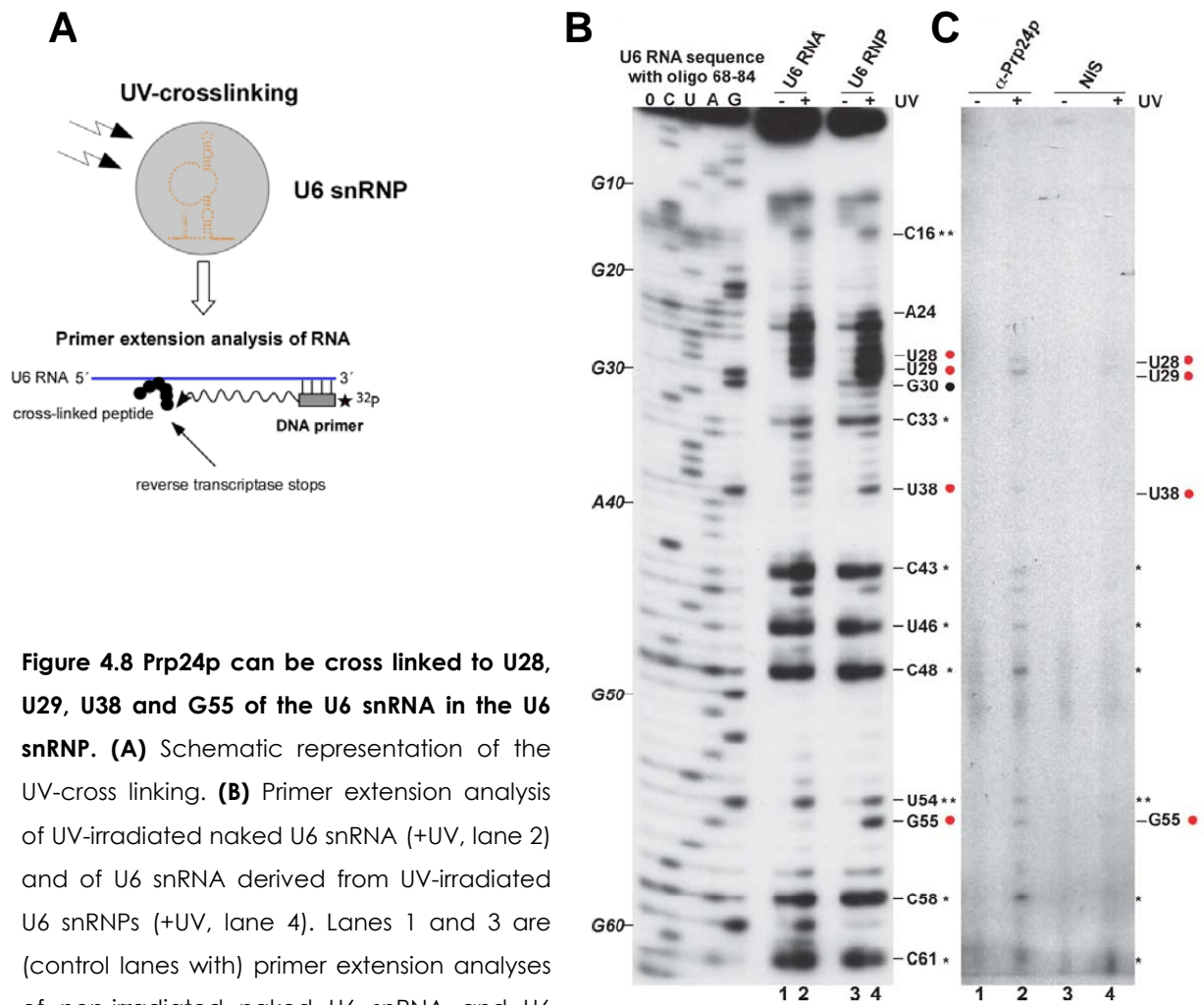


Figure 4.8 Prp24p can be cross linked to U28, U29, U38 and G55 of the U6 snRNA in the U6 snRNP. (A) Schematic representation of the UV-cross linking. **(B)** Primer extension analysis of UV-irradiated naked U6 snRNA (+UV, lane 2) and of U6 snRNA derived from UV-irradiated U6 snRNPs (+UV, lane 4). Lanes 1 and 3 are (control lanes with) primer extension analyses of non-irradiated naked U6 snRNA and U6 snRNA derived from non-irradiated U6 snRNPs (-UV). C, U; A, and G are dideoxy sequence markers. Positions of nucleotides that caused a stop are shown on the right. Note that the actual signals of reverse transcriptase stops are one nucleotide upstream of those that caused the block. UV-cross linking sites of Prp24p on the RNA of the native U6 snRNP are marked by red dots. The asterisks (*) indicate naturally occurring background stops (single asterisk) or putative RNA-RNA cross links (double asterisks). **(C)** Primer extension analysis of the U6 snRNA after immunoprecipitation of denatured U6 snRNPs with an antibody rose against Prp24p (α -Prp24p), either with (lane 2) or without UV-irradiation (lane 1). The non-immune serum (NIS) was used as a control to precipitated UV-irradiated (lane 4) and non-irradiated (lane 3) particles. Nucleotide positions of reverse transcriptase stops due to specific cross linking between Prp24p and the U6 snRNA are indicated on the right side with red dots.

Figure 4.8 B shows the primer extension analysis of the naked U6 snRNA (lanes 1 and 2) and U6 snRNA in the U6 snRNP (lanes 3 and 4). The samples were UV-irradiated before (lane 4) or after (lane 2) isolation of the RNA from the U6 snRNP. Natural strong reverse transcriptase stops in the U6 snRNA occurred at C33, C43, U46, C48, C58, and C61 as these stops were detected irrespective of whether

Figure 4.8 B shows the primer extension analysis of the naked U6 snRNA (lanes 1 and 2) and U6 snRNA in the U6 snRNP (lanes 3 and 4). The samples were UV-irradiated before (lane 4) or after (lane 2) isolation of the RNA from the U6 snRNP. Natural strong reverse transcriptase stops in the U6 snRNA occurred at C33, C43, U46, C48, C58, and C61 as these stops were detected irrespective of whether

the samples had been UV-irradiated (Figure 4.8 B, single asterisks, compare lanes 1 and 3 with lanes 2 and 4). Prominent reverse transcriptase stops were observed at nucleotides C16, A24-U27, and U54 after UV-irradiation of both naked U6 snRNA and U6 snRNPs, suggesting that they do not present protein-RNA cross links but potentially RNA-RNA cross links (Figure 4.8 B, double asterisks, compare lane 2 with lane 4). Additional UV-induced stops were detected at nucleotides G30, U38, and G55. These stops were found exclusively in the U6 snRNA isolated from UV-irradiated U6 snRNPs, indicating that they are caused by a cross linked protein. However, it cannot be excluded that the presence of proteins in the U6 snRNP induces some new RNA-RNA cross links by modulating the U6 snRNA structure. In addition, stops at U28 and U29 were enriched significantly in the U6 snRNP after UV-irradiation, when compared with the UV-irradiated, naked U6 snRNA (Figure 4.8, compare lane 2 with lane 4). This suggests that they were also due to protein specific cross links to these nucleotides.

To determine which U6 snRNP specific protein was cross linked to these nucleotides, immunoprecipitations of UV-irradiated purified U6 snRNPs were performed under conditions where protein-protein interactions in the particles were completely disrupted and only a single protein is precipitated. Specific Prp24p-U6 snRNA cross links were determined after immunoprecipitation with anti-Prp24p antibodies. Figure 4.8 C shows the results of primer extension analysis of RNA species immunoprecipitated with anti-Prp24p antibodies before (lane 1) and after (lane 2) UV-irradiation. Reverse transcriptase stops were detected after immunoprecipitation at nucleotides U28, U29, U38, and G55 with the UV-irradiated particle only (Figure 4.8 C, lane 2). The remaining stops observed after UV-irradiation correspond to naturally occurring background stops or putative intra RNA cross links (indicated by asterisks, compare Figure 4.8 B with C). Controls show that RNA-protein cross links were not immunoprecipitated with the non-immune serum either before (Figure 4.8 C, lane 3) or after (Figure 4.8 C, lane 4) UV-irradiation. We therefore conclude that Prp24p is cross linked to U28, U29, U38 and G55.

The possible contact sites of LSm proteins at uridine rich last 18 nucleotides of 3'-end of the U6 snRNA was analyzed by Northern analysis. To overcome the absence of antibodies rose against LSm proteins, individual LSm proteins were replaced by LSm-yECitrine fusion proteins by homologous recombination in the yeast strain which has also TAP-tag at the C-terminus of Prp24 protein. Extracts

were prepared from these double-tagged strains (i.e. TAP-tag at Prp24p and yECitrine-tag at either of LSM proteins) and U6 snRNPs were isolated by TAP method. Isolated U6 particles were UV-irradiated and U6 snRNA was immunoprecipitated with anti-yECitrine antibodies. Unlike Prp24p-cross links, interactions within the LSM core prior to immunoprecipitation were disrupted by the use of 1.5 % SDS (instead of 1 %) since Sm- and LSM-snRNA interactions are known to be much stronger (Urlaub *et al.*, 1999).

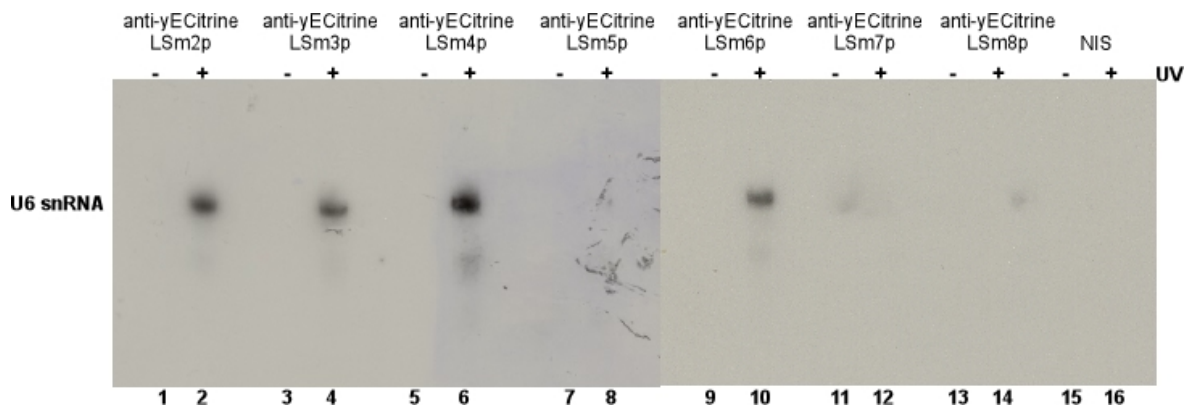


Figure 4.9 Immunoprecipitation of LSM cross links in U6 snRNA by anti-yECitrine antibodies and analysis by Northern blotting. U6 snRNPs were UV-irradiated and protein-protein interactions within LSM ring were disrupted with 1.5 % (w/v) SDS. Subsequently, U6 snRNA-LSM protein cross links were performed with anti-yECitrine antibodies (+UV lanes). As control, U6 snRNPs were immunoprecipitated without UV-irradiation (-UV). The non-immune serum (NIS) was used as a control to precipitate UV-irradiated (Lanes 15 and 16). After immunoprecipitation, samples bound to beads were digested with proteinase K and U6 snRNA was loading on a denaturing Urea polyacrylamide gel. Co-precipitated U6 snRNA bands were assayed by Northern blot using radioactively labelled cDNA probes.

Figure 4.9 shows the Northern blot analysis of the co-precipitated U6 snRNAs. U6 snRNA was efficiently immunoprecipitated with LSM2, LSM3, LSM5 and LSM6 proteins (lanes 2, 4, 6 and 10), indicating that these proteins have contact sites in U6 snRNPs, probably at G30 (see below) or at the 3'-end of the U6 snRNA. However, there was no co-precipitation of U6 snRNA with LSM5, LSM7 and LSM8 (lanes 8, 12 and 14), showing that these proteins do not have cross linking sites in U6 snRNA.

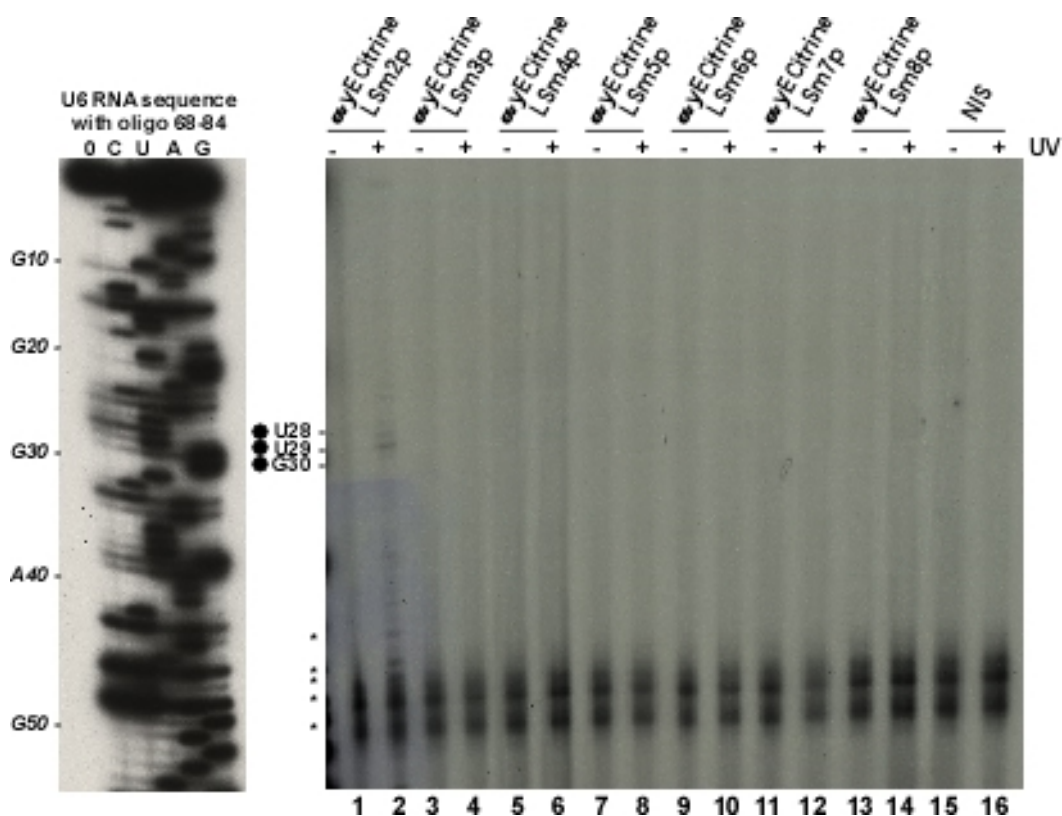


Figure 4.10 LSm2p can be cross linked to U28-G30 region of the U6 snRNA in the U6 snRNP. Figure shows the primer extension analysis of U6 snRNA after immunoprecipitation of denatured U6 snRNPs with anti-yECitrine antibody either with (+UV lanes) or without UV-irradiation (-UV lanes). The non-immune serum (NIS) was used as a control to precipitate UV-irradiated (lane 16) and non irradiated (lane 15) particles. Nucleotide positions of reverse transcriptase stops due to specific cross linking between LSm2p and the U6 snRNA are indicated on the left side with black dots. The asterisks indicate naturally occurring or UV-induced RNA-RNA background stops.

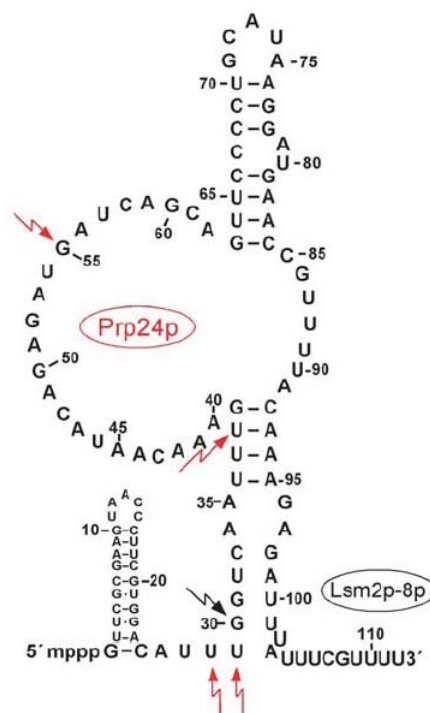
Interestingly, a protein cross linked to G30 was not immunoprecipitated by anti-Prp24p antibodies (compare lane 2 of Figure 4.8 C with lane 4 of Figure 4.8 B), suggesting that G30 may be contacted by one of LSm2, -3, -4, or -6 proteins, which have cross linking sites in the U6 snRNA. To determine which of these LSm proteins indeed contact G30 nucleotide, U6 snRNPs were UV-irradiated and immunoprecipitated with anti-yECitrine antibodies as described above and co-precipitated U6 snRNA was analyzed by primer extension.

Figure 4.10 shows the primer extension analysis of U6 snRNA immunoprecipitated with anti-yECitrine antibodies before (lanes 1, 3, 5, 7, 9, 11, and 13) and after (lanes 2, 4, 6, 8, 10, 12, and 14) UV-irradiation. Reverse transcriptase stops were detected after immunoprecipitation at nucleotides U28, U29, and to a lesser extent at G30, with the UV-irradiated particle, only when

immunoprecipitated using LSm2p-yECitrine extract (Figure 4.10, lane 2). On the other hand, anti-yECitrine antibodies did not precipitate any cross linked U6 snRNA of U6 snRNP when extracts were prepared from one of other LSm-yECitrine expressing strains (Figure 4.10, lanes 4, 6, 8, 10, 12, and 14). The remaining stops, observed after UV-irradiation, correspond to non-protein-RNA cross links as described above. To check unspecific binding on the beads, UV-irradiated and non-irradiated particles (which have TAP-tag at Prp24p and yECitrine at LSm4p) were immunoprecipitated with non-immune serum. Lane 15 and 16 show that there was no unspecific binding of U6 snRNA.

In summary, our cross linking studies reveal that Prp24p is cross linked to U28, U29, U38, and G55, and LSm2p is cross linked to U6 snRNA at region of U28-G30 region (summarized in Figure 4.10).

Figure 4.11 Summary of cross linking sites of U6 proteins within U6 snRNP. Figure shows the secondary structure of the yeast U6 snRNA in the U6 particle, which was established in this study. UV-cross linking sites of Prp24p on the RNA of the native U6 snRNP are marked by red arrows and UV cross linking region of LSm2p is shown by a black arrow.



5.2 RNA-Protein Interactions within the Prp24p-U6 snRNA Binary Complex

After studying the protein-RNA interactions within the native U6 particles, we have studied the interaction of Prp24p with U6 snRNA in an attempt to directly test the binding specificity of Prp24p and its possible role in the dynamic association of

the U4 and U6 snRNAs. To investigate specific interactions of Prp24p-U6 snRNA, full-length recombinant Prp24 protein was expressed and purified from *Escherichia coli* cells. Next, binding affinity of Prp24p for U6 snRNA was determined and the resulting U6-Prp24p binary complexes were examined for their protein-RNA interactions using hydroxyl radical footprinting and cross linking methods.

5.2.1 Purification of Recombinant Prp24 Protein

To overexpress full-length recombinant Prp24, first, the *PRP24* gene was amplified by PCR from yeast genomic DNA using Prp24p_expression oligonucleotides. The resulting fragment contained double digestion sites of NcoI/Acc65I and further subcloned in frame with the N-terminus-(His)₆-tag in pETM-11 vector, which allowed constitutive expression of Prp24p under T7 promoter. Next, this plasmid was transformed into a proper *E. coli* strain where Prp24 protein could be optimally overexpressed.

uua () 0	ugu Cys (C) 5	cug Leu (L) 3	ucg Ser (S) 3
uga () 0	total Cys (C) 8	cuu Leu (L) 8	ucu Ser (S) 7
total () 0	caa Gln (Q) 9	uua Leu (L) 12	total Ser (S) 34
gca Ala (A) 11	cag Gln (Q) 6	uug Leu (L) 7	uag Ter (.) 1
gcc Ala (A) 5	total Gln (Q) 15	total Leu (L) 44	total Ter (.) 1
gcg Ala (A) 2	gaa Glu (E) 24	aaa Lys (K) 28	aca Thr (T) 9
gcu Ala (A) 7	gag Glu (E) 8	aag Lys (K) 12	acc Thr (T) 2
total Ala (A) 25	total Glu (E) 32	total Lys (K) 40	acu Thr (T) 1
aga Arg (R) 12	gga Gly (G) 10	aug Met (M) 13	total Thr (T) 7
agg Arg (R) 6	ggc Gly (G) 1	total Met (M) 13	ugg Trp (W) 19
cga Arg (R) 6	ggg Gly (G) 2	uuc Phe (F) 7	total Trp (W) 1
cgc Arg (R) 1	ggu Gly (G) 6	uuu Phe (F) 14	uac Tyr (T) 1
cgg Arg (R) 2	total Gly (G) 19	total Phe (F) 21	aua Tyr (T) 2
cgu Arg (R) 4	cac His (H) 7	cca Pro (P) 8	total Tyr (T) 9
total Arg (R) 29	cau His (H) 3	ccc Pro (P) 3	gua Val (V) 11
aac Asn (N) 13	total His (H) 10	cpg Pro (P) 1	guc Val (V) 5
aau Asn (N) 20	aua Ile (I) 14	ccu Pro (P) 4	gug Val (V) 4
total Asn (N) 33	auc Ile (I) 4	total Pro (P) 16	guu Val (V) 11
gac Asp (D) 5	auu Ile (I) 13	agc Ser (S) 6	total Val (V) 22
gau Asp (D) 16	total Ile (I) 31	agu Ser (S) 8	TOTAL 445
total Asp (D) 21	cua Leu (L) 8	uca Ser (S) 5	
ugc Cys (C) 3	cuc Leu (L) 6	ucc Ser (S) 5	

Figure 4.11 Codon usages in *PRP24* gene. The nature of codon usage in *PRP24* gene and translated Prp24 protein were investigated by database search. The amino acids shown in grey bars are the rare codons of *PRP24* gene.

It is very well known that if the protein contains a high number of *rare E. coli* codons, it is best to express it in a strain co-expresses the tRNAs for these rare codons. For this purpose, the nature of codon usage in *PRP24* gene and translated Prp24 protein were analyzed by database search (Figure 4.11). Indeed, *PRP24* gene contained many rare codons (18 AGG/AGA (Arg), 2 CGG (Arg), 14 AUA (Ile), 8 CUA (Leu), 3 CCC (Pro), and, 10 GGA (Gly); see also grey bars in Figure 4.11). Therefore *E. coli* strain Rosetta (DE3, pLYSs), which harbours a plasmid expressing tRNAs for AGG/AGA (Arg), CGG (Arg), AUA (Ile), CUA (Leu), CCC (Pro), and GGA (Gly), was used as the host.

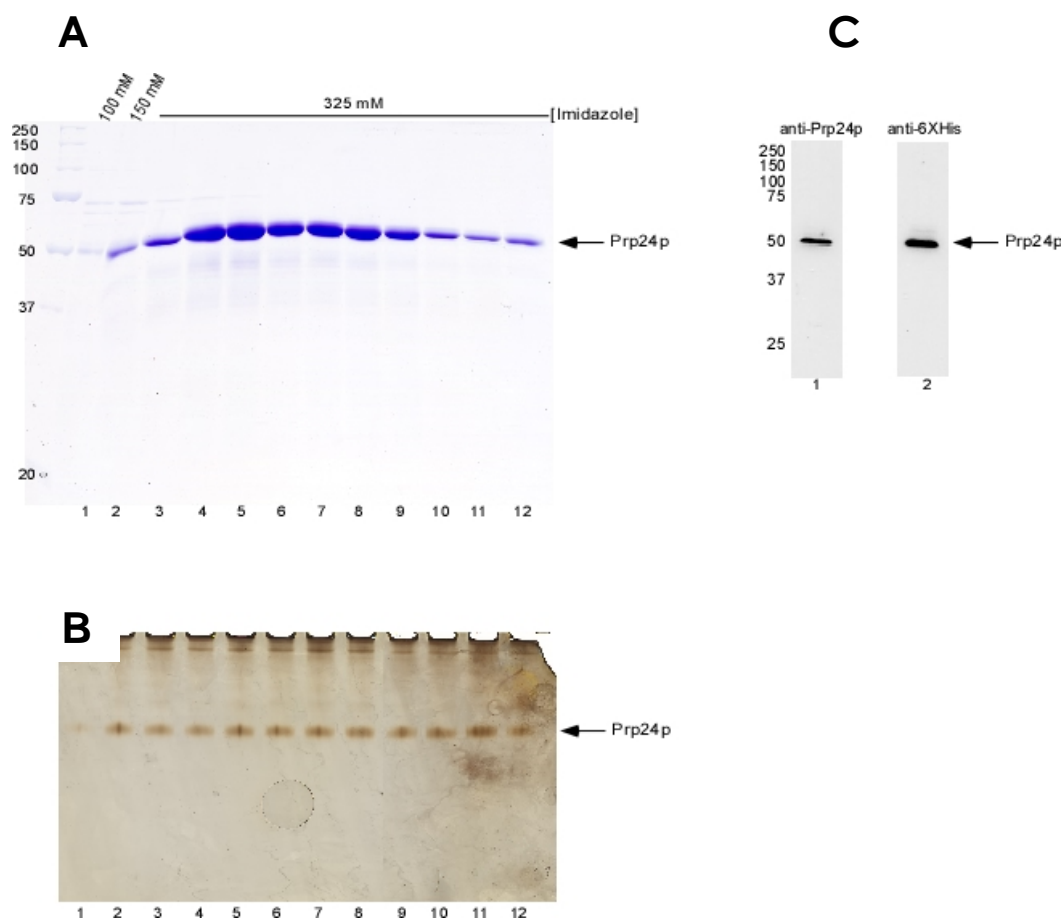


Figure 4.12 Purification of the recombinant Prp24 protein. After overexpression, recombinant Prp24p was purified from *Rosetta E. coli* cell lysate by Ni²⁺-NTA affinity chromatography. Proteins bound on Ni²⁺-NTA beads were eluted by different concentrations of imidazole (100, 150, and 325 mM). Eluted fractions were loaded on a SDS-polyacrylamide gel and visualized by Coomassie-staining (**A**). To detect likely contamination of recombinant protein with nucleic acids, the same fractions were also

loaded (without PCI-extraction) on a denaturing gel and analyzed by silver-staining **(B)**. **(C)** shows the detection of Prp24 and its (His)₆-tag by Western blot using anti-Prp24p and anti-His antibodies.

After overexpression in Rosetta strain, recombinant Prp24 protein was purified by Ni²⁺-NTA affinity chromatography. Figure 4.12 shows the elution profile of bound Prp24 protein from Ni²⁺-affinity column by 100, 150 mM, and 325 mM concentrations of imidazole. The elute protein was highly pure and was not contaminated with any other proteins (Figure 4.12 A). Since Prp24p is an RNA-binding protein, potential contamination with non-specifically bound nucleic acids was also checked by denaturing-gel electrophoresis and silver-staining. Figure 4.12 B shows that eluted Prp24p was free of any nucleic acids. The elution fractions 4-8, containing the highest amount of Prp24 protein, were pooled together and characterized further by Western blot using anti-Prp24p and anti-His antibodies. Figure 4.12 C shows that purified recombinant protein was indeed Prp24p (lane 1) and contained the (His)₆-tag (lane 2).

5.2.2 Determination of Binding Affinity of Prp24p-for U6 snRNA

After purification of recombinant Prp24 protein, its binding affinity for U6 snRNA or another words its dissociation constant (K_d) from U6 snRNA was determined. K_d is the strength of the protein for its substrate RNA: a high K_d indicates weak binding: a low K_d indicates strong binding. K_d is equal to the concentration of protein at which half of the substrate RNA is bound by proteins. For K_d fortitude, a constant amount of radioactively labelled U6 snRNA (transcribed *in vitro* by T7) was incubated with increasing amounts of recombinant Prp24p and subsequent protein-RNA complexes were assayed for binding by gel-mobility shift using a non-denaturing native polyacrylamide gel (Figure 4.13).

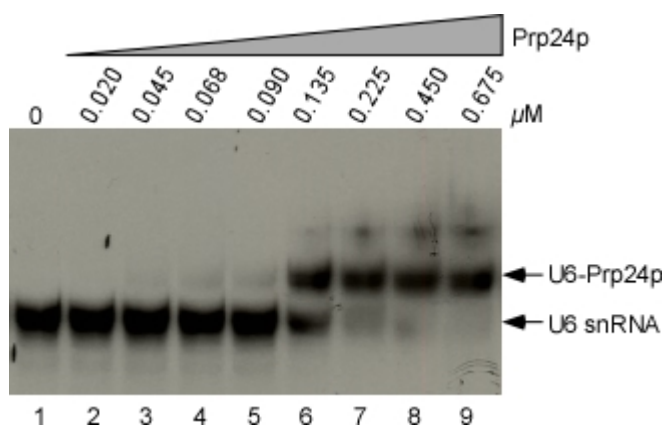


Figure 4.13 Determination of binding affinity of Prp24p for U6 snRNA. A constant amount of radioactively labelled U6 snRNA transcript (0.36 nM) was reconstituted with increasing amounts of Prp24p. Complexes and free RNA were resolved on a 6 % native polyacrylamide gel. Lane 1 is control without added protein and the wedge represents increasing protein concentrations (lane 2-9).

To calculate the dissociation constant of Prp24p for U6 snRNA, the ratio of U6 snRNA, unbound or bound with Prp24 protein, was determined by phosphor-imager analysis. K_d of Prp24p was estimated as 0.135 μM since 50 % of U6 snRNA was found to be in complex with Prp24p when 0.135 μM of protein was present (Figure 4.13, lane 6). This K_d value is similar to the previously reported value of 95 nM (Ghetti *et al.*, 1995) and the affinity of Prp24p for U6 snRNA appears to be relatively high when compared to the other RNA binding proteins.

5.2.3 Recombinant Prp24p Recognizes Similar Nucleotides of U6 snRNA as Native Prp24p does

The fact that recombinant Prp24p has a high affinity for U6 snRNA allowed us to ask whether it contacts U6 snRNA in the same region as native Prp24p does. To answer this question, UV-cross linking studies with *in vitro* reconstituted U6 snRNA-Prp24p complexes were performed. UV-cross linking experiments with binary complexes required: (1) higher amounts of U6 transcript as compared to RNA used for EMSA assays and (2) all U6 snRNA substrate had to be reconstituted homogenously with Prp24p. To set up these conditions, first, 15 nM of radioactively labelled U6 snRNA transcript was titrated with increasing concentrations of recombinant Prp24p, and the resulting complexes were analyzed initially on a non-denaturing native polyacrylamide gel (Figure 4.14). Recombinant Prp24p shifted the U6 snRNA to a slower migrating complex quantitatively already at 0.7 μM concentration (lane 4). At 0.7 and 1.0 μM concentrations of Prp24p (lane 4 and 5), only one RNP complex was observed, therefore, we conclude that, at these concentrations, the binary U6 snRNA-Prp24p complex is homogenous.

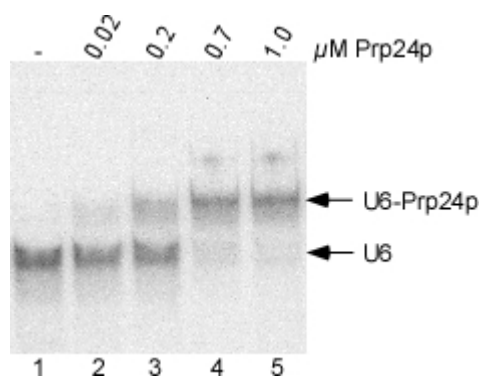


Figure 4.14 U6 snRNA-binding activity of recombinant Prp24p for UV-cross linking experiments monitored by gel mobility-shift analysis. A constant amount of radioactively labelled U6 snRNA transcript (15 nM) was titrated with increasing amounts of Prp24p. Complexes and free RNA were resolved on a 6 % native polyacrylamide gel. Lane 1 is control without added protein and increasing μM concentrations of Prp24p are shown on the top of the figure (lane 2-5).

link product was observed between U6 snRNA and recombinant Prp24p (lane 4) only upon UV-irradiation. Naked U6 RNA (independent from irradiation; lane 1 and 3) or non-irradiated U6-Prp24p (lane 2) did not result in a higher molecular complex. In order to check further whether the observed cross link, indeed, is a specific protein-RNA cross link but not a UV-induced intra-RNA cross link, two additional controls were performed: *in vitro* reconstituted U6-Prp24p complex was digested either with RNases A and T1 or with proteinase K. The radioactive cross link product completely disappeared upon proteinase K treatment (lane 6) and very faint band of RNA nucleotides cross linked with Prp24p were still visible upon reactions with RNases (lane 5), indicating that the observed cross linking band is definitely a protein-RNA cross link between U6 snRNA and recombinant Prp24p.

In order to identify the contact points of recombinant Prp24p at U6 snRNA, the sites of cross links within this cross linking product were detected by primer extension (Figure 4.15 B). As a control, identical experiments were carried out with naked U6 snRNA. Figure 4.15 B shows that several reverse transcriptase stops were observed in the U6 snRNA (compare lane 2 with lane 4). The strongest of these stops occurred at nucleotides A24, U29, U36, U37, U38, and U54 (Figure 4.15 B, lane 4). In fact, these stops took place primarily at the same nucleotides as cross links between native Prp24p and U6 snRNA were observed. In addition, weaker stops were found between recombinant Prp24p and U6 transcript at nucleotides C33, A34, A41, A42, C43, A44, and U46 (Figure 4.15 B, see nucleotides with asterisks). Our analysis with the native U6 snRNPs had shown that the stops at C33, C43 and U46 are the nucleotides where reverse transcriptase happened to stop irrespective of UV-irradiation. It had also shown that the stops at A34, A44 were observed both in naked native U6 snRNA and U6 snRNA in native U6 snRNPs. Therefore, these stops are unlikely due to specific protein-RNA cross links. However, the nucleotides A41 and A42 are very likely additional sites where recombinant Prp24p contact at U6 snRNA transcript (see Discussion for details). Nevertheless, we conclude that recombinant Prp24p recognizes primarily the same nucleotides of U6 snRNA as the native Prp24p does at U6 snRNA within native U6 snRNPs and recombinant protein can be used for our further structural analysis (see below).

5.2.4 Footprinting of Recombinant Prp24p Bound to the U6 snRNA

Hydroxyl radical footprinting performed with the native U6 snRNPs suggested that Prp24p interacts within the first 60 nucleotides of the U6 snRNA. To

investigate whether this region of the U6 snRNA is indeed bound only by Prp24p, and not by the LSm proteins, hydroxyl radical footprinting was performed with *in vitro* reconstituted U6 snRNA- Prp24p binary complex.

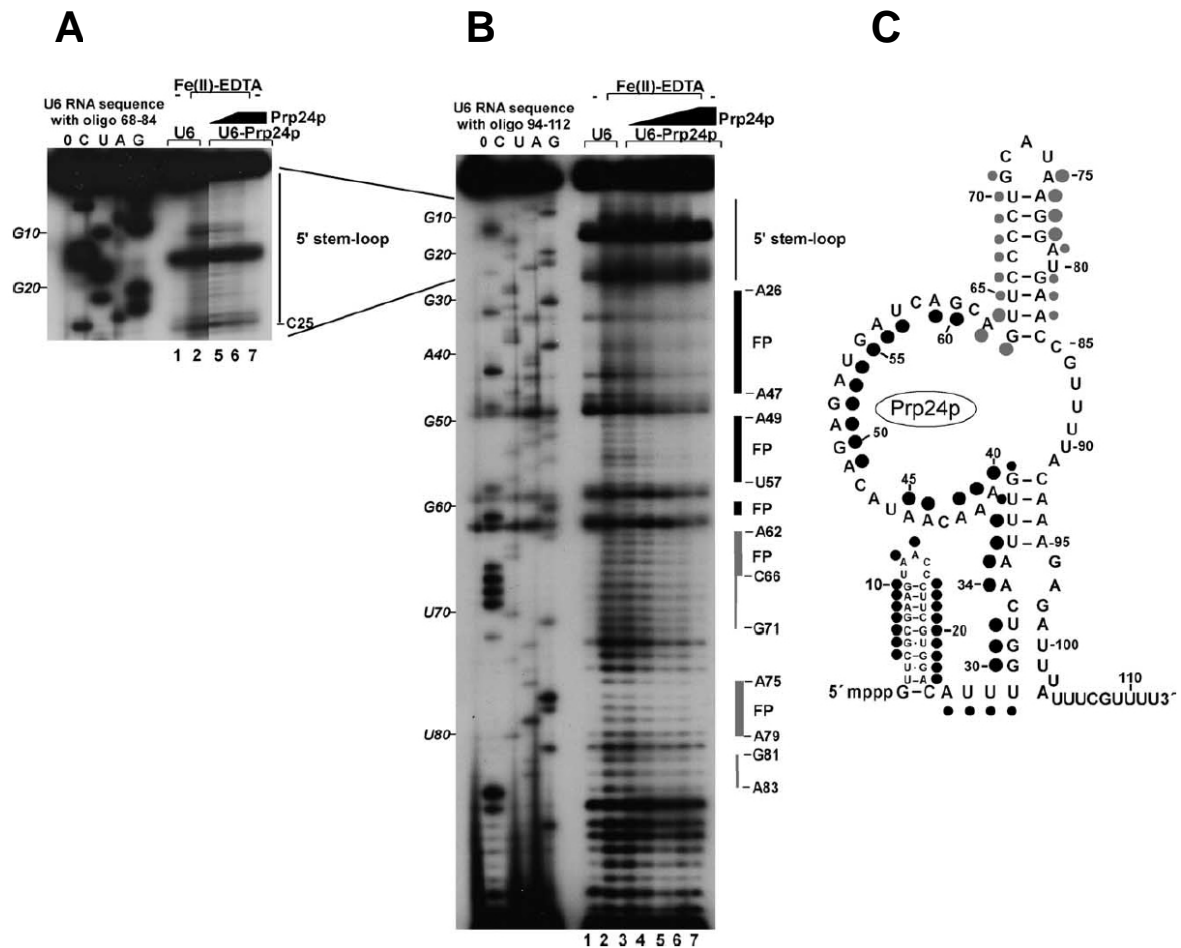


Figure 4.16 Footprinting analyses of complexes formed between recombinant Prp24p and *in vitro* transcribed U6 snRNA. The Fenton reagent-treated complexes were analyzed by primer extension using a radioactively labelled oligonucleotide complementary to the U6 snRNA at positions 68-84 (**A**) and 94-112 (**B**). The protection of the ribose backbone from hydroxyl radicals at increasing concentrations of recombinant Prp24p (lanes 3-6, 0.02 μ M, 0.2 μ M, 0.7 μ M, and 1 μ M), is marked by black bars on the right side of the (**B**) and designated as FP (footprint). Grey bars indicate protections that are not found in native U6 snRNPs. Thin grey bars indicate mild protection. Lanes 1 contains naked U6 snRNA without Fenton reagent and lane 2 is naked U6 snRNA reacted with Fenton reagent.

To analyze the RNA-protein interactions within the U6-Prp24p complex, 15 nM of U6 snRNA was incubated first with increasing amounts of Prp24p (see Figure 4.14) and subsequently incubated with the Fenton reagent. Naked U6 snRNA

transcript was also incubated with hydroxyl radicals. Additional incubations were performed to control for background RNA cleavage by omitting the *Fenton reagent* for naked U6 snRNA or for RNP complex (Figure 4.16 A and B, lanes 1 and 7). The protection pattern of the U6 snRNA in the U6 snRNP was analyzed by primer extension using the DNA oligonucleotides as described above (4.1.2).

Analysis of the U6 snRNA-Prp24p complexes by hydroxyl radical footprinting revealed a U6 snRNA protection pattern similar to that seen with the native U6 snRNP (see Figure 4.7 A). To discern the 5'-stem-loop of U6 snRNA more closely, protection pattern was analyzed by an oligonucleotide complementary to nucleotides 68-84 of U6 snRNA. Figure 4.16 A shows that the 5'-stem-loop appears to be protected, but not as strongly as in the native particle. Nucleotides A26-G60 of the U6 snRNA were protected strongly (with a few exceptions, see Figure 4.16 B), demonstrating that recombinant Prp24 protein binds the U6 snRNA in the C4-G60 region. Interestingly, the protection pattern of the large single stranded region is very similar to that of the same region in the native particle, excluding only a few nucleotides, such as, A45, G50, and U54, which seem to be protected more strongly by recombinant Prp24p. We thus conclude that the large internal loop binds exclusively Prp24p also in the native particle.

Unexpectedly, although the 3'-stem-loop was not protected by proteins in the native U6 snRNP, a protection of the 3'-stem, comprising nucleotides A62-G71, A75-A79 and G81-A83, was observed in the binary complex (Figure 4.16 B, grey bars). In agreement with previous experiments performed with recombinant Prp24p, our results indicate that recombinant Prp24p interacts also with the 3'-stem when the LSm proteins are missing (Figure 4.16 C).

5.3 Electron Microscopy Analysis of yeast U6 snRNP

The precise binding region of the LSm proteins to the U6 snRNA could not be investigated by chemical methods since primer extension had to be performed with an oligonucleotide annealing to the uridine-rich tract, which is shown to be required for LSm binding in the U6 snRNA (Vidal *et al.*, 1999). In order to learn more about the spatial rearrangement of LSm proteins and Prp24p, we used electron microscopy.

5.3.1 U6 snRNP Has Two Morphologically-Defined Subunits

For the structural analysis of U6 snRNPs with electron microscopy, U6 particles were isolated by the TAP method using yeast cells with TAP tag-Prp24p. Eluted particles were subjected to a further purification by 10 %- 30 % (v/v) glycerol gradient centrifugation (Figure 4.5 B and C and Figure 4.1X A). After fractionation, particles from fractions 16 and 17 were analyzed by electron microscopy in collaboration with P. Dube and B. Kastner in our department. The U6 snRNPs were visualized by negative staining with 2.5 % uranyl formate using the carbon double film method.

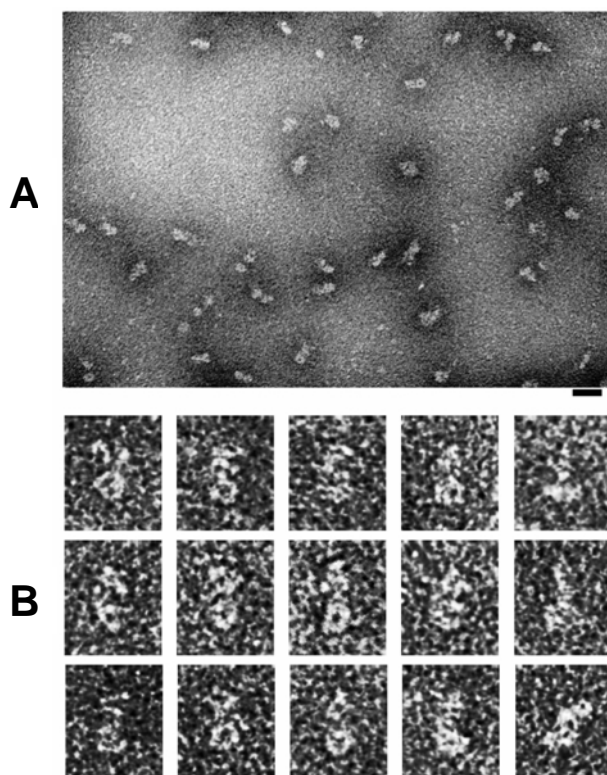


Figure 4.17 Electron microscopy analyses of U6 snRNPs negatively stained with 2.5 % uranyl formate. The particles were purified using the TAP method and TAP-tagged Prp24p, followed by a 10 %-30 % glycerol gradient. The images were obtained from fractions 16 and 17 after glycerol gradient sedimentation. **(A)** General view of a glycerol gradient fraction containing U6 snRNP. Black bar is a scale of 20 nm in length. **(B)** Gallery of selected U6 snRNP particles. The U6 snRNPs were oriented with the LSm ring downwards and Prp24 protein upwards.

Figure 4.17 A shows an overview of the U6 snRNPs. The particles have a slightly elongated shape with 14 to 16 nm length and 7 to 9 nm width. Already at low magnification, two distinct globular structures of U6 snRNP can be recognized: one substructure often exhibits a round shape whereas the other substructure has a more irregular shape (Figure 4.17 B, images oriented to the bottom with respect to the round domain). Lower substructure appeared frequently as a round projection with a diameter of 7 to 8 nm and with an accumulation of stain in the middle. This is very typical for the Sm or LSm core structure (Kastner *et al.*, 1990;

Achsel *et al.*, 1999); therefore, the lower subunit should be the LSM ring of U6 snRNP. The upper substructure of U6 snRNP should contain the Prp24 protein.

5.3.2 Topographic Labelling of LSM Proteins with yECitrine-Tag

To obtain information on the positions of individual LSM proteins within U6 snRNP, we developed a method for topographical localization of individual LSM proteins. Single entities of LSM ring were extended with an additional globular domain, which allowed visualization of expanded individual LSM proteins. For this purpose, all LSM proteins were labelled individually with yECitrine globular domain by replacing chromosomally.

The yECitrine tag was genetically introduced to each LSM protein by homologous recombination in the yeast strain, which already contained TAP tag at the C-terminus of Prp24p. The yECitrine cassette coding for the C-terminal yECitrine-tag was amplified by PCR from plasmid (pKT 175 and pKT 239) and yeast cells (YRK3) were subsequently transformed with this PCR product. Transformants were incubated at 25 °C or 30 °C to. The yECitrine tag did not interfere with the function of LSM proteins *in vivo* and the transformants grew normally like parent YRK3 cells without any detectable growth defect. The correct integration of the yECitrine-cassette in transformants was verified by PCR analyses using *LSM_check_oligonucleotides* and the proper expression of yECitrine at the C-terminus was characterized by Western blot using anti-YFP antibody.

Figure 4.18 shows the characterization results of transformants by PCR and Western blot. The yECitrine-cassette was correctly inserted at the 3'-end of each LSM gene (Figure 4.18 A) and moreover, yECitrine protein was being expressed at their C-terminal end (Figure 4.18 B)

After the fusion of the yECitrine-tag, U6 snRNP particles, labelled at various LSM proteins, were isolated using TAP method and TAP-tagged Prp24p. Figure 4.19 shows the protein composition of LSM-labelled U6 snRNPs. The analysis of protein bands by mass spectrometry in each U6 snRNP showed the presence of Prp24p and six of the LSM2-8 proteins, LSM4p, LSM7p, LSM8p, LSM2p, LSM5p, LSM6p, and the yECitrine-tag. LSM3p could not be detected in none of the U6 snRNP purifications except for the one with LSM3p-tag. Indeed, we could show that LSM3 protein (10 kDa) was shifted to about 40 kDa when tagged with the 30 kDa yECitrine tag in the Prp24p-TAP-tag strain (Figure 4.19 C). This demonstrates the presence of LSM3p in our purified U6 snRNPs.

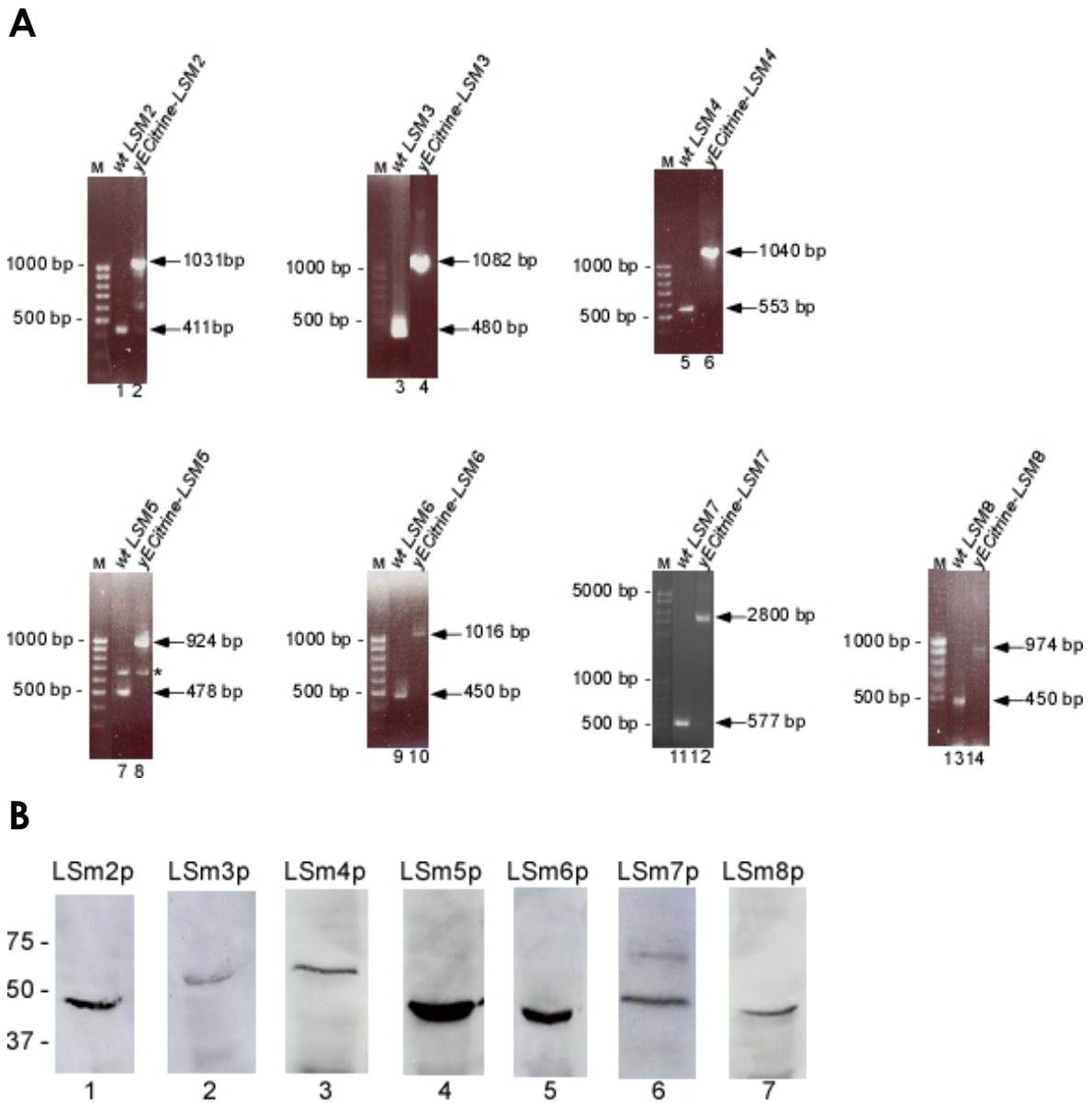


Figure 4.18 Transformant characterizations by PCR analyses and Western blot. (A) Chromosomal DNA was isolated from both wild type (lanes 1, 3, 7, 9, 11, 13) and positive colony (lanes 2, 4, 6, 8, 10, 12, 14) and PCR products amplified with corresponding *LSM_check* oligonucleotides were loaded on a 1 % Agarose gel. Arrows mark the size of the PCR product of the wild type and the positive colony. M is DNA ladder in base pairs. The band shown by an asterisk in lanes 7 and 8 is an unspecific PCR product observed both in wild type and positive colonies. **(B)** Expression of *yECitrine-tag* in positive colonies was analyzed by Western blot using anti-YFP antibody. The size marker in kDa is shown on the left.

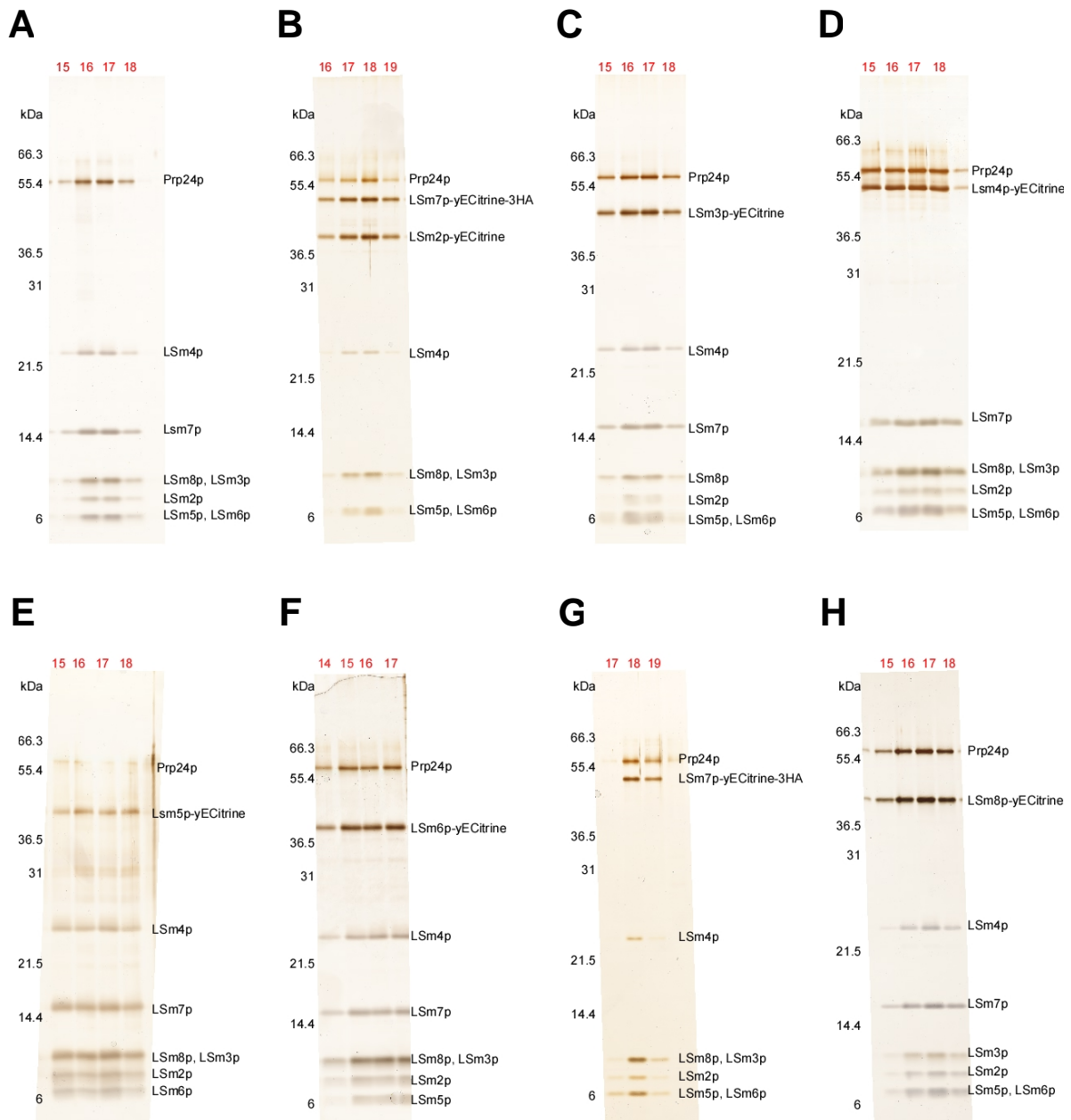


Figure 4.19 Characterization of the yeast U6 snRNPs, which contain tagged-LSm proteins. The U6 snRNP was purified from corresponding yeast whole-cell extract by TAP method using TAP-tagged Prp24p. Afterwards, isolated particles were further purified by a 10 %-30 % glycerol gradient centrifugation. Gradient fractions, numbered above each lane, were analyzed for their protein content by mass spectrometry. These fractions were also visualized by electron microscopy. **(A)** wild type U6 snRNP containing only TAP-tagged Prp24p; **(B)** U6 snRNP containing the yECitrine-tag both at LSm2p and LSm7p; U6 snRNPs with tagged yECitrine tagged-LSm3p **(C)**, -LSm4p **(D)**, -LSm5p **(E)**, -LSm6p **(F)**, -LSm7p **(G)**, -LSm8p **(H)**.

U6 snRNPs labelled at different LSM proteins from gradient fractions were then analyzed by electron microscopy as described above. Figure 4.20 A shows an overview of the U6 snRNPs tagged at LSM7p. The LSM7p-labelled particles exhibit more elongated structures (up to 20 nm) as compared with the untagged particles (Figure 4.17). At higher magnification (Figure 4.20 B), in most of the images, LSM7p-tagged U6 snRNPs contain typical round images of LSM-ring and two another globular domains next to the LSM structure: one domain is comparatively larger and exhibits the angular features of Prp24p domain; and second domain is much smaller and has a more compact arrangement with 4 nm diameter, which is indeed expected structure and size for yECitrine protein. In most pictures, the globular domains of Prp24 and yECitrine proteins were almost always found to be roughly opposite to each other, at the two opposed sides of LSM-ring periphery, indicating that the position of yECitrine-tag, therefore LSM7 protein, is clearly distant to the periphery of the LSM ring where Prp24 domain is linked. The finding, that LSM7p is distantly positioned and never observed near Prp24 domain, also suggests that the linker region of Prp24p domain should take place at the defined region of LSM-ring and, furthermore, the positions of LSM proteins within the ring are not positioned randomly relative to the Prp24p.

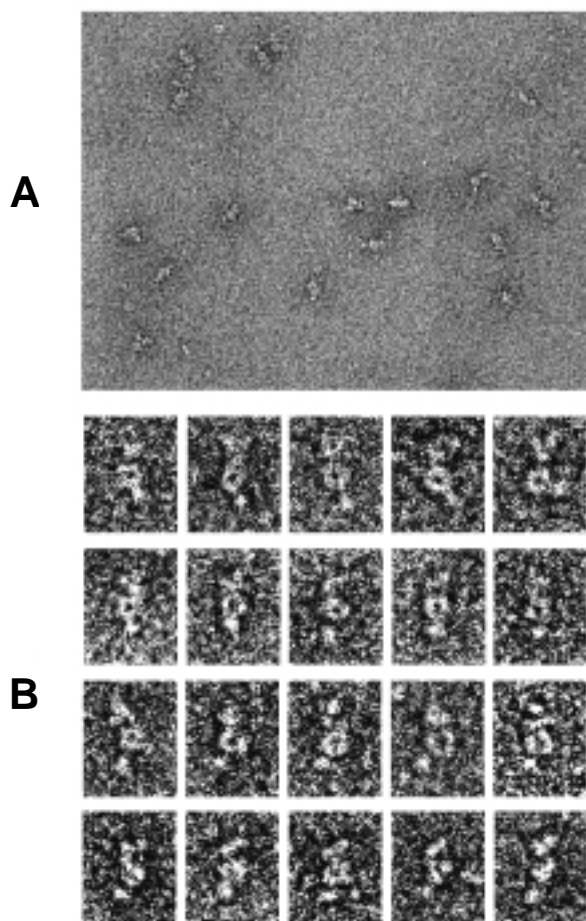
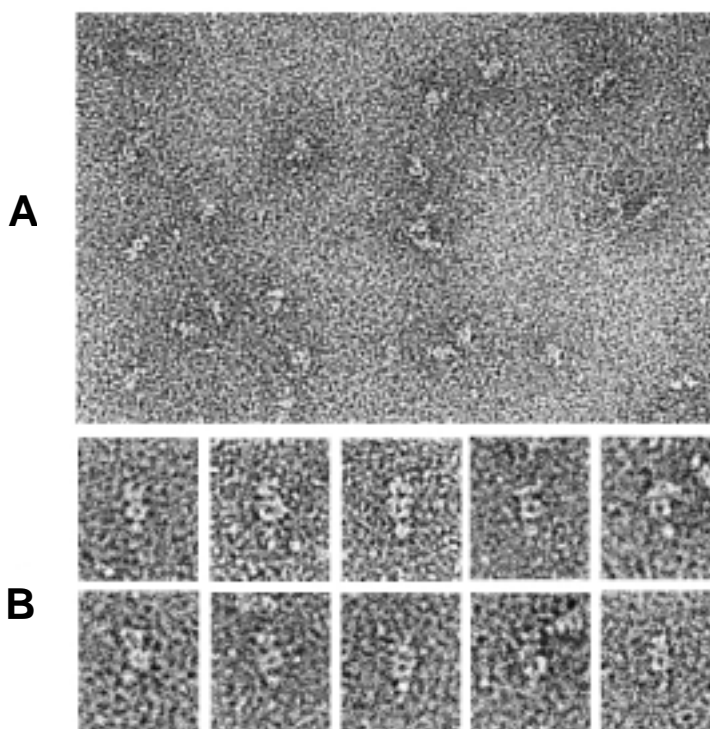


Figure 4.20 Electron microscopy analyses of U6 snRNPs labelled at LSM7p. The particles were purified using the TAP method and TAP-tagged Prp24p, followed by a 10 %-30 % glycerol gradient. **(A)** General view of the glycerol gradient fractions containing U6 snRNP. **(B)** Gallery of selected LSM7p labelled U6 snRNP particles. The U6 snRNPs were oriented with the LSM ring downwards and Prp24 protein upwards.

Next, the position of the LSm5 protein in the LSm ring was analyzed by electron microscopy using the LSm5p-yECitrine tagged U6 snRNPs. As can be already seen in overview (Figure 4.21 A), LSm5p-labelled particles show more elongated structure, similar to U6 snRNPs containing LSm7p-yECitrine tag. In most images, three essential morphological subunits in tagged U6 snRNP can be identified: LSm ring, Prp24p domain and small globular tag (Figure 4.21 B). LSm5p-labelled particles showed similar projections as LSm7p-tagged U6 snRNPs, in which yECitrine-tag and LSm5 protein were found to be at distant positions of the LSm-ring compared to Prp24p link region.

Figure 4.21 Electron microscopy analyses of U6 snRNPs labelled at LSm5p.

The particles were purified using the TAP method and TAP-tagged Prp24p, followed by a 10 %-30 % glycerol gradient. **(A)** General view of the glycerol gradient fractions containing U6 snRNP. **(B)** Gallery of selected LSm5p labelled U6 snRNP particles. The U6 snRNPs were oriented with the LSm ring downwards and Prp24 protein upwards.



The electron micrographs obtained from LSm6p and LSm8p labelled U6 snRNP showed in most images the typical LSm-ring and angular Prp24p structures, however, the position of yECitrine tag in both labelled U6 snRNPs was less frequent to distinguish (Figures 4.22 A and 4.23 A). As can be seen in the selected images (Figures 4.22 B and 4.23 B), the yECitrine tag was found to be closer to the Prp24p-LSm ring link region. As compared to LSm5p or LSm7p-tagged U6 snRNPs, the position of yECitrine tag at the LSm8p was even sometimes observed in close orientation with Prp24p domain (Figure 4.22 B). On the other hand, the tag at the LSm6p showed a more distant localization from Prp24p-LSm ring link region (up to 120 degrees) (Figure 4.23 B). These results indicate that both LSm6 and LSm8

proteins are positioned closer to Prp24p-LSm ring link region as compared to the positions of LSm5p and LSm7p.

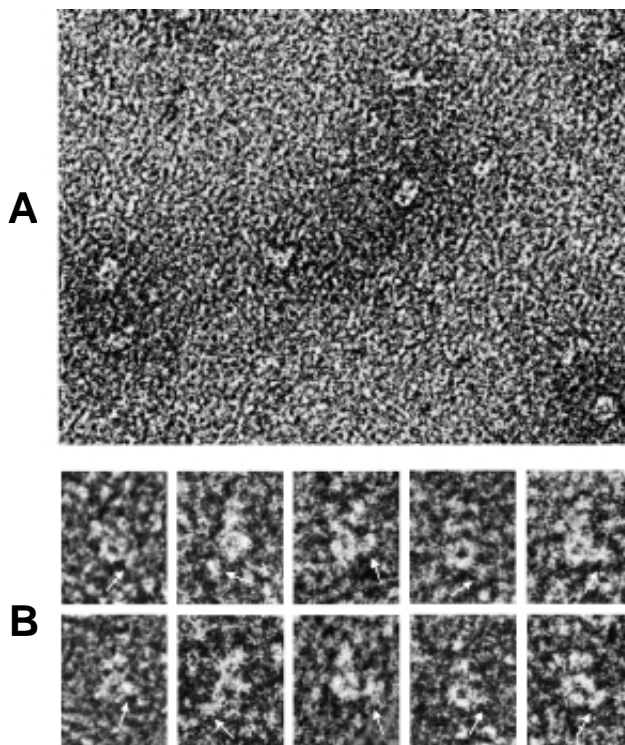


Figure 4.22 Electron microscopy analyses of U6 snRNPs labelled at LSm8p. The particles were purified using the TAP method and TAP-tagged Prp24p, followed by a 10 %-30 % glycerol gradient. **(A)** General view of the glycerol gradient fractions containing U6 snRNP. **(B)** Gallery of selected LSm8p labelled U6 snRNP particles. The U6 snRNPs were oriented with the LSm ring downwards and Prp24 protein upwards.

Figure 4.23 Electron microscopy analyses of U6 snRNPs labelled at LSm6p. The particles were purified using the TAP method and TAP-tagged Prp24p, followed by a 10 %-30 % glycerol gradient. **(A)** General view of the glycerol gradient fractions containing U6 snRNP. **(B)** Gallery of selected LSm6p labelled U6 snRNP particles. The U6 snRNPs were oriented with the LSm ring downwards and Prp24 protein upwards.

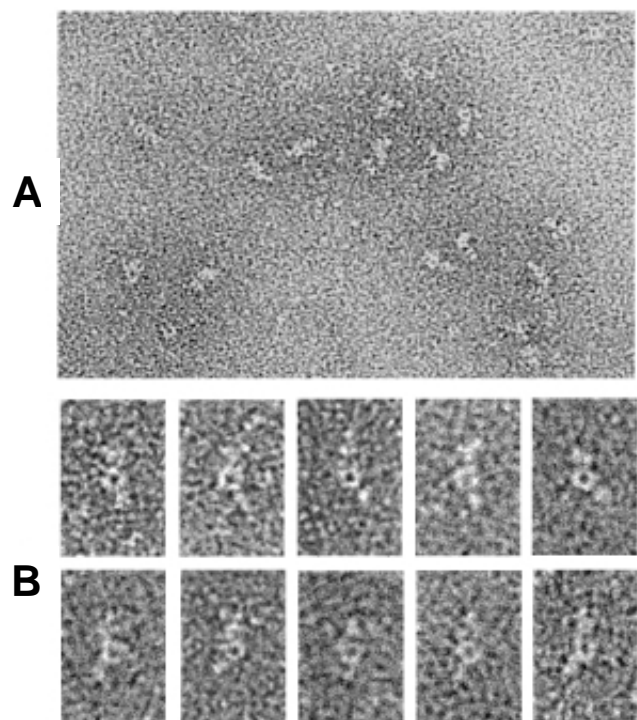


Figure 4.24 Electron microscopy analyses of U6 snRNPs labelled at LSm4p. The particles were purified using the TAP method and TAP-tagged Prp24p, followed by a 10 %-30 % glycerol gradient. **(A)** General view of the glycerol gradient fractions containing U6 snRNP. **(B)** Gallery of selected LSm4p labelled U6 snRNP particles. The U6 snRNPs were oriented with the LSm ring downwards and Prp24 protein upwards

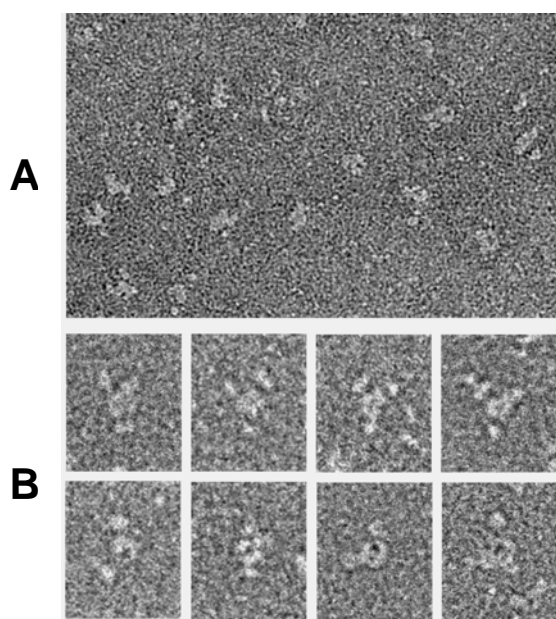
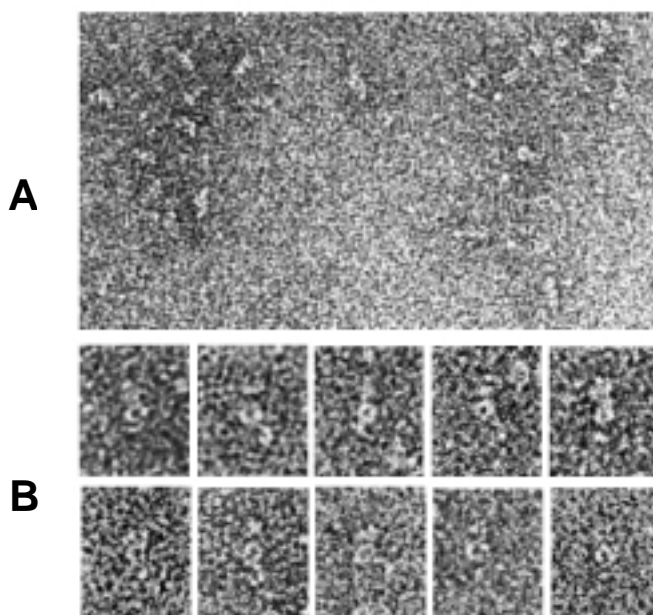


Figure 4.25 Electron microscopy analyses of U6 snRNPs double-labelled at LSm2p and LSm7p. The particles were purified using the TAP method and TAP-tagged Prp24p, followed by a 10 %-30 % glycerol gradient. **(A)** General view of the glycerol gradient fractions containing U6 snRNP. **(B)** Gallery of selected LSm2p and LSm7p labelled U6 snRNP particles. The U6 snRNPs were oriented with the LSm ring downwards and Prp24 protein upwards

Electron microscopy analysis of LSm4p-labelled U6 snRNPs showed that in these particles, γ ECitrine tag was not found anymore at the periphery of the LSm-ring, which makes it difficult to localize (Figure 4.24) but in some images, a long connection between the tag and the LSm-ring could be identified. This could be due to the fact that the LSm4 protein contains a 60 amino acid-long C-terminus in addition to the Sm motifs 1 and 2; therefore, the additional mass of the tag could be visualized as a domain distant to LSm-ring. Nevertheless, the tag at LSm4p is

located at a farther position compared to the location of LSm8p relative to Prp24p link site, but much closer than the site of LSm7p.

Finally, LSm2p- and LSm3p-tagged U6 snRNPs were analyzed by electron microscopy. In none of the projections from both labelled particles, γ ECitrine tag could be identified clearly (Figure 4.25 and 4.26). A reason for that could be that both LSm2 and LSm3 proteins are located near Prp24p domain and γ ECitrine-tag and Prp24p domain cannot be identified as distinct morphological subunits. This could also further suggest that Prp24p domain is linked to LSm-ring periphery in a region where LSm2p and LSm3p are located.

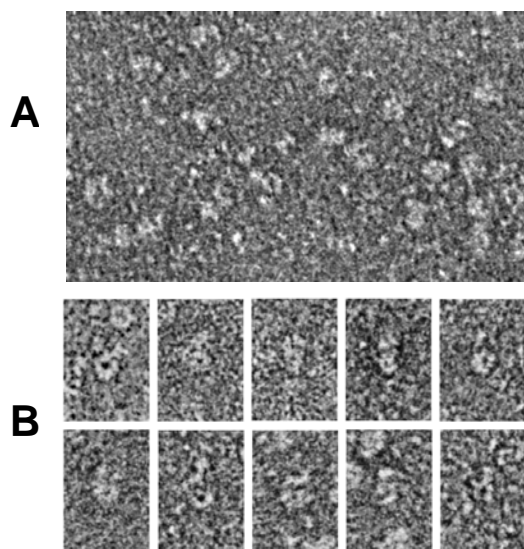


Figure 4.26 Electron microscopy analyses of U6 snRNPs -labelled at LSm3p. The particles were purified using the TAP method and TAP-tagged Prp24p, followed by a 10 %-30 % glycerol gradient.

(A) General view of the glycerol gradient fractions containing U6 snRNP. **(B)** Gallery of selected LSm3p labelled U6 snRNP particles. The U6 snRNPs were oriented with the LSm ring downwards and Prp24 protein upwards

5.3.3 Further Image Analysis of U6 snRNP Reveals Potential Flexibility within its Domains

To discern typical structural features of the U6 snRNP (without γ ECitrine-tag), single particle image analysis and image classification were performed. Electron-microscopic images of U6 snRNPs were aligned translationally and rotationally. Then these images were averaged in order to obtain a set of similar views of the molecules. By using IMAGIC-V software and the usual procedure of treating the U6 snRNPs as structural entities, the resulting class averages did not give rise to clear outlines even after increased number of analyzed particles (up to 12,000). However, a few class sums revealed detailed features of either Prp24p or LSm-ring domain, suggesting a conformational structural heterogeneity caused by flexible connection between Prp24p and LSm-ring. To overcome this, statistical image analysis was performed for the two well-defined subunits separately and image

classes were obtained for the upper and the lower substructures, individually. The particles found in each class were finally averaged by using the whole particle image again. Figure 4.27 A shows typical class averages obtained after classifying only the upper Prp24p domain and Figure 4.27 B illustrates the when classifying only the lower LSm-ring domain. In each case, due to classification of only one of the domains, the other domain is less discernible. This confirms that both domains are not rigidly bound to each other.

The class averages obtained from only upper Prp24p domain show clear outlines and internal finer structures (Figure 4.27 A). The Prp24 protein appears to consist of 3 to 4 arms (with about 3 nm thickness), which are oriented mostly in a triangular manner. While one or two arms are located away from LSm-ring, the other arms appear to contact the LSm-ring via one or two protrusions (Figure 4.27 A, see arrows).

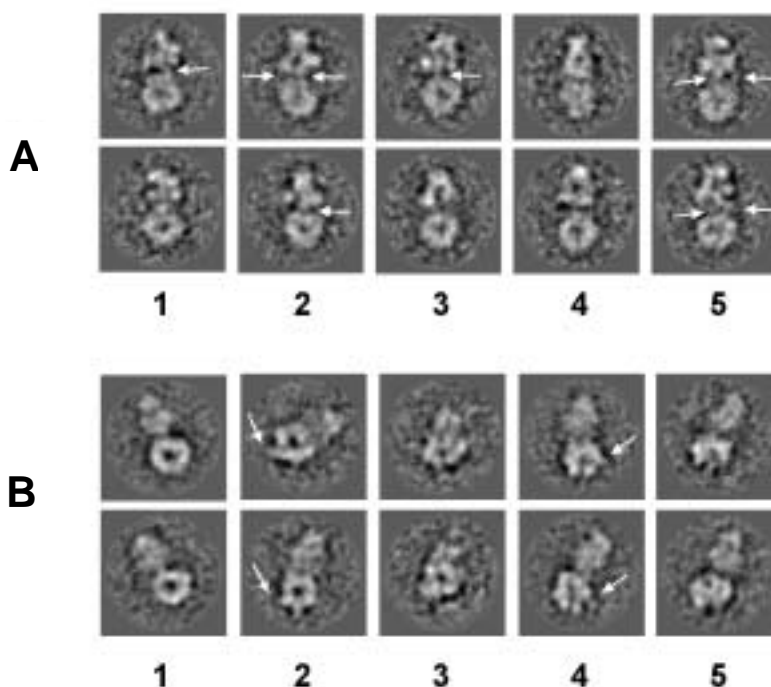


Figure 4.27 Class averages of U6 snRNP particles. The images from U6 snRNP particles were sorted, classified and finally averaged into class sums. The U6s snRNPs were oriented with the LSm-ring downwards and Prp24 protein upwards. **(A)** The class averages focused on only Prp24p domain by masking the LSm-ring structure. Arrows indicate the interaction area of Prp24p and and LSm-ring. **(B)** The class sums after focused-averaging on the LSm-ring domain by masking Prp24 protein. Arrows mark the position of the most pronounced protuberance within the LSm-ring.

After masking the Prp24p domain and averaging only the lower LSm-domain, more structural details of the LSm-ring can be recognized (Figure 4.27 B). In most images, the LSm-ring was observed as an asymmetrical heptameric ring with individually defined structural elements. The most pronounced of such elements is marked by an arrow in Figure 4.27 B. In some class averages, the characteristic staining of LSm-ring in the middle could not be seen easily. These projections results very likely from side views of the LSm-ring (Figure 4.27, columns lanes 4 and 5).

Various class averages obtained from U6 snRNPs using only the LSm-domain for classification also showed that Prp24p domain (where Prp24p domain appeared fussy) has a defined contact position at the LSm ring periphery. This can be best understood when the location of Prp24p domain is compared with the position of the most pronounced protuberance (marked by an arrow at LSm-periphery in 4.27 B). This protuberance very likely contains the C-terminus of the biggest LSm protein, LSm4p, and is located distant from the LSm-Prp24 contact site (Figure 4.27 B). Furthermore, it confirms the experiments when the position of LSm4p labelled with γ ECitrine is also found distant from the interaction surface between Prp24p and LSm ring.

5.3.4 Chemically Cross Linked Particles Exhibit a Compact Structure

Single particle image analysis of the U6 snRNPs showed that better class sums were obtained when two substructures were averaged separately instead whole particle was used. In order to stabilize the apparent flexibility between two domains of U6 snRNP, the particles were fixed chemically with 0.1 % glutaraldehyde in solution before adsorbing to the carbon film. Figure 4.28 A shows the overview of U6 snRNPs after fixing with glutaraldehyde. The fixed U6 particles have a less elongated shape with 12 nm length and 9 nm width, exhibiting a more compact structure as compared to the particles without glutaraldehyde fixation. Two distinct substructures, as could be seen in unfixed U6 particles, are hardly discernable and the typical angular structure of Prp24p domain or a ring-like structure can barely be seen in the overviews (Figure 4.28).

To determine the typical views of fixed U6 snRNPs, image classification and averaging of the U6 projections were done as described above. Using only 2,000 single particle images, the stabilized whole U6 particle revealed well-defined classes (Figure 4.28 B). In some class averages of fixed U6 snRNPs, typical structures

of LSm-ring and Prp24p-domain can be presumed (Figure 4.28 B lanes 1 and 2). In some views, partly LSm-ring structure can be recognized at the bottom as the upper domain represents more angular structure of Prp24p-domain.

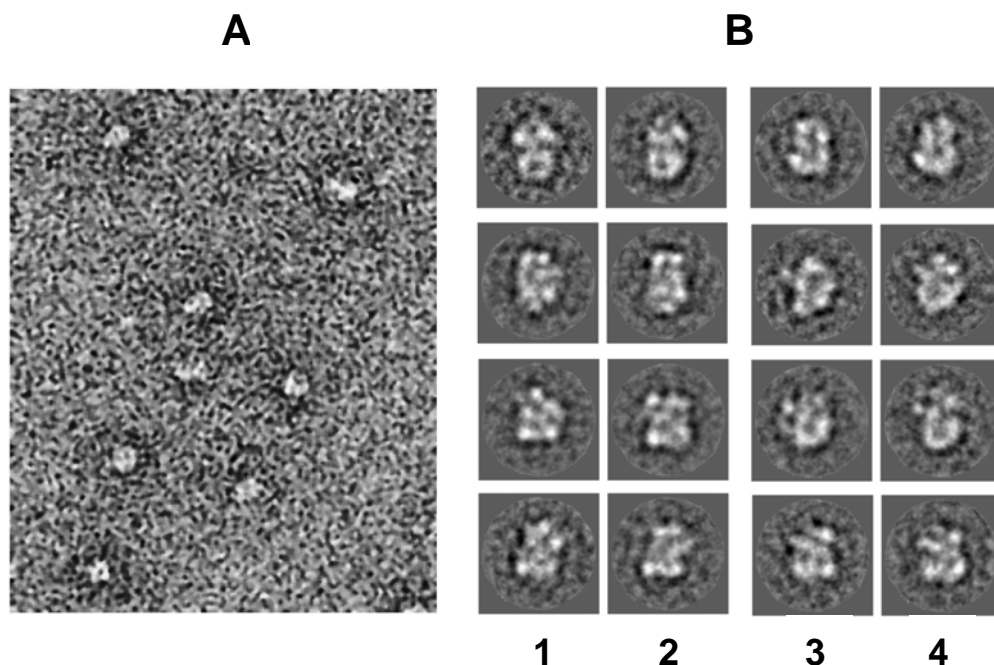


Figure 4.28 Electron microscopy analyses of the chemically fixed U6 snRNPs. The particles were purified using the TAP method and TAP-tagged Prp24p, and fixed by chemical cross linking with 0.1 % glutaraldehyde prior to binding to carbon film. **(A)** General view of the fixed U6 snRNPs. **(B)** Gallery of selected fixed U6 snRNP particles.

Next, chemically fixed U6 snRNPs containing yECitrine label at the C-terminal of individual LSm proteins were analyzed to map the location of the LSm ring as well as the nature of LSm ring-Prp24p interaction. Figure 4.29 B, C and D shows the class averages obtained after statistical analysis and classification of images from glutaraldehyde fixed U6 snRNPs with yECitrine label at LSm7p, LSm2p and LSm7p, or LSm3p. Like non-labeled U6 snRNPs (Figures 4.28 and 4.29 A), a more compact structure is observed with the labeled U6 snRNPs and the globular yECitrine-tag can be identified in most class averages (marked with arrows). Compared to corresponding class averages from unlabelled U6 snRNPs, yECitrine can be visually identified in some class averages of the tagged U6 particles. (Figure 4.29 B). Although no direct conclusion on relative position tag and Prp24p can be drawn, it can be now observed that LSm7p might be considerably close to the Prp24p domain in the U6 particle.

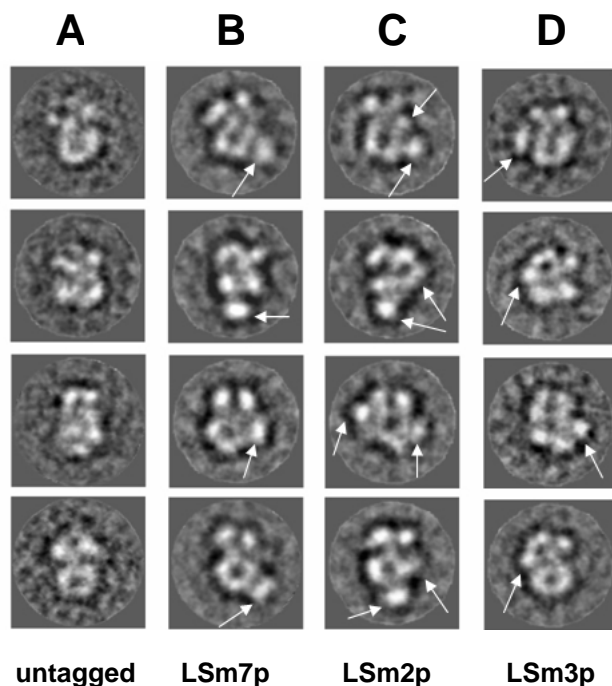


Figure 4.29 Electron microscopy analyses of the yECitrine labeled and chemically fixed U6 snRNPs. The particles were purified using the TAP method and TAP-tagged Prp24p, and fixed by chemical cross linking with 0.1 % glutaraldehyde prior to binding to carbon film. Gallery of selected fixed and untagged (**A**), LSm7p-tagged (**B**), LSm2p and LSm7p double-tagged (**C**), and LSm3p-tagged (**D**). The positions of yECitrine tags are shown by arrows.

As described above, electron microscopy analysis of LSm2p-LSm7p-double yECitrine-tagged unfixed U6 snRNP particles did not result in images where yECitrine tags could be clearly identified. However, after fixing with glutaraldehyde and image processing, the double-tagged U6 snRNP particles brought about better class averages where the yECitrine-tag could be better identified. Figure 4.29 shows such class averages where Prp24p, LSm-ring and globular domains of two different yECitrine-tags could be distinguished. In the images, the tag seen in lower position is very likely the yECitrine tag of LSm7 protein since yECitrine-tag in mono-LSm7p-tagged U6 snRNPs is oriented from similar positions (compare Figure 4.29 B and C). In most the images the position of the second yECitrine-tag of LSm2p is relatively difficult to identify. Similar results were obtained when U6 snRNPs tagged at LSm3p were analyzed by electron microscopy (Figure 4.29 D). yECitrine tag of LSm3p could be identified close to Prp24p domain.

DISCUSSION

5.1 RNA Structure and RNA-Protein Interactions in Purified U6 snRNPs

5.1.1 The Secondary Structure of U6 snRNA in Purified U6 snRNPs

Our chemical modification data demonstrate that the naked U6 snRNA structure is dramatically different from the structure of the U6 snRNA in U6 snRNP particles (Figure 5.1). The structure of the naked U6 snRNA is very compact, (Figure 5.1 A) whereas the presence of Prp24p and the LSm2p–8p proteins leads to a more open snRNA structure in the U6 particle (Figure 5.1 B). This is particularly apparent for the 3'-stem loop (also called intramolecular stem-loop, ISL, nucleotides 63–84), in which several nucleotides are inaccessible to chemical modification in the naked U6 snRNA, but are accessible in the U6 snRNP. Our data for the naked RNA are consistent with the NMR structure of a portion of the U6 ISL. For example, the proposed C67⁺A79 wobble pair (Reiter *et al.*, 2004) is consistent with the total (A79) and partial (C67) protection from chemical modification that we observe. Similarly, the complete protection of U80 under our conditions, is consistent with NMR studies performed at pH 7.0 that showed that U80 is sequestered within the helix (Reiter *et al.*, 2004). In the U6 snRNP, we observe a significant increase in the reactivity of bases C67 and A79 and, to a certain extent, of U80. Remarkably, we observe that the reactivity of bases C72–A75 of the loop structure is also enhanced when compared with that of the naked RNA.

In addition, our chemical modification data show that several nucleotides below the 3'-stem loop (e.g. 54–62 and 87–89) are paired in the naked U6 snRNA. A different result was obtained for the small internal loop, in which only three of the nucleotides are inaccessible; the latter could potentially form intramolecular base-pairings, as shown in Figure 5.1 A (broken lines). In this whole region, there is a very pronounced difference between the structure of the naked U6 snRNA and the U6 snRNA in the U6 particle (compare Figure 5.1 A with B). The presence of the U6 proteins leads to restructuring of these nucleotides, as can be seen especially for nucleotides 54–62 and 87–89, which are single-stranded only in the U6 snRNP. As the presence of Prp24p and the LSm complex leads to a number of local

structural rearrangements, U6 snRNA in the native U6 snRNP results in a more open structure. Dissociation of base-pairing results in the formation of the large asymmetric internal loop, which consists of nucleotides A40-A62 (on the left; Figure 5.1) and C85-A91 (on the right; Figure 5.1). This has important functional implications, as discussed below.

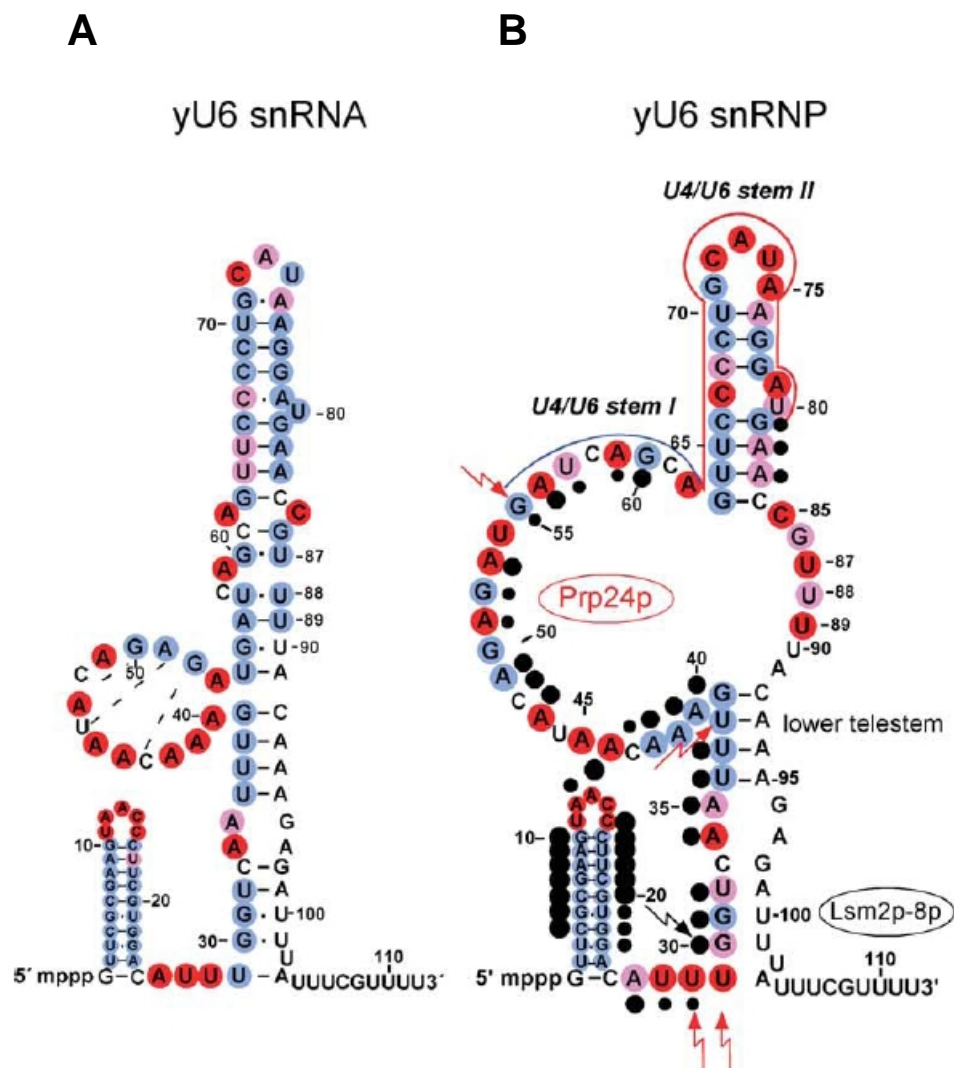


Figure 5.1 Comparison of the proposed secondary structure of yeast U6 snRNA in the naked (A) and in native U6 snRNPs (B) obtained by chemical structure probing. The binding region of Prp24p on the U6 snRNA was determined by hydroxyl-radical footprinting (black dots) and UV cross-linking (red arrows); for details, see the text. Bases protected from modification, blue; bases weakly modified, pink; bases strongly modified, red.

A similar structure opening is true for the base of the lower telestem of the U6 snRNA, where nucleotides 29–33 can base-pair with nucleotides 96–103 in the naked RNA. The RNA within the U6 particle seems to be less compact also in this

region. Indeed, nucleotides in the region 28–54 were previously found to be available for oligonucleotide-directed RNase H cleavage in the yeast U6 snRNP in cell extracts (Fabrizio *et al.*, 1989). This may be due to the fact that several nucleotides of the large internal loop are single stranded and available for base-pairing with an oligonucleotide. This would again indicate that the presence of proteins opens the U6 snRNA structure (Figure 5.1).

Our data do not support the presence of the upper half of the previously proposed telestem (nucleotides A40–C43 and G86–U89) in the purified U6 snRNP. We show that bases A40–A42 are single-stranded in the naked U6 snRNA, whereas they are protected from modifications in the U6 snRNP, indicating that these bases are either paired or shielded by Prp24p. However, we demonstrate clearly that bases A40–A42 are not paired, since their proposed binding partners, U87–U89, are accessible to the chemical probing reagents (Compare Figure 5.1 A with B). This is consistent with data reported by Ryan *et al.*, [2002] who proposed that this half of the telestem, which would form between bases A40–C43 and G86–U89, binds Prp24p even when the Watson–Crick base-pairing is disrupted by mutation of nucleotides G87–U89. Moreover, Ghetti *et al.*, [1995] observed that mutation of bases A40 and C43 decreased binding of recombinant Prp24p to naked U6 snRNA, suggesting that Prp24p contacts these bases in a sequence-specific manner. In addition, our footprinting analysis shows that nucleotides A40–C43 are protected from hydroxyl radical cleavage in native U6 snRNPs. Thus, this demonstrates that bases A40, A41, A42 and C43 are unpaired, but protected by direct binding of Prp24p, as discussed below.

In agreement with previously proposed yeast U6 secondary structures, we demonstrate that bases U36–G39 of the lower half of the telestem are paired in both the naked U6 snRNA and the RNA of the U6 particle (Figure 5.1 A and B) but bases A26–U28 (between 5′-stem loop and the base of lower telestem) are accessible to modification reagents, both in the naked U6 snRNA and in the U6 snRNP particle, suggesting that they are unpaired (Mougin *et al.*, 2002).

5.1.2 The Binding Site of Prp24 and LSm2-8 Proteins on the U6 snRNA in the U6 snRNP particles

Our hydroxyl radical footprinting experiments revealed that U6 proteins protect most of the nucleotides in the region C4–G60 of the U6 snRNA in native U6 snRNPs (see the black dots in Figure 5.1 B). A similar region was protected when

footprinting was performed with a binary recombinant Prp24p-U6 snRNA complex. The combined results of these footprinting studies indicate that the 5'-half of the U6 snRNA is the major binding region of Prp24p. Consistent with our footprinting data, we show by UV cross-linking that Prp24p contacts the U6 snRNA directly at four positions within the C4-G60 region (see the red arrows in Figure 5.1 B). The left part of the large asymmetrical loop (A40-A62) is the most striking binding site of Prp24p. Two types of Prp24p protections are found in this region: (1) bases protected at the Watson-Crick positions and on the ribose moieties; and (2) bases freely accessible at the Watson-Crick positions but protected on the ribose moieties. A40-C43, A49, G52, G55 and G60, whose bases should form intimate contacts with Prp24p belong to the first type of protection (Figure 5.1 B, see blue rounds). It is interesting to note that A40-A42 are among these rare type of nucleotides. As they are freely available in the naked U6 snRNA they could represent a recognition motif for nucleation of Prp24p. A47, A51, A53, A56 and A59 belong to the second type (Figure 5.1 B, red rounds). Interestingly, two of them are in the upper portion of the large loop (i.e. G55-A60), which is the region of U6 snRNA involved in base-pairing with U4 snRNA to form the stem I duplex.

For both yeast and human, uridine-rich sequence at the 3'-end of U6 snRNA (nucleotides 93-112) was suggested to involve in binding of LSm2-8 proteins (Achsel *et al.*, 1999; Mayes *et al.*, Vidal *et al.*, 1999). Our hydroxyl footprinting experiments could not detect a detectable binding region of LSm proteins in the U6 snRNP. This is due the fact that an oligonucleotide which annealed at the 3'-end of U6 snRNA (at nucleotides 94-102), was used to perform primer extension analysis. To detect which of the LSm protein(s) contacts the uridine-rich sequence of U6 snRNA, a different strategy was used. UV-irradiated purified U6 snRNPs containing yECitrine-labelled LSm proteins at their C-terminus were first immunoprecipitated by anti-yECitrine antibodies (see also section 4.1.4). The resulting possible cross links between U6 snRNA and LSm proteins were then detected by Northern blotting. By these experiments, LSm2p, -3p, -4p and -6p were observed to UV-cross link the U6 snRNA in native U6 snRNPs. Further analysis of these immunoprecipitated LSm-cross linked U6 snRNAs by primer extension analysis (which allows detection of cross linking sites upstream of nucleotide A93) indicated that only LSm2 protein cross links in this region, specifically to nucleotide G30. Unlike the U6 snRNA-LSm2p cross link, the other immunoprecipitated U6 snRNAs with LSm3p, -4p, or -6p cross links did not result in a specific reverse

transcriptase stop. This might indicate that LSm3p, -4p, and -6p cross links occur by means of the 3'-end of U6 snRNA and therefore not detected by this method. Additional experiments are required to confirm the presence of the cross linking sites between LSm3p, -4p and -6p and the 3'-terminus of U6 snRNA.

Our structural investigation experiments showed that the stem (nucleotides 29-33 and 96-103) at the base of U6 snRNA involves in more than one protein-RNA interactions. We showed by hydroxyl radical footprinting experiments that Prp24p binds strongly to G30-U32 in that region. Our cross linking experiments showed direct contact sites between U28-U29 and Prp24p and between G30 and LSm2p. Moreover, we showed by chemical probing experiments that nucleotides in the base of the lower telestem are somehow less involved in base pairing when compared to the naked U6 snRNA. The less compact structure in this region might suggest that Prp24p and LSm proteins might be in close proximity in the stem at the base of the U6 snRNA (see also section 5.2.2).

Interestingly, using only recombinant Prp24p and *in vitro* transcribed U6 snRNA, we observe that the footprint by Prp24p on the U6 snRNA extends to the entire 3'-stem. One possibility to explain this broader binding region (compared to native U6 snRNPs containing both Prp24p and LSm proteins) is that Prp24p expressed in *E. coli* binds less accurately than native Prp24p. Another possibility might be that Prp24p has indeed a larger binding site but becomes restricted when the LSm proteins are present. A reverse situation is observed in part for the 5'-stem loop structure. A protection of the 5'-stem loop is clearly seen after hydroxyl radical footprinting in the native U6 snRNP. This protection at the 5'-stem loop is also in the *in vitro* reconstituted U6-Prp24p binary complex; however, recombinant Prp24p binds the 5'-stem loop less efficiently. Again, this could, in part, be due to different behaviour of recombinant Prp24p. However, we favour the hypothesis that the LSm complex helps Prp24p to bind the 5'-stem loop more tightly and, overall, to recognize its binding regions in the U6 snRNA more correctly.

5.1.3 Prp24p and the LSm Complex Facilitate U4/U6 Association by Opening the U6 Structure

Our results demonstrate that a large asymmetric internal loop region of the U6 snRNA in the U6 particle is unpaired and protected from chemical modification by bound Prp24p. Prp24p interacts mostly in an alternating way with bases or ribose moieties in this region, and thus several of the bases whose sugar backbone

It is interesting to note that the 3'-stem loop of U6 snRNA can form linear/loop interactions with U4 snRNA. This type of interaction was suggested to play a role in helix propagation between two complementary RNA strands. (Zeiler and Seimons, 1998). U6 and U4 intermolecular base-pairing may begin between the unstructured free 5'-end of the U4 snRNA and the complementary 3'-stem loop of the U6 snRNA, leading to helix propagation to form stem II in the U4/U6 di-snRNP (Figure 5.2). Helix propagation would indeed be greatly facilitated in the snRNP, since the presence of Prp24p and the LSm2p-8p proteins, as shown above, destabilizes the stem. U80 and A79 of the bulge, as well as C72, A73 and U74 of the loop, are unpaired and therefore readily available for interaction with their binding partners in the U4 snRNA. Such initial recognition of the U4 snRNA by the 3'-stem loop of the U6 snRNA may lead to destabilization of surrounding RNA structures located on either side of the binding site, thereby allowing new RNA/RNA interactions to form. After formation of stem II, Prp24p may "hand over" to the U4 snRNA the single-stranded binding region G55-A62 for the formation of stem I.

In conclusion, our data suggest that the combined association of Prp24p and the LSm complex confers upon U6 nucleotides a conformation favourable for U4/U6 base-pairing. Thus, Prp24p and the LSm proteins may act as RNA chaperones (Beggs, 2005; Kwan and Brow, 2005). It has been hypothesized that RNA chaperones and specific RNA-binding proteins can solve different problems in RNA folding (Lorsch, 2002; Schroeder *et al.*, 2004). A role as RNA chaperones for the LSm proteins was proposed previously (Shannon and Guthrie, 1991). The LSm complex would help facilitate U6 snRNA restructuring, and the specific RNA binding protein Prp24p would stabilize the active U6 snRNA structure, which would not be sufficiently stable on its own. Indeed, recombinant Prp24p in the absence of the LSm proteins binds to the entire 3'-stem of U6 snRNA. This binding would probably block or slow the opening of this sequence, which is required to form the stem II duplex with the U4 snRNA.

5.1.4 The Structure of the Yeast U6 snRNA in Native snRNPs can be adopted by Human U6 and U6_{atac} snRNAs

In contrast to the other yeast spliceosomal RNAs, U6 is very similar in size and sequence to its human counterpart. Therefore, U6 snRNA from yeast and man may be expected to assume similar secondary structures. In fact, these molecules

have a 3'-stem loop of similar length (Figure 2.13; Harada *et al.*, 1980; Brow and Guthrie, 1988; Fortner *et al.*, 1994). The same holds true for the U6_{atac} snRNA, the 3'-stem loop of which has been shown to be phylogenetically conserved (Shukla and Padgett, 2001). Up to now, human U6 mono-snRNPs have not been isolated; however, the structure of naked U6 snRNA of higher eukaryotes was obtained by theoretical calculations of maximal base-pairing and by chemical and enzymatic probing (Harada *et al.*, 1980; Mougin *et al.*, 2002). In both cases, the structure of naked human U6 snRNA is very compact and resembles very much the structure of our naked yeast U6 snRNA. The existence of an internal loop was predicted (Rinke *et al.*, 1985), and it may be analogous to the loop adopted by bases 40–53 of the yeast U6 snRNA (Figure 2.13 A).

It was shown recently that the mammalian counterpart of Prp24p, p110/SART3, binds an internal region of the human U6 snRNA (bases 38–57) and a 5'-stem loop of the U6_{atac} snRNA from the same species (bases 10–30) (Figure 2.13; Bell *et al.*, 2002; Damianov *et al.*, 2004). These nucleotides exhibit a high level of evolutionary conservation between these two functionally related snRNAs, so it would be unexpected if they differ significantly in their secondary structure. Taking into consideration evolutionarily conserved nucleotides, the binding region of Prp24p to the yeast U6 snRNA in the native particle, and the binding region of recombinant p110 to the human U6 and U6_{atac} snRNAs, we propose on the base of our results from yeast U6 snRNA the following structures as they are shown in Figure 5.3. These structures suggest that the binding of both Prp24p and its mammalian orthologue p110 to the U6 snRNA would occur mostly at an internal loop of RNA consisting of several highly evolutionarily conserved bases.

Figure 5.3 shows also that two of the nucleotides (in yeast U6, U38 and G55), which are cross-linked to Prp24p, are 100% conserved in evolution (arrow heads in Figure 5.3), and that G55 (corresponding to nucleotides G49 and G22 in human U6 and U6_{atac} snRNAs, respectively) is situated in a highly conserved region. This suggests that conservation of these nucleotides in U6 snRNA may be related to their role in Prp24p/p110 binding and in spliceosomal function, such as base-pairing with the U4 and subsequently with the U2 snRNAs.

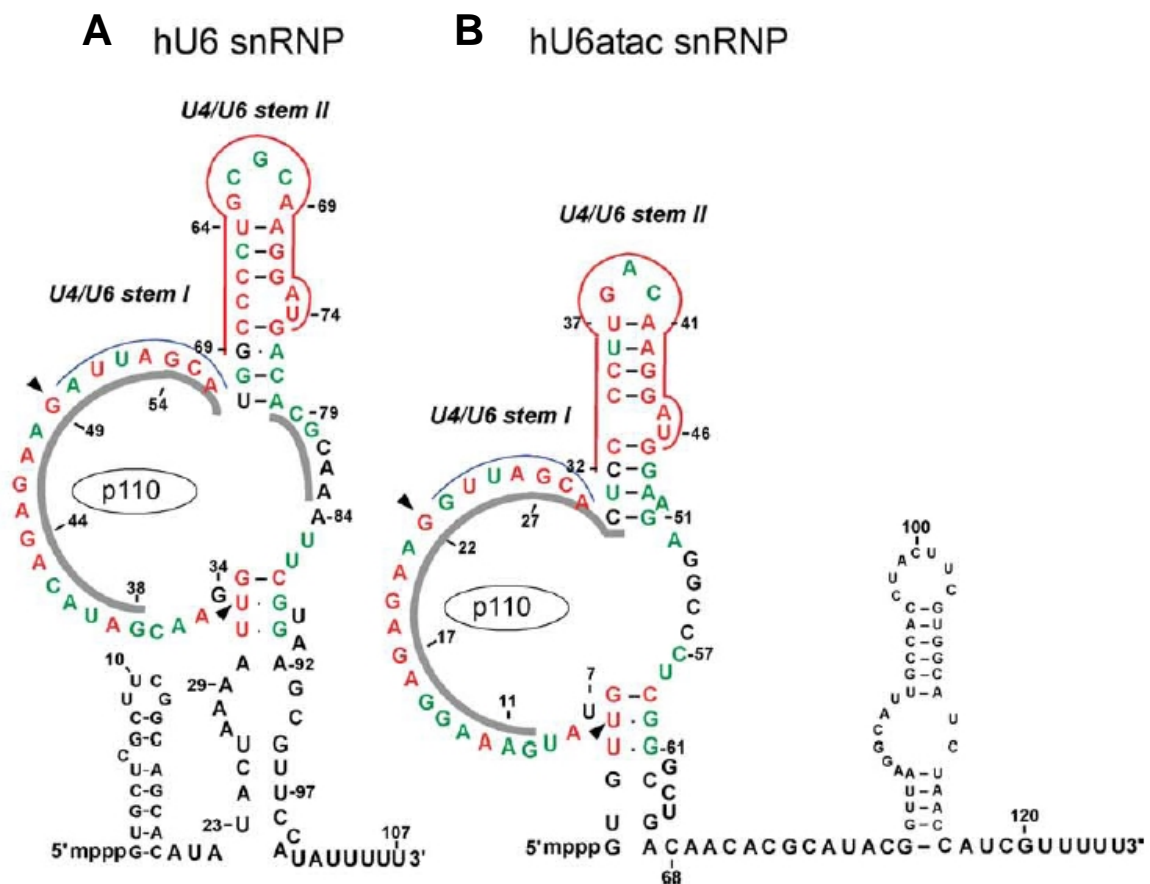


Figure 5.3 The structures of the U6 (A) and U6atac (B) snRNAs in the human U6 and U6atac particles. The structures have been extrapolated from the structure of the yeast U6 snRNA with the U6 snRNP shown in Figure 5.1. The recognition element of the human orthologue of Prp24p, p110/SART3, is depicted in grey. The black arrowheads point to two of the evolutionarily conserved nucleotides that in yeast are UV-crosslinked to Prp24p. Nucleotides that are 100% evolutionarily conserved between yeast U6, tomato U6, nematode U6, fly U6, mouse U6, human U6 and human U6atac snRNAs are shown in red. Nucleotides that are 70% conserved are shown in green. In each part of the Figure, nucleotides that are involved in the formation of stems I and II with the U4 snRNA, are highlighted with blue and red lines, respectively.

5.2 Electron Microscopy of Yeast U6 snRNPs Reveal Structural Arrangement between Prp24p and the LSm Ring

5.2.1 U6 snRNPs Exhibit Two Structural Configurations

In this study, in addition to determination of U6 snRNA structure and U6 snRNA-protein interactions, ultra structure of the yeast U6 snRNPs were analyzed by electron microscopy. Depending on whether U6 snRNP particles were chemically fixed prior to electron microscopy sample preparation or not, yeast U6 snRNPs

show two different structural configurations: (1) an open or (2) a close form.

Electron microscopy analysis of U6 snRNPs with open form shows two morphologically different substructures: (1) a round ring-like domain and (2) a more angular, jagged domain. The two domains appear to link with each other via a flexible region since statistical image analysis of the two subunits separately revealed better class averages than when classification of images was applied for the whole particle. The round substructure shows an accumulation of the stain in its middle, which is typical for the ring-shaped heptameric LSm (or Sm core) structure (Kastner *et al.*, 1990; Achsel *et al.*, 1999). The other Prp24p domain appears to have a roughly triangular shape that includes thick fine structure about 3 nm, which presumably the latter might represent the various RRM of the Prp24 protein.

Chemically cross linked U6 snRNP particles exhibit a close form. The typical elongated shape of U6 snRNPs observed by unfixed U6 particles is not seen anymore when U6 particles were fixed. Moreover, two morphologically different substructures, Prp24p and LSm ring, which can be very well identified in the unfixed U6 snRNPs, cannot be easily distinguished in the fixed U6 particles. Only some class averages showed parts of the typical views of LSm ring structure, suggesting that in the fixed U6 snRNPs, Prp24p domain superimposes largely the LSm ring and makes it more difficult to recognize. Remarkably, close form in the fixed U6 snRNP reveals better class averages and a more uniformly defined structure as compared with the unfixed U6 particles. Therefore, the close form of U6 snRNPs might represent the more native structure and might indicate a biologically relevant configuration of U6 snRNPs. In solution, both open and close forms of U6 snRNP might be at equilibrium. It is very likely that during electron microscopy sample preparation, if not fixed chemically, the open form is induced since U6 snRNP particles in such an open form will have a larger binding surface to adsorb on the carbon film, which is used during EM-specimen preparation.

Interestingly, yeast two-hybrid data showed that the highly conserved 12 amino acids long C-terminal motif of Prp24 protein is responsible for strong interaction of Prp24p with LSm5p, -7p and 8p (Fromont-Racine *et al.*, 2000; Rader and Guthrie, 2002). In the open form, the two substructures of U6 snRNP are positioned relatively distant to each other and it is hard to suggest any interaction between two substructures. However, in the close form, Prp24p and LSm ring must be situated nearer. For such a transition, Prp24p could bend over the LSm ring,

consequently, would allow the observed two-hybrid interactions between Prp24p and LSm proteins.

5.2.2 Topographic Labelling of the LSm Proteins Reveals the Arrangement of Prp24p, LSm Proteins and U6 snRNA

To identify the positions of LSm protein entities in U6 snRNP, we developed a new method for topographical localization of proteins by electron microscopy. For localization of the LSm proteins each individual LSm protein was extended by manipulating genetically with the yECitrine protein sequence at their C-terminus, which introduced a 4 nm-long globular domain that could be visualized by electron microscopy. First of all, our study showed that yECitrine is well suited for topographical labelling of small complexes like yeast U6 snRNP and depending on the position of the yECitrine-tag; it allowed us direct visualization and localization of the individual LSm proteins. The big advantage of the tagging method is that label is introduced by genetic recombination into all of the targeted protein. As an additional result, isolated tagged-complexes are particularly suitable for statistical image analysis as compared to other labelling methods such as immunolabelling of target proteins with antibodies, where often only a fraction of the particles is efficiently labelled.

The positions of LSm proteins were investigated in U6 snRNPs that had been singly labelled (LSm3p, -4p, -5p, -6p, -7p and -8p in separate particles) and doubly labelled (LSm2p-LSm7p in the same particle). The electron micrographs obtained from labelled and unfixed U6 snRNPs showed that LSm4p, -5p, 6p, 7p, and -8p are found in the LSm ring at distant positions to the Prp24p domain (Figure 5.4 A). Both LSm5 and LSm7 proteins are found clearly at very distant positions to the region where Prp24p and LSm ring is linked to each other. Both labelled U6 snRNPs revealed images with more elongated U6 particles as seen at the unlabelled U6 snRNP, suggesting that LSm5p and LSm7p are located at nearly opposite positions relative to Prp24p domain. LSm6 and LSm8 labelled U6 snRNPs exhibited particles in similar length or only slightly longer than the untagged U6 snRNP. Like the tag at LSm5p and LSm7p, in both LSm6 and LSm8 labelled particles, yECitrine was clearly visible. However, LSm6p and in particular LSm8p exhibited a closer localization to the Prp24p-LSm ring link region, suggesting that LSm 6 and LSm 8 proteins in the LSm ring are located still distant from Prp24p domain but closer than the positions of LSm5p or LSm7p.

The position of the tag at LSm4 protein was more difficult to locate. It varied in position and appeared not to be located directly attached to the ring structure. Among the LSm proteins, LSm4p is particular as it contains about 90-amino acid long C-terminal sequence in addition to its Sm domain. Other LSm proteins contain in maximum only 30 amino acids long additional sequences. As the yECitrine-tag is placed at the very C-terminal of the 60-amino acid long extension, it probably protrudes out of the LSm-ring and places the tag in some distance to the ring. Indeed, class averages focused on the LSm domain of the unfixed U6 snRNP particle revealed fine structural features like a 3 nm-long protuberance extending the LSm ring. This long protuberance is very likely the C-terminal extension of LSm4p. It was previously shown that RNA-free human LSm complexes exhibit also a round structure with a conspicuous peripheral protuberance (Figure 2.8; Achsel *et al.*, 1999). As the isolated human LSm complex contained neither U6 snRNA nor another protein, such a big protuberance at the periphery of the LSm ring can derive only from LSm4p. In human, LSm4p has by far the longest extension as compared to the other LSm proteins. In conclusion, comparing the long LSm4p protuberance and the label position with the Prp24p-LSm ring link region suggested that LSm4p is localized at a distant position from Prp24p-LSm ring link region.

Electron microscopy analysis of LSm2p and LSm3p labelled unfixed U6 snRNPs did not result in clear localization of the yECitrine tag. The position of the yECitrine tags at LSm2p or LSm3p could be first identified when the labelled U6 particles at these LSm proteins were chemically fixed and the images were analyzed by image processing. Class averages obtained from these labelled and fixed U6 snRNPs indicated that the positions of LSm2 and LSm3 proteins might be in close proximity to the Prp24p domain. Indeed such a localization of LSm2p and LSm3p is expected if the arrangement of LSm4p, -5p, 6p-, 7p, and -8p is considered in the LSm ring. If the LSm5 and LSm7 proteins are located opposite to the Prp24p domain, LSm2p and LSm3p should be situated close to Prp24p-LSm link region as these proteins are placed at opposite to LSm5p and LSm7p in the ring sequence of the LSm proteins (Figure 5.4 B). The sequence of the LSm proteins in this LSm ring structure indeed fully agrees with our yECitrine labelling results. In addition, all our results clearly show that the arrangement of the LSm proteins in the LSm ring relative to the Prp24p domain is not random. Moreover, our results predict that the Prp24p domain is linked to the LSm ring at well defined positions

close to LSm2p and/or LSm3p.

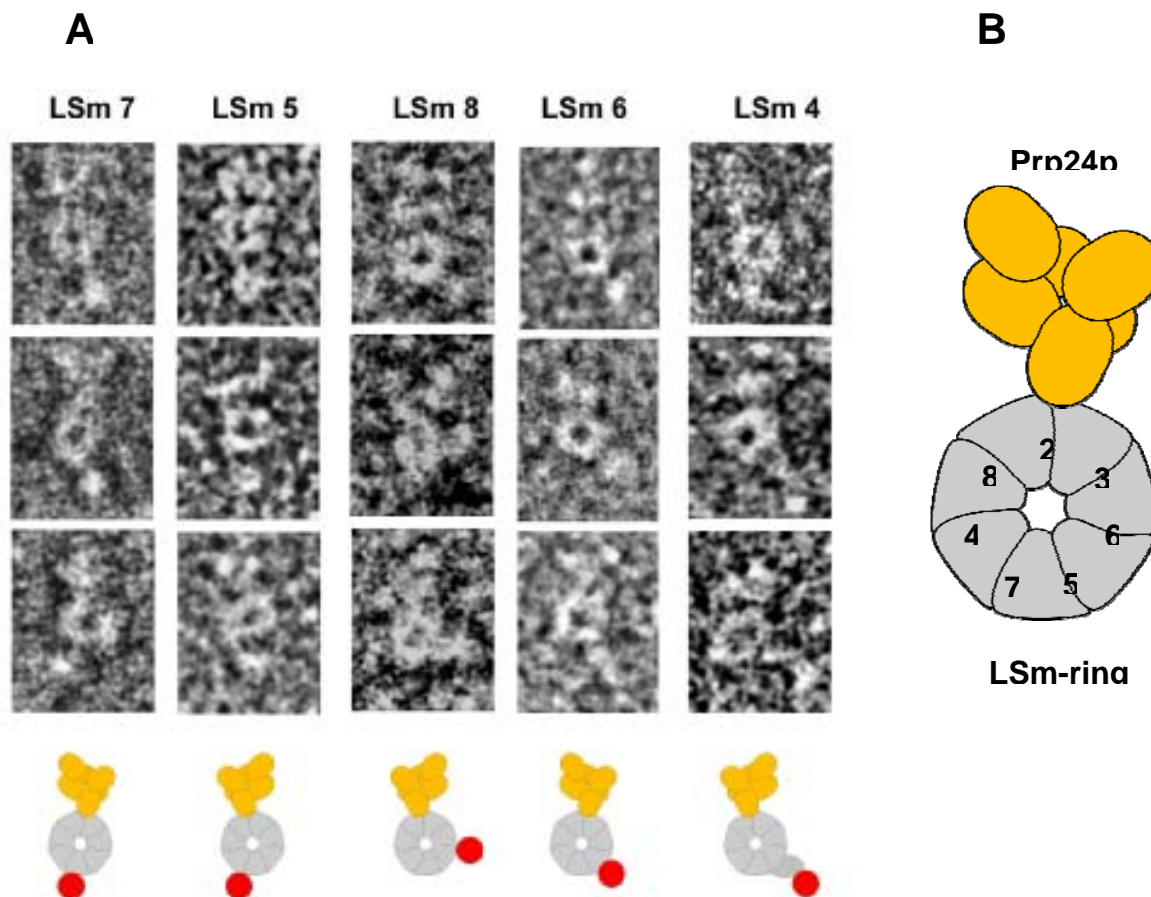


Figure 5.4 Summary of electron microscopy analysis of γ ECitrine-labelled U6 snRNPs. (A) Most frequent images from γ ECitrine-LSm7p, -5p, -8p, -6p, or -4p labelled unfixed U6 snRNP particles are shown. Below image projections, the positions of γ ECitrine-tag relative to Prp24p-LSm-ring contact region are shown schematically with red rounds. **(B)** Interaction between Prp24p and LSm-ring is shown schematically. The identities of the LSm proteins in the LSm-ring are shown with numbers from 2 to 8.

A direct evidence was obtained from our UV-cross linking experiments with the LSm proteins. LSm2p was observed to cross link at the base of the lower telestem of the U6 snRNA. Prp24p was also found to interact with the nucleotides of this stem region (see section 5.1.2.). This is indeed in perfect agreement with our electron microscopy analysis of the positions of LSm proteins and furthermore confirms that the LSm2 protein is located close to the Prp24p domain. In conclusion, our data provide the first direct confirmation about the proposed arrangement in the LSm ring (Panone *et al.*, 2001; Ingelfinger *et al.*, 2002) that LSm proteins assume an order of 4-8-2-3-5-6-7. Our data also show that in U6 snRNP,

LSm2p, eventually together with LSm3p, is the closest LSm proteins to Prp24p domain (Figure 5.4 B).

Interestingly, the Prp24 protein by yeast two-hybrid analysis showed weak or no interactions with LSm2p or LSm3p, on the other hand, we show by electron microscopy analysis that in the open form of U6 snRNP, these two LSm proteins are located near Prp24p. Indeed, the observed flexibility between Prp24p domain and the LSm ring does not argue for strong protein-protein interactions. It is very likely that in the open form of U6 snRNP, Prp24p and LSm proteins do not interact at protein level. Therefore, U6 snRNA is the only element of U6 snRNP, which can provide the link between Prp24p and the LSm ring in the open form. The Prp24p domain and LSm ring are linked to each other at the position where LSm2p is also located, as Prp24p and LSm2p, both cross links to the nucleotides U28-G30 at the base of lower telestem. Therefore, this stem region of U6 snRNA is the putative candidate to grant a link region between Prp24p domain and LSm ring.

The manner of RNA binding to the Sm/LSm rings is still not very well understood. Although there are available crystal structures of RNA bound to Sm ring (Mura *et al.*, 2003), it is not clear in which direction, 5'- to 3'-, RNA is oriented along the ring aperture, which is the known binding site for the 3'-end of U6 snRNA. In addition, it is still unknown how the 3'-terminus of U6 snRNA is aligned along LSm proteins, whether LSm nucleotide binding pocket prefer LSm 2-3-6-5-7-4-8 or another way around LSm 3-2-8-4-7-5-6. We showed by cross linking experiments that three LSm proteins -3, -4 and -6 contain putative contact sites probably at the 3'-end of U6 snRNA in addition to the cross link between LSm2 protein and nucleotide G30. It can be suggested that at the Prp24p-LSm ring link region, where the stem region at the base of U6 snRNA leaves Prp24p domain, LSm2p contacts this stem region first and as next, the neighbouring LSm3p and LSm6p could hand over the first 5'-nucleotides of uridine rich sequence of U6 snRNA. Such an assumption would favour the alignment of the LSm proteins as 2-3-6-5-7-4-8 with the U6 snRNA. Clearly, further experiments are needed to elucidate these points. Electron microscopy analysis of labelled LSm proteins together with the U6 snRNA labelled at its 3'-end will help us to define the alignment of the U6 snRNA in the LSm ring aperture.

5.2.3 Possible Functional Implications of Two Forms of U6 snRNP

During subsequent rounds of splicing, U4- and U6 snRNAs must re-associate to assemble into new [U4/U6.U5] tri-snRNP particles. We showed by chemical probing experiments (see sections 5.1.1 and 5.1.2) that the binding of Prp24 and the LSm2-8 proteins to U6 snRNA causes a number of local structural rearrangements and confer U6 snRNA a conformation favourable for U4/U6 base pairing. It has been shown that either Prp24p or LSm2p-8p alone can promote the annealing of the U4/U6 snRNAs but it is more efficient when both Prp24 and LSm2-8 proteins are present. Moreover, during the cooperation between Prp24p and LSm2p-8p, the interaction between C-terminal motif of Prp24p and the LSm5p, -7p and -8p is important for the efficient promotion of the base pairing association between U4- and U6 snRNAs (Rader and Guthrie, 2002; Verdonne *et al.*, 2005). Therefore, the observed close form of U6 snRNPs, which suggested multiple Prp24p-LSm ring interaction, must be functionally important. During the transition from close to open form or vice versa, the postulated structural rearrangements could be important for the alignment and formation of the stems I and II of U4/U6 di-snRNA. In solution, if open and close forms of U6 snRNP are at an equilibrium state, close form could correspond to the functionally active configuration of U6 snRNP. The transition from close to open form can begin with the annealing of U6 snRNA with U4 snRNA. The open form will then allow the initial base pairing with U4 snRNA and subsequent helix propagation, which leads the formation of stems I and II in the U4/U6 di-snRNP.

REFERENCES

A

Achsel, T., Brahms, H., Kastner, B., Bachi, A., Wilm, M., and Lührmann, R. (1999) A doughnut-shaped heteromer of human Sm-like proteins binds to the 3'-end of U6 snRNA, thereby facilitating U4/U6 duplex formation *in vitro*. *EMBO J.*, 18, 5789-5802.

Albrecht, M. and Lengauer, T. (2004) Novel Sm-like proteins with long C-terminal tails and associated methyltransferases. *FEBS Lett.*, 569, 18-26

B

Beggs, J. D. (2005). Lsm proteins and RNA processing. *Biochem. Soc. Trans.* 33, 433-438.

Bell, M., Schreiner, S., Damianoy, A., Reddy, R., and Bindereif, A. (2002) p110, a novel human U6 snRNP protein and U4/U6 snRNP recycling factor. *EMBO J.*, 21, 2724-2735

Berglund, J. A., Chua, K., Abovich, N., Reed, R. and Rosbash, M. (1997) The splicing factor BBP interacts specifically with the pre-mRNA branchpoint sequence UACUAAC. *Cell*, 89, 781-787.

Berglund, J. A., Abovich, N., Rosbash, M. (1998) A cooperative interaction between U2AF65 and mBBP/SF1 facilitates branchpoint region recognition. *Genes Dev.*, 12, 858-867.

Black, D. L. and Pinto, A. L. (1989) U5 small nuclear ribonucleoprotein: RNA structure analysis and ATP-dependent interaction with U4/U6. *Mol. Cell. Biol.*, 9, 3350-3359.

Blum, H., Beier, H., and Gross, H.J. (1987) Improved silver staining of plant proteins, RNA, and DNA polyacrylamide gels. *Electrophoresis*, 8, 93-99.

Bochnig, P., Reuter, R., Bringmann, P. and Lührmann, R. (1987) A monoclonal antibody against 2,2,7-trimethylguanosine that reacts with intact U1 snRNPs as well as with 7-methylguanosine-capped RNAs. *Eur. J. Biochem.*, 168, 461-467.

Bordonne R., Banroques J., Abelson J. and Guthrie C. (1990) Domains of yeast U4 spliceosomal RNA required for PRP4 protein binding, snRNP-snRNP interactions and pre-mRNA splicing in vivo. *Genes Dev.*, 4(7): 1185-96

Bradford, M.M. (1976) *Anal. Biochem.*, 72, 248-254

Brimacombe, R., Stiege, W., Kyriatsoulis, A., and Maly, P. (1988) Intra-RNA and RNA-protein cross-linking techniques in *Escherichia coli* ribosomes. *Methods Enzymol.*, 164, 287-309.

Brow, D.A. and Guthrie, C. (1988) Spliceosomal U6 RNA is remarkably conserved from yeast to mammals. *Nature*, 334, 213-218

Brow, D.A. (2002) Allosteric Cascade of Spliceosome Activation. *Annu Rev Genet.*, 26: 333-60

Burge, C.B., Tuschl, T., and Sharp, P.A. (1999) Splicing of precursors to mRNAs by the spliceosomes. In Gesteland, R.F., Cech, T.R., and Atkins, J.F., Editors, *The RNA World* (Second edition), Cold Spring Harbor Laboratory Press, New York, pp. 525-560.

C

Celander D.W. and Cech T.R. (1990) Iron(II)-ethylenediaminetetraacetic acid catalyzed cleavage of RNA and DNA oligonucleotides: similar reactivity toward single- and double-stranded forms. *Biochemistry*, 13, 29(6): 1355-61.

Chanfreau, G., Elela, S. A., Ares, M. and Guthrie, C. (1997) Alternative 3'-end processing of U5 snRNA by RNase III. *Genes Dev.*, 11, 2741-2751.

Chen C-H, Yu W-C, Tsao TY, Wang LY, Chen H-R, et al. 2002. Functional and physical interactions between components of the Prp19p-associated complex. *Nucleic Acids Res.* 30:1029–37

Cheng, S. C. and Abelson, J. (1987) Spliceosome assembly in yeast. *Genes Dev.*, 1, 1014-1027.

D

Damianov A., Schreiner S. and Bindereif A. (2004) Recycling of the U12-type spliceosome requires p110, a component of the U6 atax snRNP. *Mol Cell Biol.*, 24(4): 1700-8

Dixon, W.J., Hayes, J.J., Levin, J.R., Weidner, M.F., Dombroski, B.A., and Tullius, T.D. (1991) Hydroxyl radical footprinting. *Methods Enzymol.*;208, 380-413.

E

Ehresmann, C., Baudin, F., Mougél, M., Romby, P., Ebel, J.P., and Ehresmann, B. (1987) Probing the structure of RNAs in solution. *Nucleic Acids Res.*, 15, 9109-9128

F

Fabrizio, P., McPheeters, D.S., and Abelson, J. (1989) *In vitro* assembly of yeast U6 snRNP: a functional assay. *Genes & Dev.*, 3, 2137-2150.

Fortes, P., Bilbao-Cortés, D., Fornerod, M., Rigaut, G., Raymond, W., Séraphin, B. and Mattaj, I. W. (1999) Luc7p, a novel yeast U1 snRNP protein with a role in 5' splice site recognition. *Genes Dev.*, 13, 2425-2438.

Fortner, D.M., R.G. Troy, and D.A. Brow, (1994) A stem/loop in U6 snRNA defines a conformational switch required for pre-mRNA splicing. *Genes & Dev.*, 8, 221-233.

Friendewey, D. and Keller, W. (1985) Stepwise assembly of a pre-mRNA splicing complex requires U-snRNPs and specific introns sequences. *Cell*, 42, 355-367

Fromont-Racine M., Mayes A.E., Brunet-Simon, A., Rain, J.C., Colley, A., Dix, I., Decourty, L., Joly, N., Ricard, F., Beggs, J.D., and Legrain, P. (2000) Genome-wide protein interaction screens reveal functional networks involving Sm-like proteins. *Yeast*, 30, 17(2): 95-110.

G

Ghetti, A., Company, M., and Abelson, J. (1995) Specificity of Prp24p binding to RNA: A role for Prp24p in the dynamic interaction of U4 and U6 snRNAs. *RNA*, 1, 132-145.

Guthrie C. and Patterson C. (1988) Spliceosomal snRNAs. *Annu Rev Genet.*, 49(5): 613-24

H

Hamm, J. and Mattaj, I.W. (1990) Monomethylated cap structures facilitate RNA export from the nucleus. *Cell*, 63(1), 109-118.

Harada, F., Kato, N. & Nishimura, S. (1980). The nucleotide sequence of nuclear 4.8S RNA of mouse cells. *Biochem. Biophys. Res. Commun.* 95, 1332–1340.

Hartmuth, K., Raker, V.A., Huber, J., Branlant, C., and Lührmann, R. (1999) An unusual chemical reactivity of Sm site adenosines strongly correlates with proper assembly of core U snRNP particles. *J. Mol. Biol.*, 285, 133-147.

Hartmuth, K., Urlaub, H., Vornlocher, H.P., Will, C.L., Gentzel, M., Wilm, M., and Lührmann, R. (2002) Protein composition of human pre-spliceosomes isolated by a tobramycin affinity-selection method. *Proc. Natl. Acad. Sci. USA*, 99, 16719-16724.

He, W., and Parker, R. (2000) Functions of Lsm proteins in mRNA degradation and splicing. *Curr. Opin. Cell Biol.*, 12, 346-350.

Hermann, H., Fabrizio, P., Raker, V.A., Foulaki, K., Hornig, H., Brahms, H., and Lührmann, R. (1995) snRNP Sm proteins share two evolutionarily conserved sequence motifs which are involved in Sm protein-protein interactions. *EMBO J.*, 14, 2076-2088;

Hertzberg, R.P. and Dervan, P.B. (1984) Cleavage of DNA with methidiumpropyl-EDTA-iron(II): reaction conditions and product analyses. *Biochemistry*, 23(17), 3934-3945.

Huppler A., Nikstad L.J., Allmann A.M., Brow D.A. and Butcher S.E. (2002) Metal binding and base ionization in the U6 snRNA intramolecular stem-loop structure. *Nat Struct Biol.*, 9(6):431-5

I

Igel, A. H. and Ares, M. Jr. (1988) Internal sequences that distinguish yeast from metazoan U2 snRNA are unnecessary for pre-mRNA splicing. *Nature* , 334, 450-453.

Ingelfinger D., Arndt-Jovin D.J., Lührmann R. and Achsel T (2002) The human LSm1-7 proteins colocalize with the mRNA-degrading enzymes Dcp1/2 and Xrn1 in distinct cytoplasmic foci. *RNA.*, 8(12): 1489-501

J

Jandrositz, A. and Guthrie, C. (1995) Evidence for a Prp24p binding site in U6 snRNA and in a putative intermediate in the reannealing of U6 and U4 snRNAs. *EMBO J.*, 14, 820-832.

K

Kambach, C., Walke, R., Young, R., Avis, J.M., and De La Fortelle (1999) Crystal structures of two Sm protein complexes and their implications for the assembly of the spliceosomal snRNPs. *Cell*, 96, 375-387

Kastner, B., Bach, M., and Lührmann, R. (1990) Electron microscopy of small nuclear ribonucleoprotein (snRNP) particles U2 and U5: evidence for a common structure-determining principle in the major U snRNP family. *Proc. Natl. Acad. Sci. USA*, 87, 1710-1714.

Kastner, B. and Lührmann, R. (1999) Purification of U small nuclear ribonucleoprotein particles. *Methods Mol. Biol.*, 118, 289-298.

Khusial P., Plaag R. and Zieve G. (2005) LSm proteins form heptameric rings that bind to RNA via repeating motifs. *TIBS.*, 30: 522-528

Konarska, M. M. and Sharp, P. A. (1988) Association of U2, U4, U5, and U6 small nuclear ribonucleoproteins in a spliceosome-type complex in absence of precursor RNA. *Proc. Natl. Acad. Sci., USA*, 85, 5459-5462.

Krol, A. and Carbon, P. (1989) A guide for probing native small nuclear RNA and ribonucleoprotein structures. *Methods Enzymol.*, 180, 212-227

Kwan S.S. and Brow D.A. (2005) The N- and C-terminal RRM of splicing factor Prp24 have distinct functions in U6 snRNA binding. *RNA.*, 11(5): 808-20

L

Lange, T.S. and Gerbi, S.A. (2000) Transient nucleolar localization of U6 small nuclear RNA in *Xenopus laevis* oocytes. *Mol. Biol. Cell.*, 11, 2419-2428.

Lorsch, J. R. (2002). RNA chaperones exist and DEAD box proteins get a life. *Cell*, 109, 797-800.

M

Madhani, H.D. and Guthrie, C. (1994) Dynamic RNA-RNA interactions in the spliceosome. *Annu. Rev. Gen.*, 28, 1-26.

Maroney, P. A., Romfo, C. M. and Nilsen, T. W. (2000) Functional recognition of 5' splice site by U4/U6.U5 tri-snRNP defines a novel ATP-dependent step in early spliceosome assembly. *Mol. Cell*, 6, 317-328.

Mayes, A.E., Verdone, L., Legrain, P., and Beggs, J.D. (1999) Characterization of Sm-like proteins in yeast and their association with U6 snRNA. *EMBO J.*, 18, 4321-4331.

Merril, C.R., Goldman, D., Sedman, S.A., and Ebert, M.H. (1981) Ultrasensitive stain for proteins in polyacrylamide gels shows regional variation in cerebrospinal fluid proteins. *Science*, 211(4489), 1437-1438.

Miura, K., Tsuda, S., Harada, F., and Ueda, T. (1983) Chemical modification of cytosine residues of U6 snRNA with hydrogen sulfide (nucleosides and nucleotides. Part 49 [1]). *Nucleic Acids Res.*, 11(17), 5893-5901.

Moine, H., Ehresmann, B., Ehresmann, C., and Romby P. (1997) Probing RNA structure and function in solution. *RNA Structure and Function*, Cold Spring Harbor Laboratory Press, 77-115.

Moore, M.J., Query, C.C., and Sharp, P.A. (1993) Splicing of precursors to mRNA by the spliceosome. In Gesteland, R.F. and Atkins, J.F., Editors, *The RNA World*, Cold Spring Harbor Laboratory Press, New York, pp. 303-357.

Mougin, A., Gottschalk, A., Fabrizio, P., Lührmann, R., and Branlant, C. (2002) Direct probing of RNA structure and RNA-protein interactions in purified Hela cell's and yeast spliceosomal U4/U6.U5 tri-snRNP particles. *J. Mol. Biol.*, 317, 631-649.

Mura C., Philips M., Kozhukhovskiy A. and Eisenberg D. (2003) Structure and assembly of an augmented Sm-like archaeal protein 14-mer. *Proc Natl Acad Sci USA.*, 100(8): 4539-44

N

Nilsen, T.W. (1998) RNA-RNA interactions in nuclear pre-mRNA splicing. In Silmons, R.W. and Grunberg-Manago, M.G., Editors, *RNA Structure and Function*. Cold Spring Harbor, New York, 35, pp. 279-307.

P

Pannone, B.K., Kim, S.D., Noe, D.A., and Wolin, S.L. (2001) Multiple Functional Interactions Between Components of the Lsm2p-Lsm8p Complex, U6 snRNA, and the Yeast La Protein. *Genetics*, 158, 187-196.

Plessel, G., Lührmann, R., and Kastner, B. (1997) Electron microscopy of assembly intermediates of the snRNP core: Morphological similarities between the RNA-free (E.F.G.) protein heteromer and the intact snRNP core. *J Mol Biol*, 265, 87-94

Powers, T. and Noller, H.F. (1995) Hydroxyl radical footprinting of ribosomal proteins on 16S rRNA. *RNA*, 1(2), 194-209.

Puig, O., Gottschalk, A., Fabrizio, P. and Séraphin, B. (1999) Interaction of the U1 snRNP with nonconserved intronic sequences affects 5' splice site selection. *Genes Dev.*, 13, 569-580.

Puig O., Caspary F., Rigaut G., Rutz B., Bouveret E., Bragado-Nilsson E., Wilm M., and Séraphin B. (2001) The tandem affinity purification (TAP) method: A general procedure of protein complex purification. *Methods* 24, 218-229.

Q

Qu, H.L., Michot, B., and Bachellerie, J.P. (1983) Improved methods for structure probing in large RNAs: a rapid 'heterologous' sequencing approach is coupled to the direct mapping of nuclease accessible sites. Application to the 5' terminal domain of eukaryotic 28S rRNA. *Nucleic Acids Res.*, 11(17), 5903-20.

R

Rader, D.S. and Guthrie, C. (2002) A conserved Lsm-interaction motif in Prp24 required for efficient U4/U6 di-snRNP formation. *RNA*, 8, 1378-1392.

Ragunathan, P.L. and Guthrie, C. (1998) A spliceosomal recycling factor that reanneals U4 and U6 small nuclear ribonucleoprotein particles. *Science*, 279, 857-860.

Reed, R. and Chiara, M.D. (1999) Identification of RNA-protein contacts within functional ribonucleoprotein complexes by RNA site-specific labeling and UV crosslinking. *Methods*, 18(1), 3-12.

Reiter N.J., Nikstadt L.J., Allmann A.M., Johnson R.J. and Butcher S.E. (2004) *Biochemistry.*, 43(43): 13739-47

Rigaut G., Shevchenko A., Rutz B., Wilm M., Mann M., and Séraphin B. (1999) A generic protein purification method for protein complex characterization and proteome exploration. *Nat. Biotechnol.* 17, 1030-1032.

Rinke, J., Appel, B., Digweed, M. & Lührmann, R. (1985). Localization of a base-paired interaction between small nuclear RNAs U4 and U6 in intact U4/U6 ribonucleoprotein particles by psoralen crosslinking. *J. Mol. Biol.* 185, 721–731.

Ryan, D.E., Stewens, S.W., and Abelson, J. (2002) The 5' and 3' domains of yeast U6 snRNA: Lsm proteins facilitate binding of Prp24p protein to the U6 telestem region. *RNA*, 8, 1011-1033.

S

Salgado-Garrido, J., Bragado-Nilsson, E., Kandels-Lewis, S., and Séraphin, B. (1999) Sm and Sm-like proteins assemble in two related complexes of deep evolutionary origin. *EMBO J.*, 18, 3451-3462.

Schroeder, R., Barta, A. & Semrad, K. (2004). Strategies for RNA folding and assembly. *Nature Rev. Mol. Cell Biol.* 5, 908–919.

S raphin, B. and Rosbash, M. (1989) Identification of functional U1 snRNA-pre-mRNA complexes committed to spliceosome assembly and splicing. *Cell*, 59, 349-358.

Schumperli, D. and Pillai, R.S. (2004) The special Sm core structure of the U7 snRNP: far-reaching significance of a small nuclear ribonucleoprotein. *Cell. Mol. Life Sci.*, 61, 2560-70

Shannon, K.W. and Guthrie, C. (1991) Suppressors of a U4 snRNA mutation define a novel U6 snRNP protein with RNA-binding motifs. *Genes Dev.*, 5, 773-785.

Shevchenko, A., Wilm, M., Vorm, O., and Mann, M. (1996) Mass spectrometric sequencing of proteins silver-stained polyacrylamide gels. *Anal Chem.*, 68(5), 850-858.

Shukla, G. C. & Padgett, R. A. (2001). The intramolecular stem-loop structure of U6 snRNA can functionally replace the U6atac snRNA stem-loop. *RNA*, 7, 94–105.

Siliciano, P.G. and Guthrie, C. (1988) 5' splice site selection in yeast: genetic alterations in base pairing with U1 reveal additional requirements. *Genes & Dev.*, 2, 1258-1267.

Siliciano, P. G., Kivens, W. J. and Guthrie, C. (1991) More than half of yeast U1 snRNA is dispensable for growth. *Nucleic Acids Res.*, 19, 6367-6372.

Singh, R. and Reddy, R. (1989) γ -Monomethylphosphate: A cap structure in spliceosomal U6 small nuclear RNA. *Proc. Natl. Acad. Sci., USA*, 86, 8280-8283.

Staley, J.P. and Guthrie, C. (1998) Mechanical devices of the spliceosome: motors, clocks, springs, and things. *Cell*, 92, 315-326.

Stark H., Dube P., Luhrmann R. and Kastner B. (2001) Arrangement of RNA and proteins in the spliceosomal U1 snRNP. *Nature.*, 409(6819): 539-42

Stevens, S.W., Barta, I., Ge, H.Y., Moore, R.E., Young, M.K., Lee, T.D., and Abelson, J. (2001) Biochemical and genetic analysis of the U5, U6, and U4/U6.U5 small nuclear ribonucleoproteins from *Saccharomyces cerevisiae*. *RNA*, 7, 1543-1553.

T

Tanner, N.K. and Linder, P. (2001) DexD/H box RNA helicases: from generic motors to specific dissociation functions. *Mol. Cell.*, 8, 251-262.

U

Urlaub, H., Hartmuth, K., Kostka, S., Grelle, G., and Lührmann, R. (2000) A general approach for identification of RNA-protein crosslinking sites within native human spliceosomal small nuclear ribonucleoproteins (snRNPs). *Journal of Biol. Chem.*, 275. 41458-41468.

Urlaub H., Raker V.A., Kostka S. and Lührmann R. (2001) Sm protein-Sm site RNA interactions within the inner ring of the spliceosomal snRNP core structure. *EMBO J.*, 20(1-2): 187-96

Urlaub, H., Hartmuth, K., and Lührmann, R. (2002) A two-tracked approach to analyze RNA-protein cross-linking sites in native, nonlabeled small nuclear ribonucleoprotein particles. *Methods*, 26, 170-181

V

Valcárcel, J., Gaur, R. K., Singh, R. and Green, M. R. (1996) Interaction of U2AF65 RS region with premRNA branch point and promotion of base pairing with U2 snRNA. *Science*, 273, 1706-1709.

Verdone L., Galardi S., Page D. and Beggs J.D. (2004) LSM proteins promote regeneration of pre-mRNA splicing activity. *Curr Biol.*, 14(16): 1487-91

Vidal, V.P., Verdone, L., Mayes, A.E., and Beggs, J.D. (1999) Characterization of U6 snRNA-protein interactions. *RNA*, 5, 1470-1481.

Vidaver R.M., Fortner D.M., Loos-Austin S.L., and Brow D.A, (1999) Multiple Functions of *S. cerevisiae* Splicing protein Prpr24p in U6 RNA Structural Rearrangements. *Genetics.*, 153, 1205-18.

Vorm O., Roepstorff P., and Mann M. (1994) Matrix surface made by fast evaporation yield improved resolution and MALDI TOF. *Anal. Biochem.*, 66:328

W

Will, C.L. and Lührmann, R. (1997) snRNP structure and function. In Krainer, A.R., Editor, *Eukaryotic mRNA Processing*, IRL Press, Oxford, pp. 130-173.

Will, C.L. and Lührmann, R. (1997) Protein functions in pre-mRNA splicing. *Curr. Opin. Cell. Biol.*, 9, 320-328.

Wolff, T. and Bindereif, A. (1993) Conformational changes of U6 RNA during the spliceosome cycle: an intramolecular helix is essential both for initiating the U4-U6 interaction and for the first step of slicing. *Genes Dev.*, 7,1377-89.

Z

Zeiler, B. N. & Simons, R. W. (1998). Antisense RNA Structure and Function. In *RNA Structure and Function* (Simons, R. W. & Grundberg-Manago, M., eds), pp. 437–464, Cold Spring Harbor Laboratory Press, Cold Spring Harbor, NY.

Zhang, D. and Rosbash, M. (1999) Identification of eight proteins that cross-link to pre-mRNA in the yeast commitment complex. *Genes Dev.*, 13, 581-592.

APPENDIX

List of Abbreviations

°C	degree Celsius
•OH	hydroxyl radical
A	adenosine
APS	ammonium peroxy sulfate
bp	base pair
C	cytosine
Ci	Curie
CMCT	1-cyclohexyl-3-(2-morpholinoethyl) carbodiimide metho-p-toluene sulfonate
DMS	dimethylsulfate
DMSO	dimethylsulfoxide
DNA	deoxyribonucleic acid
DTE	1,4-dithioerythrol
ddNTPs	dideoxynucleotide-5'-triphosphates
dNTPs	deoxynucleotide-5'-triphosphates
DTT	1,4-dithiothreitol
E. coli	Escherichia coli
EDTA	ethylenediamine-N, N, N', N'-tetraacetic acid
G	guanosine
h	hour
HY-mix	hybridization mix
IgG	immunoglobulin G
kb	kilo base
kDa	kilo dalton
KE	β -ethoxy- α -ketobutyral aldehyde
L	liter
Lsm	Sm-like proteins
μ	micro
min	minute
ml	milliliter

mRNA	messenger RNA
NP-40	Nonidet P-40
OD	optical density
PAGE	polyacrylamide gel electrophoresis
PAP	peroxidase-antiperoxidase complex
PBS	phosphate-buffered saline
PCR	polymerase chain reaction
PCV	packed cell volume
PEG	polyethylene glycol
pmole	picomole
PNK	polynucleotide kinase
pre-mRNA	pre-messenger RNA
poly (U)	poly uridine
RNA	ribonucleic acid
RNP	ribonucleoprotein
rNTPs	ribonucleotide-5'-triphosphates
RRM	RNA recognition motif
RT	reverse transcriptase
RT-mix	reverse transcriptase mix
<i>S. cerevisiae</i>	<i>Saccharomyces cerevisiae</i>
SDS	sodium dodecyl sulfate
snoRNP	small nucleolar ribonucleoprotein
T	thymidine
TAP	tandem affinity purification
TBE	Tris-Borate-EDTA buffer
TE	Tris-EDTA buffer
TEMED	N, N, N', N'-tetramethylethylenediamine
TEV protease	tobacco etch virus protease
TPR	tetratricopeptide repeat
TRP1	tryptophane
U	uridine
UsnRNA	uridine-rich small nuclear ribonucleic acid
UsnRNP	uridine-rich small nuclear ribonucleoprotein
UV	ultra violet
YPD	yeast extract, peptone, dextrose
SC-TRP	synthetic complete lacking tryptophane

Acknowledgements

Here I would like to thank ...

... first of all, **Prof. Dr. Reinhard Lührmann** for this interesting topic, his encouragement, his guidance and his incredible support during my PhD work. I would like to express my gratitude to him for being always open and available for discussion.

... **Dr. Patrizia Fabrizio**, for supervising me during my experiments.

... members of our small yeast team, **Irina Häcker** and **Marion Killian**, as well as former member **Dr. Cornelia Bartels**, for being always around to help me and many interesting discussions.

... electron microscopy team members: **Dr. Berthold Kastner** for always encouraging me, very useful discussions, and for proofreading my PhD thesis; **Dr. Prakash Dube** for all sample analyses and moral support and **Dr. Holger Stark** for structural analysis of U6 snRNP.

... **Dr. Henning Urlaub**, **Dr. Klaus Hartmuth** and **Dr. Stephanie Nottrott** who helped me a lot in structure probing experiments. Also **Monika Raabe** for being always patient to analyze my samples by mass spectrometry.

... **Irina**, with whom I always feel free to talk about everything.

... **Irene Öchsner** who always gave me many useful stuff both in the lab and at home (my lovely neighbour).

... **Heike Behr** for simply her loud laughs which motivate me and I always enjoy to hear.

... **Ilonka Bartoszek**, who joined to our group recently but helped me incredibly.

... our “Hexenküche”, **Uschi Drössler** and **Gertrud Nowak**. How I would be able to grow my yeast cells without your help.

... **Juliane Moses**, for her help in all kind of paper-work problems.

... of course **all my colleagues**, whose names I could not mention here, for their patience and for creating such a friendly atmosphere; for providing discussions, ideas and suggestions during our group seminars, essential to the planning and execution of my PhD work.

... finally and specially **my parents**, who encouraged me and provided financial support during the time; **Prof. Dr. Neş’ e Bilgin**, who persuaded me to choose the road of science and also provided me incredible moral support during the time I was applying for PhD; and **Benedikt Heiming**, who is always by my side and ready for every kind of support. Without him, I might not have finished this PhD work.

Curriculum Vitae

First Name Ramazan
Family Name Karaduman
Date of birth August 30, 1979
Place of birth Istanbul, Turkey
Nationality Turkish
Adress Friedrichstraße 1, 37073 Göttingen, Germany
E-mail rkaradu@gwdg.de

School Education 1985-1989 Primary School in Bahçelievler, Istanbul
 1989-1992 Secondary School in Yeşilköy, Istanbul
 1992-1995 College of Science in Fatih, Istanbul

University Education 1995-2000 Bachelor of Molecular Biology and Genetics at Boğaziçi University, Istanbul
 2000-2001 M.Sc. Program in Molecular Biology, Georg-August University, Göttingen
 2002-2003 Master of Science, "Tandem Affinity Purification and Characterization of the U6 snRNP from the yeast *Saccharomyces cerevisiae*" in Dept. of Cellular Biochemistry, at Max-Planck-Institute of Biophysical Chemistry, Göttingen under supervision of Prof. Dr. R. Lührmann
 2003-2006 Dissertation, "Determination of the structure of the spliceosomal U6 snRNP from yeast, *Saccharomyces cerevisiae*", in Dept. of Cellular Biochemistry, at Max-Planck-Institute of Biophysical Chemistry, Göttingen under supervision of Prof. Dr. R. Lührmann

Awards and Fellowships	1995	Bronz Medal in 6 th International Biology Olympiad, Bangkok
	1995-2000	Undergrad Scholarship by Foundation of Turkish Education, Istanbul
	2000-2001	M.Sc. Fellowship by International MSc Program in Molecular Biology, Göttingen
	2003-2005	Ph.D. Stipend by Max-Planck-Institute of Biophysical Chemistry, Göttingen

Presentations

Poster Presentation, 9th Annual Meeting of the RNA society, June 2004, Madison, USA

Title "Elucidation of the Structure of Purified U6 snRNP from *S. cerevisiae* using Biochemical Methods and Electron Microscopy"

Oral Presentation, Eukaryotic mRNA Processing, August 2005, Cold Spring Harbor Laboratory, Cold Spring Harbor, New York, USA

Title "Structure Probing and EM Analyses of the yeast U6 snRNP Reveal New Insights into the Structure of the U6 snRNA and its Interaction with Prp24p and LSm2p-8p"

Publications

Karaduman R., Fabrizio P., Hartmuth K., Urlaub H. and Luhrmann R.
RNA structure and RNA-protein interactions in purified yeast U6 snRNPs
Journal of Molecular Biology, **356**, 1248-62

Karaduman R., Dube P., Stark H., Fabrizio P., Kastner B. and Luhrmann R.
Electron microscopy of LSm-protein labelled yeast U6 snRNPs reveals the structural arrangement of Prp24p and the LSm complex (in preparation)